

# Theoretical Analysis and Experimental Investigation of Simulated Moving Bed Chromatography for the Purification of Protein Mixtures

---

**Chris J. Wayne**

Department of Biochemical Engineering  
University College London  
Gower Street  
London  
WC1E 6BT

A thesis submitted for the degree of  
DOCTOR OF PHILOSOPHY  
September 2018

## **DECLARATION**

I confirm that the work presented in this thesis is my own unless indicated otherwise. The work presented was carried out under the supervision of Prof Ajoy Velayudhan at the Department of Biochemical Engineering, University College London between September 2014 and September 2018. This thesis has not been submitted, either in whole or in part, for another degree or another qualification at any other university.

Christopher James Wayne  
London, September 2018

## **ABSTRACT**

Stepwise-Elution Simulated Moving Bed Chromatography (SE-SMB) is a promising method for 'intensification' of polishing chromatographic processes in downstream bioprocessing. This is because SE-SMB systems are continuous, capable of high-resolution separations, efficient in their utilization of chromatographic resins, well-suited to non-isocratic proteinaceous separation problems operated under high feed-loading conditions, and highly productive.

However, there are a number of theoretical and practical problems which have impeded industrial interest in the adoption of SE-SMB separations into downstream processes. Fundamental phenomena, such as the modulator dynamics of SE-SMB systems, have yet to be theoretically analysed. Consequently, important practical questions – such as how productive and high-resolution separations may be best achieved through SE-SMB systems – remain unanswered. Furthermore, the complexity and operational fragility of SE-SMB systems require much improvement in their 'robustness' before any consideration of their application to industrial purification of therapeutic proteins may be entertained.

This thesis constitutes an initial investigation of the theoretical and practical issues which arise concerning the application of SE-SMB to industrial bioseparations. Regarding the theoretical issues, an analysis of modulator dynamics in SE-SMB systems is presented. This provides new insights into how such systems – both for binary and ternary separations - should be designed for productive and robust operations. Furthermore, the behaviour of SE-SMB systems under high feed-loading conditions is also investigated. Regarding practical issues, experimental SMB separations of a challenging proteinaceous mixture are demonstrated, and simulated comparisons are used to investigate the comparative performance of various intensified processes. Finally, an exploration of SE-SMB fault detection and diagnosis methods is undertaken. The results suggest that SE-SMB chromatography may be 'de-risked' to such an extent that, with future development, it becomes an attractive option for incorporation into industrial bioprocesses.

## IMPACT STATEMENT

It is hoped that the body of work summarized by this thesis will be of immediate and future use to academic and industrial practitioners of continuous chromatography. This thesis is based upon three results chapters which address some of the scientific and practical problems of the design and robust operation of SE-SMB systems.

First, the formal analysis of modulator perturbations and subsequent definition of two new design constraints – presented as the dimensionless numbers  $\Psi$  and  $\Omega$  – should be of immediate use to investigators who wish to perform ion-exchange SE-SMB chromatographic separations productively and to a high purity. These constraints define the design space of SE-SMB separations in the limit of linear-isotherm binding behaviour.

Second, for non-linear SE-SMB separations, the use of the  $\Psi$  constraint in addition to the analysis of the interaction between zone-lengths and non-linear isotherm behaviour should aid chromatographers in empirical SE-SMB optimization efforts. The behaviour of SE-SMB systems operated under high loading conditions also has a bearing on the optimal design of centre-cut SE-SMB systems; this topic is also analysed within this thesis.

Finally, in regards to the problems posed by failure modes for the adoption of SE-SMB processes by industrial operators, a preliminary account in this thesis is given of how rapid and easy detection and diagnosis of such faults may be achieved. While this area of investigation is still at a very early stage, it is hoped that the further development of so-called 'expert systems' for industrial SE-SMB chromatography can benefit from the initial results documented in the following pages.

A number of publications and presentations have arisen as a result of work on this thesis:

- 1) Cell Culture and Downstream World Congress, in Munich (Germany) 2017 ; Oral Presentation; Title: 'Continuous Chromatography of Proteins'
- 2) Continuous Biomanufacturing Conference, Oxford (U.K.) 2017; Oral Presentation; Title: 'Robust operation of protein SMB'
- 3) As first-author, published in Biotechnology Journal the research article titled: 'Modulator Dynamics Shape the Design Space for Stepwise-Elution Simulated Moving Bed Chromatographic Separations'; see the following reference[1] .
- 4) American Chemical Society (ACS) spring conference, New Orleans (U.S.A.) 2018; Poster Presentation; Title: 'Failure Mode Detection, Diagnosis and Recovery in SMB Chromatography'.

5) A research article titled: 'Failure Mode Detection and Diagnosis in Stepwise-Elution Simulated Moving Bed Chromatography'. At the time of writing, this paper is in preparation.

## ACKNOWLEDGEMENTS

This thesis would not have been possible but for my supervisor, Professor Ajoy Velayudhan. I have been very fortunate to benefit from Ajoy's long industrial experience, critical insight, and excellent book recommendations. He has my gratitude for helping me find my feet in a new (for me) scientific area, and for helping me pursue what I found to be a very interesting PhD project.

In addition to my supervisor, I'd like to thank my lab colleagues for their help and training. Particular thanks go to Kosma Jurlewicz, Nick Field, Spyridon Konstantinidis, Gareth Mannall, Mike Sulu, Haiyuan Goh, Trish Krishnan, Anshul Sharma, Sushobhan Bandyopadhyay, and Greta Jasulaityte.

I'd also like to thank the EPSRC and UCL for giving me the opportunity to do a PhD. I hope that the vast quantities of money and resources you have spent on my training as a scientist will turn out to be a good investment!

During the last four years at UCL, I've been lucky enough to accumulate a good number of new friends and acquaintances. Having these people around has brightened each day of lab work, every conference trip, and many informal weekends and evenings. I'm thankful to them and my department at UCL for bringing such a friendly, interesting, and fun group of people together under one roof.

Finally, I would like to thank my family. In particular, my parents and my aunt deserve special thanks for their support and encouragement over the years - I am very fortunate to be related to them. I am also grateful for my sister, who has put her first-class Oxford degree to excellent use in supplying a thesis proof-reading service in combination with remedial lessons on the basic rules of English grammar. While I have tried to write this thesis intelligibly and without errors, if mistakes are present, she alone is to blame.

# LIST OF FIGURES

Figure 1-1 True Moving Bed chromatography of a binary separation .....	24
Figure 1-2 Classic binary SMB operation scheme .....	25
Figure 1-3 Binary SE-SMB scheme .....	26
Figure 1-4 Two examples of isocratic integrated (or ‘single train’) SMB systems .....	27
Figure 1-5 Modified Four-Zone SMB (MF-SMB) .....	28
Figure 1-6 The two-column MCSGP .....	30
Figure 1-7 Triangle theory for the design isocratic binary separations .....	34
Figure 3-1 Standing Waves in SMB separation .....	56
Figure 3-2 SE-SMB design within 3D design space .....	64
Figure 3-3 Transient modulator profiles in SE-SMB systems .....	66
Figure 3-4 Differences between the Real and Ideal SE-SMB operation spaces .....	70
Figure 3-5 Sequential design and theoretical approximations of theory .....	74
Figure 3-6 Experiments and simulations to test theory .....	78
Figure 3-7 Experiments and simulations to demonstrate application of theory for robust and productive SE-SMB design .....	81
Figure 4-1 Integrated ternary SE-SMB schemes. ....	92
Figure 4-2 A centre-cut separation of a ternary mixture through a raffinate-coupled SE-SMB 6-zone cascade configuration with intermediary buffer tank .....	93
Figure 4-3 Resolving Power differences between chromatographic processes .....	99
Figure 4-4 Single column batch chromatogram of model ternary protein separation .....	100
Figure 4-5 Experimental Separations of Model Ternary Protein Mixture .....	101
Figure 4-6 Three fractions (Extract, Wash and Raffinate) of ovalbumin variants (overlaid) from a SAW SMB separation .....	103
Figure 4-7 Chromatogram of ovalbumin variants in the SMB feed .....	104
Figure 4-8 Evidence for ‘asymmetric productivity’ in simulated non-linear system .....	105
Figure 4-9 SMB productivity and zone length (Z3) in simulated non-linear system .....	106
Figure 4-10 SMB productivity and zone length (Z2) in simulated non-linear system .....	107
Figure 4-11 Separation resolution affects single-train SMB performance in simulated non-linear system .....	108
Figure 4-12 Comparison between intensified processes (purity constrained to >95%) in simulated non-linear system .....	109
Figure 5-1 Cyclic signal variation from singular failure-mode .....	119
Figure 5-2 Conductivity measurement of SE-SMBs .....	120
Figure 5-3 UV signal feature extraction .....	121
Figure 5-4 Feature extraction from SMB outlet conductivity patterns .....	122
Figure 5-5 Failure-mode signatures in SE-SMB extract and raffinate outlet concentration patterns	124
Figure 5-6 Single failure-modes classification decision trees .....	126
Figure 5-7 Decision tree for classification of general failure modes .....	128
Figure 5-8 Mechanisms of failure-mode pattern generation .....	130
Figure 5-9 Overlaid internal concentration profile snapshots of single-fault SE-SMBs .....	131

Figure 5-10 Decision trees for locating malfunctioning component (post-failure-mode classification)	133
Figure 5-11 Generating false-positive failure-mode signals	136
Figure 5-12 Failure-mode patterns in an SMB cascade	138

## LIST OF TABLES

Table 1-1 Elution programs in batch chromatography .....	20
Table 1-2 Important literature contributions on the subject of proteinaceous, centre-cut, and stepwise-elution SMBs.....	31
Table 2-1 Model Parameters for Competitive Langmuirian Isotherm Simulations .....	41
Table 2-2 Properties of model system used in laboratory SMB experiments .....	42
Table 2-3 Simulation parameters used to investigate failure mode signal patterns.....	44
Table 2-4 Signal Feature Analysis.....	52
Table 3-1 Isotherm and void fraction parameter determination .....	75
Table 3-2 Experiment to demonstrate N-theory first MP constraint .....	76
Table 3-3 Properties of simulated system used to demonstrate N-theory second MP constraint .....	79
Table 3-4 Operation conditions used to demonstrate N-theory operation window boundaries .....	80
Table 3-5 Properties of simulated system used to demonstrate N-theory design of robustness to ligand loss.....	82
Table 3-6 Experimental operation conditions used to demonstrate N-theory robust design .....	83
Table 3-7 Operation conditions used to demonstrate N-theory design of productive separations ....	84
Table 4-1 Model ternary mixture separations through various chromatographic approaches .....	100
Table 4-2 Operation conditions of centre-cut experiments .....	102
Table 4-3 Operation conditions of SAW SMB ovalbumin experiment.....	104
Table 5-1 Summary of the effects of various common failure modes on binary SE-SMB processes operated under high feed-loading conditions .....	117
Table 5-2 Cyclic signal features indicative of failure mode class in step-down SE-SMB system with Z2 pump. Codes for features (of type F#) are detailed in the Materials and Methods Table 2-4.....	127
Table 8-1 MOO final generation's individuals for T1 binary separation Product collected at Raffinate port.....	156
Table 8-2 MOO final generation's individuals for T1 binary separation Product collected at Extract port.....	156
Table 8-3 MOO final generation's individuals for Recycle-batch chromatography.....	157
Table 8-4 MOO final generation's individuals for batch chromatography .....	158
Table 8-5 MOO final generation's individuals for SAW SMB .....	158

## **ABBREVIATIONS**

<b>DSP</b>	Downstream Processing
<b>IEX</b>	Ion-Exchange
<b>LRC</b>	Less Retained Component
<b>mAbs</b>	Monoclonal Antibodies
<b>MRC</b>	More Retained Component
<b>MOO</b>	Multi-Objective Optimization
<b>MP</b>	Modulator Perturbation
<b>OVA</b>	Ovalbumin
<b>P</b>	Product
<b>S</b>	Strong Impurity
<b>SAW</b>	Step and Wash
<b>SE-SMB</b>	Stepwise-Elution Simulated Moving Bed
<b>SMB</b>	Simulated Moving Bed
<b>SMT</b>	Solute Movement Theory
<b>SWA</b>	Standing Wave Analysis
<b>TMB</b>	True Moving Bed
<b>W</b>	Weak Impurity
<b>ZLB</b>	Zero Lower Bound

## NOMENCLATURE

$A_C$	[cm <sup>2</sup> ]	Column cross-sectional area
$c_{i,j,x}$	[g/L]	Liquid concentration of species i in zone j at node x
$c_{i,j,x}^p$	[g/L]	Pore liquid concentration of species i in zone j at node x
$C_{M,j,x}$	[M]	Modulator concentration in zone j at node x
$C_{\ddagger}$	[M]	Modulator concentration in MPP pulse
$C_D$	[M]	Modulator concentration in desorbent solution
$C_F$	[M]	Modulator concentration in feed solution
$C_j$	[M]	Modulator concentration in zone j
$d_p$	[cm]	Particle Diameter
$D_i$	[m <sup>2</sup> second <sup>-1</sup> ]	Axial dispersion coefficient for species i or the modulator
$\Delta C_D$	[mM]	Desorbent modulator concentration deviation
$\Delta C_F$	[mM]	Feed modulator concentration deviation
$\Delta Q_E$	[%]	Extract pump flow rate deviation
$F_i$	[mLmin <sup>-1</sup> ]	Feed solution concentration of species i
$H$	[mLmin <sup>-1</sup> ]	Harmonic mean of liquid flow rates in Zone 2 & Zone 3
$k_{m,i}$	[second <sup>-1</sup> ]	Solid Phase mass-transfer rate coefficient
$k_{f,i}$	[second <sup>-1</sup> ]	Liquid Phase mass-transfer rate coefficient
$K_{0,i}$	[-]	Partition coefficient at OM modulator for species i
$k'_{i,C_j}$	[-]	k prime value for species i in Zone j at $C_j$ modulator concentration
$L$	[cm]	Column Length
$M_j$	[-]	Flow-rate ratio in Zone j
$q_{i,j,x}$	[g/L]	Adsorbed phase concentration of species i in zone j at node x
$q_{i,j,x}^*$	[g/L]	Equilibrium adsorbed phase concentration of species i in zone j at node x
$Q_D$	[mLmin <sup>-1</sup> ]	Desorbent liquid flow rate

$Q_E$	[mLmin <sup>-1</sup> ]	Extract liquid flow rate
$Q_{Eq}$	[mLmin <sup>-1</sup> ]	Equilibrium flow rate
$Q_F$	[mLmin <sup>-1</sup> ]	Feed liquid flow rate
$Q_R$	[mLmin <sup>-1</sup> ]	Raffinate liquid flow rate
$Q_j$	[mLmin <sup>-1</sup> ]	Liquid flow rate in Zone j
$S_i$	[-]	Coefficient for salt-dependency of partition for species i
$t_2$	[mins]	Time for ideal solvent front to travel one column's distance in Zone2
$t_S$	[mins]	Switching Time
$v_{i,j}$	[cm/min]	Velocity of species i in zone j
$V$	[mL]	Total Column Volume
$V_0$	[mL]	Void volume of column
$V_{Eq}$	[mL]	Equilibration Volume
$V_{i,C_{\ddagger}}$	[mL]	Retention volume at transitional modulator concentration for species i
$V_{i,C_M}$	[mL]	Retention volume at a given modulator concentration for species i
$V_{i,C_3}$	[mL]	Retention volume at Zone 3 modulator concentration for species i
$V_{lag}$	[mL]	Volumetric difference between theoretical step change in [modulator] at end of single column and actual change due to non-idealities
$x_i$	[cm]	Distance travelled by species i

### Subscripts

i	Feed species component, i=a,b
a	Feed species 'a', the more-retained component (MRC)
b	Feed species 'b', the less-retained component (LRC)
j	Zone number, j=1:3 or j=1:4
x	Node number, x=1:n per column
n	nodes per column
$C_M$	Relating to Modulator

### Greek letters

$\alpha$	[cm <sup>-1</sup> ]	coefficient, equal to $6/d_p$
$\varepsilon_{T,C_M}$	[-]	Total void fraction available to modulator
$\varepsilon_{T,i}$	[-]	Total void fraction available to species i
$\varepsilon_{p,i}$	[-]	Particle porosity available to species i
$\varepsilon_e$	[-]	Interstitial void fraction
$\varphi_i$	[-]	Phase ratio $\left(\frac{1-\varepsilon_{T,i}}{\varepsilon_{T,i}}\right)$ for species i
$\Psi$	[-]	Dimensionless number describing the first MP constraint
$\omega$	[min <sup>-1</sup> ]	Port switching frequency
$\Omega_i$	[-]	Dimensionless number describing the second MP constraint for species i

# TABLE OF CONTENTS

IMPACT STATEMENT .....	4
LIST OF FIGURES.....	7
LIST OF TABLES.....	9
ABBREVIATIONS .....	10
NOMENCLATURE.....	11
Chapter 1 Literature Review .....	17
1.1 Chromatography in Downstream Processing (DSP).....	17
1.1.2 Ion Exchange Chromatography: Isocratic, Gradient, and Stepwise Operation .....	18
1.1.3 Motivations for replacing or improving batch chromatography processes .....	21
1.2 Intensified and Continuous Approaches to Industrial Downstream Processing .....	22
1.2.1 Recycle Batch Chromatography .....	23
1.2.2 SMB Chromatography.....	23
1.2.3 Centre-Cut SMB and Hybrid-SMB schemes .....	26
1.2.4 The Multi-Column Solvent Gradient Process (MCSGP).....	28
1.2.5 Important literature contributions involving non-isocratic, ternary, and proteinaceous SMB separations .....	30
1.3 Adoption of intensified and continuous processes in industry .....	32
1.3.1 Robust design of isocratic SMB operations .....	33
1.3.2 Control engineering of intensified processes .....	34
1.4 Aims and Organization of Thesis.....	35
Chapter 2 Materials and Methods with THEORETICAL CONSIDERATIONS.....	38
2.1 Computational Methods.....	38
2.1.1 Modelling of Ideal and Real SMB chromatography .....	38
2.1.2 Modelling of SMB failure modes.....	42
2.1.3 Multi-Objective Optimization (MOO) methods .....	44
2.1.4 Modelling of single-column batch and recycle-batch chromatography.....	46
2.2 Experimental Methods.....	48
2.2.1 SMB and single-column batch chromatography experiments.....	48
2.2.2 Isotherm determination.....	49
2.2.3 Construction of failure-mode experimental models .....	50
2.2.4 Analytical chromatography methods for purity assessment.....	51

2.3 Analytical Methods .....	52
2.3.1 Failure-mode signal-analysis methods.....	52
Chapter 3 Robust and Productive Design of Stepwise-Elution SMB Binary Separations .....	54
3.1 Introduction .....	54
3.1.2 Design of non-isocratic countercurrent systems .....	56
3.1.3 Motivation for Chapter 3 .....	56
3.2 Theory .....	57
3.2.1 A new 3D design space for SE-SMB systems.....	57
3.2.2 Design of ideal SE-SMB systems.....	58
3.2.3 The Modulator Perturbation (MP) problem in real SE-SMB systems .....	65
3.2.4 Design of real SE-SMB systems with account of MPs: the $\Psi$ constraint .....	67
3.2.5 Design of real SE-SMB systems with account of MPs: the $\Omega$ constraint.....	71
3.2.5 Robust design of SE-SMB systems .....	74
3.3 Results.....	75
3.3.3 Experiments to demonstrate robust and productive design.....	80
3.4 Discussion.....	85
Chapter 4 Stepwise-Elution SMB Systems for Non-Linear Ternary Bioseparations .....	87
4.1 Introduction .....	87
4.1.1 Motivation for Chapter 4 .....	88
4.2 Theory .....	89
4.2.1 Optimal approaches to integrated stepwise elution centre-cut SMB separations .....	90
4.2.2 Optimal approaches to cascade centre-cut SE-SMB separations .....	92
4.2.3 Performance differences in integrated and cascade centre-cut SE-SMB separations .....	97
4.3 Results and Discussion .....	100
4.3.1 Experimental batch, SE-SMB cascade, and SAW SMB separation of a model ternary proteinaceous mixture.....	100
4.3.2 Experimental SAW separation of challenging ternary proteinaceous mixture .....	103
4.3.3 Asymmetry in binary SMB performance under overload conditions .....	104
4.3.4 Effect of Z3 length on binary SMB performance under overload conditions.....	105
4.3.5 Effect of Z2 length on binary SMB performance under overload conditions.....	106
4.3.6 Purity limitations of integrated separation schemes.....	107
4.3.7 Simulated comparison between various intensified approaches to preparative chromatography.....	108

4.3.8	Towards the global optimization of SE-SMB cascades .....	110
4.3.9	On the utility of Integrated SMB, MCSGP and single-train 'pseudo-SMB' processes for bioprocessing .....	113
	Conclusion.....	114
Chapter 5	Failure mode detection and diagnosis in SE-SMB systems.....	115
5.1	Introduction .....	115
5.1.1	Single-column batch chromatography expert systems .....	116
5.1.2	Countercurrent chromatography expert systems .....	116
5.1.3	Motivation for Chapter 5 .....	117
5.2	Theory.....	118
5.3	Results and Discussion .....	122
5.3.1	The outlet concentration patterns produced by singular column and leak SMB failure modes are cyclical.....	122
5.3.2	Identification of general column failure modes.....	127
5.3.3	Mechanism of generation of cyclic signal features.....	128
5.3.4	Localization of Faults by column-signal features .....	132
5.3.5	Robustness of fault detection methods to false-positive signals .....	133
5.3.6	Failure modes in a directly-coupled SMB ternary cascade .....	137
	Conclusion.....	138
Chapter 6	CONCLUSION.....	141
Chapter 7	BIBLIOGRAPHY.....	145
Chapter 8	APPENDIX .....	156

# CHAPTER 1 LITERATURE REVIEW

## 1.1 Chromatography in Downstream Processing (DSP)

In the industrial manufacture of biological macromolecules (i.e. 'biologics') for therapeutic applications, chromatographic processes are very often employed for purification tasks. As an established industrial separation process, chromatography is capable of purifying single components from complex mixtures with high yield and purity.

Purification tasks are a feature of many bioprocesses, and most therapeutic proteins are manufactured through the use of cultured cells. While the use of living cells permits the manufacture of structurally-complex and highly chiral macromolecules - which would otherwise be very difficult and expensive to manufacture through alternative synthetic chemistry routes - there are drawbacks to the use of biological organisms in the bioprocess.

One significant problem in upstream bioprocessing is the co-production of product and impurities during upstream manufacturing processes. Impurities, such as host-cell proteins (HCPs), host-cell DNA, viruses, product fragments, and product aggregates, need to be separated from the target biologic product before a drug may be administered to a patient. Failure to remove such impurities from an injected drug is dangerous to patients, as – among other possible hazards – undesired ('secondary') immunogenic reactions may occur.

Chromatographic processes are key to most industrial bioseparations. These processes purify components of complex mixtures by exploiting the ability of different chromatographic stationary-phases ('sorbents') to separate molecules based upon differences in their charge, size, hydrophobicity, van der Waals' interactions, and affinity to a particular ligand (e.g. Protein A, immobilised metal ions, lectins). The choice of the number, type, and sequence of chromatographic steps in a bioprocess is a common engineering design task. However, in general, most bioprocesses feature at least one purification step involving an Ion-Exchange chromatography (IEX). In IEX, products are separated from contaminants based upon differences in the strength of their electrostatic interactions with sorbents.

There have traditionally been two possible operation modes for chromatographic steps: 'bind-and-elute' and 'flow-through' chromatography. In the bind-and-elute mode, a separation mixture is first loaded onto a chromatographic column, and then all feed species are eluted sequentially. Purified and concentrated product may be collected during the course of this elution as

a 'fraction' (a discrete volumetric sample) of a column's eluted contents. In contrast to the bind-and-elute mode, the flow-through chromatographic mode operates by allowing continuous loading of a mixture with a product that does not interact with the stationary phase. The product therefore 'flows through' the column, but it emerges for collection stripped of a number of impurities which bind to, and accumulate in, the solid phase [2]. Most bioprocesses make use of both bind-and-elute and flow-through operation modes in order to meet the regulatory requirements on therapeutic biologics.

### **1.1.2 Ion Exchange Chromatography: Isocratic, Gradient, and Stepwise Operation**

The 'work-horse' of current industrial polishing chromatography is the single-column batch separation. Batch bind-elute separations involve two processing stages: feed mixture is first loaded onto a column, and subsequently an 'elution' buffer is pumped through the column. The purpose of the elution stage of chromatography is to sequentially elute different feed mixture components from the column, such that one or more of the feed components may be collected as a pure fraction at the column outlet.

Optimization of the elution stage of IEX and HIC chromatography is a common engineering task, and there are three possible elution modes (or 'programs') on which optimization work is generally focused. These three programs are isocratic, stepwise, and gradient elution modes. Isocratic elution involves use of a single modulator concentration, whilst stepwise elution involves sequentially 'stepping' the modulator concentration. In the extreme case of stepwise-elution schemes, when modulator steps are very small, numerous, and evenly-spaced, a 'linear-gradient' scheme is generated.

While isocratic elution can maximise the difference of retention times between the peaks of sequentially-eluting components, there is rarely a suitable global optimum of modulator concentration for non-binary isocratic separations. Also, isocratic elution of multi-component separation mixtures can be time-consuming, and can thus increase the band-broadening of more retained components which results in poorer separation resolution. These considerations make isocratic elution conditions a rare choice in most industrial preparative chromatography of protein mixtures.

A popular elution program which retains the ability of isocratic elution schemes to generate large differences between the retention times of sequentially-eluting peaks, whilst at the same time shortening the required process time and band-broadening of later-eluted components, is a

stepwise-elution program. These programs 'step' the modulator concentration at uniform or non-uniform temporal intervals during the elution stage of a process. Stepwise-elution programs aim to achieve necessary resolution between feed components, so as to enable their individual fractionation, whilst at the same time permit shortening of the required processing-time.

A related method to the stepwise-elution mode is the linear modulator-gradient elution mode. Linear gradients can be generated experimentally by serially 'stepping' the elution buffer's modulator concentration by small increments. These multiple, discrete micro-steps in the modulator concentration are generally smoothed by mixing within the buffer preparation apparatus and the column flow-path, thus producing a smooth modulator gradient. Linear-gradients are often characterized by three values: 1) A chosen gradient-starting modulator concentration, 2) A gradient-ending modulator concentration, and 3) The number of column/membrane volumes over which the buffer pumps linearly 'step' the modulator between the gradient start and finish concentrations.

Table 1-1 summarizes some of the advantages and disadvantages of each elution program [3].

**Table 1-1** Elution programs in batch chromatography

	<b>Isocratic</b>	<b>Stepwise</b>	<b>Linear-gradient</b>
<b>Advantages</b>	<p>For binary separations, the maximum difference between peak retention times is obtained through isocratic elution.</p> <p>Capable of separation of challenging mixtures with small separation factors (small <math>k'</math> range).</p>	<p>Large number of degrees of freedom in design, thus challenging multi-component separations are possible.</p> <p>Capable of separations across a large range of separation factors (large <math>k'</math> range).</p> <p>Capable of separation of challenging mixtures with small separation factors (small <math>k'</math> range).</p> <p>Depending on method, peaks can be significantly more or less concentrated than peaks from linear-gradient elution program alternatives.</p>	<p>Peaks are generally Gaussian-shaped, and thus easily recognisable and manually fractionable.</p> <p>Capable of separations across a large range of separation factors (large <math>k'</math> range).</p>
<b>Disadvantages</b>	<p>For binary and multi-component separations, gains in retention-time differences between binary elution peaks are often undermined by increased process time and concomitant band-broadening (worse resolution).</p> <p>Peaks can be less concentrated than is the case for linear-gradient and stepwise-elution programs.</p> <p>Not well suited to separation of mixtures with large separation factors (large <math>k'</math> range).</p>	<p>Generation of 'ghost' peaks from modulator steps can confuse manual fractionation in certain (type II elution) processes.</p>	<p>Less suited to fine, multi-component separations from challenging mixtures than stepwise-elution programs due to fewer degrees of design freedom.</p> <p>Not so well suited to separation of mixtures with small separation factors (small <math>k'</math> range) without use of a very shallow gradient.</p>

Of the three modes described, industrial polishing batch-chromatography tends to employ stepwise-elution programs or linear-gradient elution programs. There are advantages and disadvantages to both. For example, stepwise-elution programs allow for optimized spacing between components of complicated mixtures, whilst linear-gradient elution programs can help operators to concentrate peaks into easily-collectable and easily-recognisable fractions. It is also possible to combine the strengths of stepwise-elution programs and linear gradients into so-called 'multi-segment gradient-elution' programs [4,5]. Whilst such 'multi-segment gradient-elution' programs have shown impressive results for analytical separations, whether this type of elution program has been widely adopted into industrial biopharmaceutical processes is unknown to the author.

### **1.1.3 Motivations for replacing or improving batch chromatography processes**

Whilst single-column batch chromatography forms an integral part of very many existing industrial bioprocesses, recent years have seen increasing interest in its improvement or replacement. There are a couple of reasons for this.

One reason for finding alternatives to batch chromatography in industrial bioprocessing stems from concerns about manufacturing and capital costs. Chromatographic processes that are more productive than traditional single-column batch processes can both reduce the required volume of chromatographic sorbent, as well as reduce the processing time of the product batches. In this manner, increases to the productivity of chromatographic processes may enable cost savings in capital and utilization expenses.

However, many commercially-available therapeutic proteins currently apportion much of their price to non-manufacturing costs. Indeed, the manufacturing cost of certain 'on-patent' therapeutic proteins has been estimated to be as low as 5% of the final drug's price [6,7]. While it is true that the manufacturing cost of 'off-patent' therapeutic proteins comprises a larger proportion of the sales price than newer drugs, there are cost-independent reasons for why improvements and alternatives to traditional chromatographic processes are currently sought after.

A desire to improve final product quality animates much industrial interest in improved chromatographic processes. For example, it is well established that different glycosylation variants of therapeutic proteins have different properties of efficacy and half-life when administered to patients [8]. Separation of glyco-variants, such as sialylated from asialylated mAbs, requires a high

chromatographic separation resolution that is not always economical -due to low recovery - through traditional single-column batch processes.

An additional reason for interest in intensified and continuous chromatographic bioprocesses is that they are enabling technologies for a number of continuous upstream processes. Continuous upstream bioprocesses, such as perfusion bioreactors, can produce higher quality products to a higher yield than otherwise possible through traditional batch fermentation methods. In particular, for cell-lines which are low-yielding and produce fragile products, continuous downstream processes can realize significant improvements to a bioprocesses' final product quality and manufacturing cost [7].

## **1.2 Intensified and Continuous Approaches to Industrial Downstream Processing**

'Intensified processes' are novel engineering methods and/or equipment which, compared to methods and equipment in current use, bring 'dramatic improvements in manufacturing and processing' [9]. In the context of downstream processing, 'dramatic improvements' to chromatographic processes are generally assessed in terms of productivity, throughput, and purity improvements. When measured along these dimensions, there are a large number of proposed chromatographic processes that can out-perform traditional single-column batch processes.

A subset of intensified processes is also referred to as 'continuous' processes. While many definitions of 'continuous' chromatography processes exist, a common definition is that a continuous process must have non-intermittent feed and outlet flow streams [10]. By this definition, SMB processes are continuous and intensified processes, because they out-perform single-column batch equivalents while also continuously producing outlet products and receiving a feed input at a constant rate.

It is possible to transform certain discontinuous processes, such as single-column batch processes, into continuous processes by the use of parallel batch processes with well-planned process scheduling. The use of multiple smaller columns in parallel, instead of using large columns in serial batch processes, can significantly shorten the processing time and residence time of biologics in a column; this is highly advantageous in the processing of fragile products. However, these parallel batch processes – also known as carousel processes –retain the productivity (defined as product per unit time and unit sorbent) and purity performance of single-column batch processes.

There is industrial interest in finding chromatographic processes which are both intensified and continuous.

While the promise of intensified and continuous downstream polishing chromatographic processes is clear, with the exception of recycle-batch chromatography, there has yet to be widespread adoption of intensified and continuous chromatography processes in industrial manufacturing [10]. The following section gives an overview of candidate intensified and continuous chromatography processes.

### **1.2.1 Recycle Batch Chromatography**

Recycle-batch chromatography ‘recycles’ a number of impure outlet fractions by collecting them from the outlet stream of a batch process and then using them as feed components in subsequent batch processing. In this way, instead of being discarded, chromatographic outlet fractions which would fail product-purity requirements are ‘saved’ for further attempts at purification. Recycle-batch chromatography has been shown to improve either process productivity, product recovery, or both [2,11–15]. A number of configurations of multi-column recycle-batch chromatographic systems have been proposed to traditional single-column recycle batch techniques to enable a higher throughput [16,17].

### **1.2.2 SMB Chromatography**

Countercurrent separation processes involve the simultaneous movement of liquid phase (‘desorbent’) and solid phase (‘sorbent’) in opposite directions, whilst contact is maintained between the two phases. The theoretical countercurrent chromatography process which achieves separation by such simultaneous and directionally-opposed movement of the two phases is termed True Moving Bed (TMB) Chromatography; a schematic of a TMB binary separation is shown by the figure below. Figure 1-1 illustrates how a TMB can continuously separate a binary feed mixture by continuous circulation of fluid and solid around the system, and continuous withdrawal of purified feed species collected at the so-called ‘Extract’ and ‘Raffinate’ outlet ports. In such a four-zone system, the different zones (represented by four rectangular ‘blocks’ in the figure) have various functions. The purpose of the first zone (Z1) is to ‘regenerate’, or strip, the circulating solid phase of any retained feed components. By contrast, the purpose of Zone 4 (Z4) is to re-generate the liquid phase before its re-insertion into Z1. For Zones 2&3 (Z2&Z3), the purpose is to effect separation between the binary feed species.

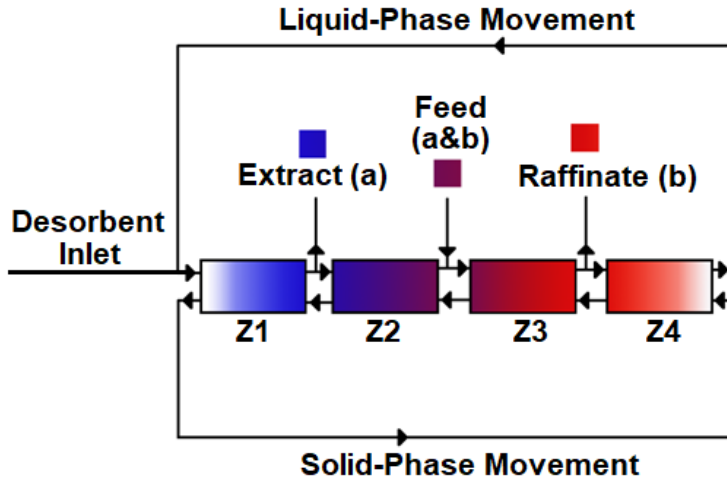


**Figure 1-1 True Moving Bed chromatography of a binary separation**

*True Moving Bed chromatographic separation of binary feed mixture (components a&b) in a four zone system*

Continuous countercurrent chromatography is capable of performing challenging separations ‘efficiently’ with respect to batch chromatography alternatives. This gain in performance of continuous countercurrent systems derives from the fact that full-resolution of the various chromatographic peaks is not necessary to achieve high-purity and high-recovery separations; resolution need only be achieved locally around the outlet-collection ports. Furthermore, the productivity of countercurrent systems – in terms of product produced per volume sorbent/desorbent per unit time – is far superior to that of bind-elute batch chromatography systems [2,18].

TMB chromatography is difficult to implement in experimental systems because of issues with mechanical shear and axial-mixing of the moving sorbent. However, it is possible to capture the performance advantages of TMB systems whilst avoiding this ‘true’ movement of the solid phase. Simulated Moving Bed (SMB) chromatography uses a stationary solid phase, but ‘simulates’ the countercurrent effect of solid-phase movement by continuous movement of inlet and outlet ports around a circle of interconnected, fixed-bed, chromatographic columns [19]. This is illustrated by Figure 1-2, where the inlet and outlet ports rotate clockwise around zones in order that pure extract and raffinate product streams are continuously withdrawn from the system.

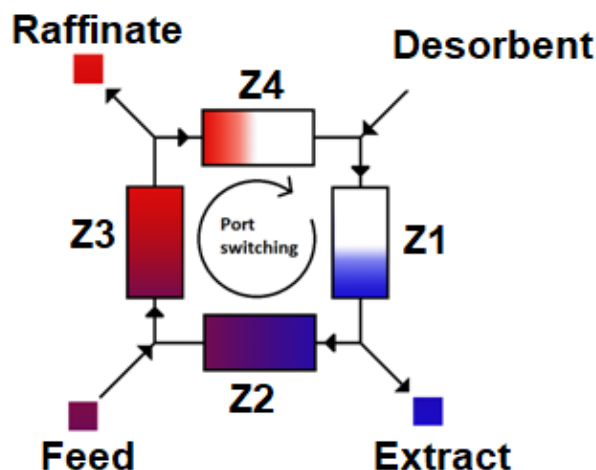


**Figure 1-2 Classic binary SMB operation scheme**

SMB ‘simulates’ countercurrent flow of sorbent through periodic port-switching of valves around a column series. Zones 1-4 are each composed of multiple columns, and every port-switching event simultaneously moves all inlet and outlet ports across their respective downstream columns. The figure’s arrows indicate how the port-switching and the liquid-flow directions are concurrent, and thus simulate countercurrent sorbent flow.

A number of modifications to the classical SMB operation mode shown by the above figure have been proposed. These modifications include the use of multiple columns per zone, intermittent feeding, internal reflux (a.k.a. ‘side-stream’) connections, fraction recycling, temperature variation between zones, asynchronous port-switching, and periodic modulation of the feed concentration [18,20–29].

One particularly successful modification to traditional SMB operation modes is the so-called stepwise-elution SMB (SE-SMB), which has also been termed ‘solvent-gradient SMB’. SMB has traditionally been operated isocratically, such that the modulator concentration is uniform across all zones of the SMB. However, for application of SMB to IEX or HIC chromatography, it has been shown that the introduction of a ‘solvent gradient’ or ‘modulator step’ (as shown by Figure 1-3) can significantly improve the specific sorbent and desorbent productivity of an SMB [1,30–37]. The modulator step is created by a difference in the modulator concentration of the desorbent and feed inlet streams; as shown by the figure below, this difference in modulator concentration creates a discontinuity in modulator concentration around the feed port.

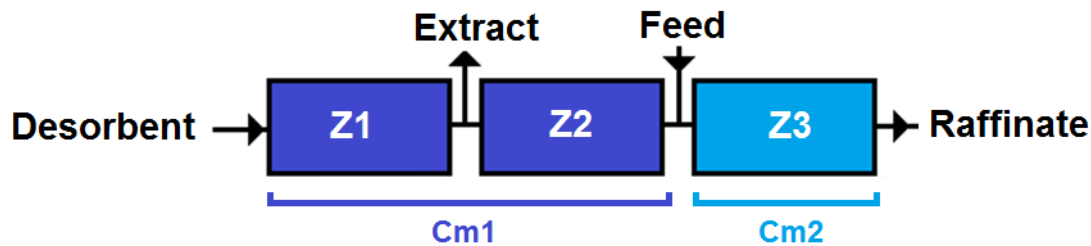


**Figure 1-3 Binary SE-SMB scheme**

A difference in the modulator concentration between the desorbent and feed inlet streams creates two regions of modulator concentration ('Cm1' & 'Cm2') in an example 3-Zone SE-SMB. In the figure, liquid in the zones flows across columns in each zone in the left-to-right direction, and port-switching occurs across columns in the same direction. Note that port-switching re-inserts the previously most-upstream column of Z1 into the final column position of Z3, and thus maintains the number of columns contained within each zone.

Most biotechnological separation challenges involve the separation of an intermediately-retained product from a ternary mixture of flanking more- and less-retained impurities. SMB separation systems have been historically used for a number of binary separation challenges, but they may be easily repurposed for ternary separations by connecting sequential binary SMB separation trains into a so-called SMB 'cascade'. However, there are other methods to achieve centre-cut ternary separations apart from through such a cascade configuration; the following section details a number of these alternative centre-cut SMB methods.

### 1.2.3 Centre-Cut SMB and Hybrid-SMB schemes

A classic SMB cascade performs a ternary separation on three feed components, which are: 1) the product, 2) the weakly-retained impurities ('W' impurities), and 3) the strongly-retained impurities ('S' impurities). In the first separation train of an SMB cascade, one of either the 'S' or 'W' impurities is separated from the product and the other impurity. After this binary separation has been performed, a second binary SMB separation train separated the remaining impurity ('S' or 'W') from the product.

Many design permutations of the classic SMB cascade configuration exist; these include: the use of different inter-train coupling options (i.e. raffinate or extract-coupling), the use of different SMB operation modes or chromatographic sorbents between the separation trains, and the use of reflux streams to enhance the purity and recovery of the centre-cut fraction [31,38–42].

SMB ternary separations have also been designed as ‘integrated’ systems, which involve the use of a single ‘ring’ of inter-connected columns to effect ternary separations [43–51]. These integrated systems can involve the use of internal ‘bypass’ streams to perform sequential binary separations, such as the schematic of an integrated 8-zone SMB shown by Figure 1-4 (bottom), or alternatively separate ternary mixtures without any by-pass streams, as shown for a generic 5-zone integrated SMB by Figure 1-4 (top).

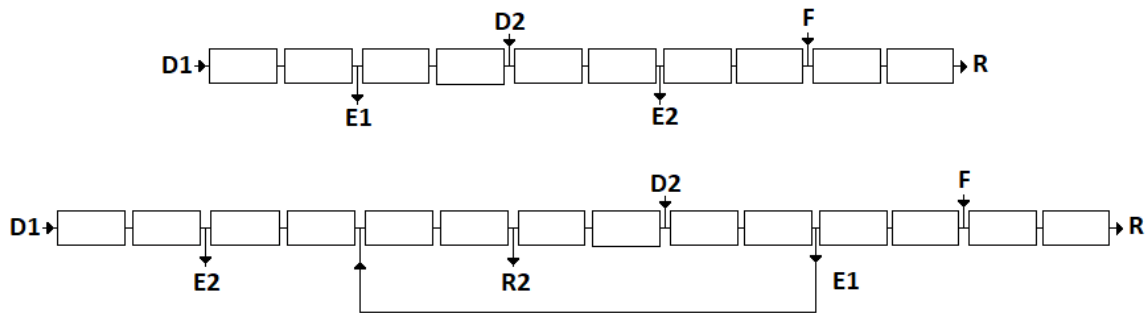


**Figure 1-4 Two examples of isocratic integrated (or ‘single train’) SMB systems**

The ternary mixture input at the feed port (*F*) is collected continuously from three outlet ports in single train systems, which – unlike cascade systems – involve only one ‘ring’ of SMB columns. The first and second desorbent input streams are labelled *D1* and *D2*, and the rectangles represent individual columns in each integrated SMB system. Port-switching progresses left-to-right across columns, and newly-regenerated columns are re-inserted into the SMB train immediately upstream of the raffinate (*R*). **Top)** An ‘Integrated SMB’, where the three feed fractions are continuously collected from the first and second extract ports (*E1* & *E2*) in addition to the Raffinate port (*R*). The intermediate-eluting component exits the system at port *E2*. **Bottom)** Integrated SMB with bypass stream, where the three feed components are collected from the two Raffinate ports (*R* and *R2*) in addition to an extract port (*E2*). The intermediate-eluting component exits the system at port *R2*.

Whilst single-train ternary SMB separations have demonstrated ability to purify centre-cut components to high purity, as SMB systems do not entail the inevitable pollution of the centre-cut fraction that is predicted from TMB models, various additional modifications have been proposed to enhance the chromatographic performance of such systems by intermittent opening and closing of the second extract port. The temporal opening and closing of outlet ports is one method of collecting pure product fractions from an integrated SMB’s internal concentration profile [21,49,52]. Another method of product fractionation is to collect pure fractions directly from a continuous outlet stream – as shown by Figure 1-5, the Modified Four-zone SMB (MF-SMB) family of SMB operation modes employ fractionation schemes to effect ternary separations in single-train configurations[27,38,53,54].

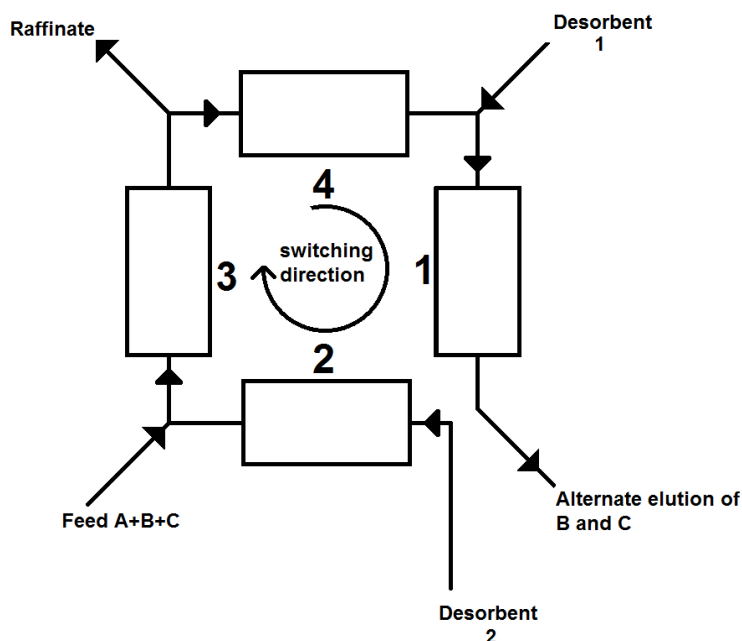


**Figure 1-5 Modified Four-Zone SMB (MF-SMB)**

An integrated SMB configuration for ternary separations where the intermediate-eluting component ('B') of the ternary feed mixture is collected discontinuously (i.e. fractionated) from the outlet of Zone 1. This integrated configuration is but one example from a large number of proposed single-train SMB methods which involve discontinuous collection of product fractions [21,49,52].

The potential for asynchronous valve operation in SMB systems has been further exploited in other configurations of SMB-type systems. The 'Pseudo-SMB', 'Hybrid' SMBs, JO-process, and Intermittent-SMB (I-SMB) are based on a sequence of asynchronous port-switching and fraction collection steps designed for the purpose of single-train centre-cut separations [55–61].

#### 1.2.4 The Multi-Column Solvent Gradient Process (MCSGP)

The Morbidelli group have proposed and demonstrated intensified chromatographic methods which apply linear modulator gradients to single-train ternary separations. These methods may be grouped into the so-called MCSGP 'family' of processes, as they share the common traits of: linear modulator gradients, intermittent product collection, and the use of multiple columns configured for centre-cut separations in a single-train (i.e. non-cascade) formation [10,62]. MCSGP configuration elude simple classification as either SMB-type processes, countercurrent processes, or even continuous processes, because differences in opinion exist as to how these terms should be applied other than to non-traditional SMB processes [10,63].

Though originally conceived as a 6 zone process, variants of MCSGP systems have been proposed which improve upon the original process' productive performance as well as simplify its operational complexity. Of these variants, the two-column MCSGP has received the most promotion and development by the Morbidelli group for its application to polishing chromatography tasks in bioprocessing [10,17,64,65].

The operation scheme of a two-column MCSGP is illustrated below. As shown in part by Figure 1-6, there are two steps in the two-column MCSGP 'cycle'; in the first step, feed is loaded onto one column and then a linear modulator gradient is applied for elution of the feed species – this step is mostly identical to a single-column batch gradient process. As feed species are eluted from this first column, fractions are collected. A pure product fraction is sequestered from the outlet stream, whilst the impure product fractions flanking this pure fraction are loaded (or 'recycled') onto a second column through use of an input dilution stream to promote binding to the sorbent. Fractions which contain impurities and/or very low concentrations of the product are not loaded onto a second column; they are discarded. Subsequently, the first column is washed and re-equilibrated with loading buffer. As this wash step of the first column proceeds, the second column is loaded with some additional 'fresh' feed, and is then subject to elution through a linear modulator gradient. The process of outlet fractionation is repeated for this second column, but impure fractions are loaded onto the re-generated first column. The second column is then washed, whilst the first column is loaded with additional feed. This scheme therefore represents one 'cycle' of the two-column MCSGP process; the cycle of wash-load-elute-fractionate repeats on an offset schedule between the processes' two columns.

### Half-cycle of two-column MCSGP process

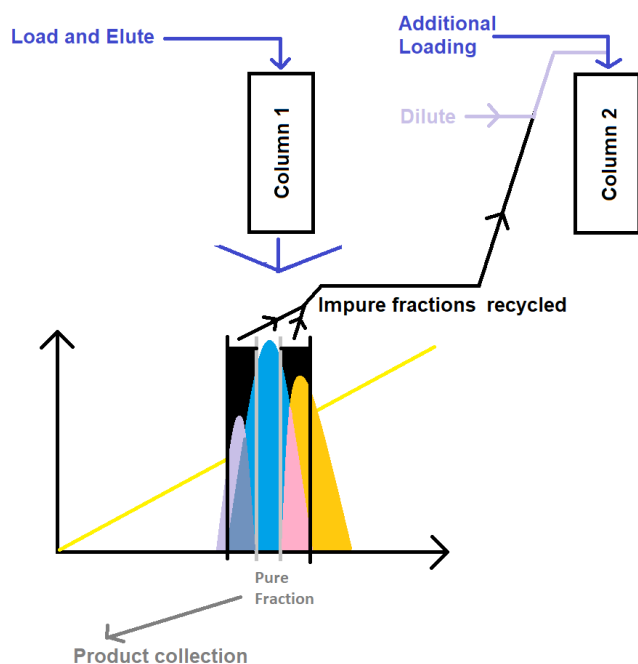


**Figure 1-6 The two-column MCSGP**

*A half cycle of process is shown; a recycle-batch chromatography step is run in one column while the second column acts as a collection vessel for the impure fractions.*

### 1.2.5 Important literature contributions involving non-isocratic, ternary, and proteinaceous SMB separations

There are few examples in the literature of SE-SMB chromatography applied to centre-cut proteinaceous separation problems. However, various investigators have often separately demonstrated: 1) The use of different centre-cut SMB configurations; 2) The use of SE-SMB for separations; and 3) The use of SMB for proteinaceous mixtures. The table below details important literature contributions in each of the three fields of proteinaceous, centre-cut, and stepwise-elution SMB systems. Included are examples of intensified processes, such as MCSGP, which are often considered to be variants of SMB systems.

**Table 1-2** Important literature contributions on the subject of proteinaceous, centre-cut, and stepwise-elution SMBs.

Year	SMB scheme	Isotherm	System	Reference
1996	SMB 8-zone cascade (ternary)	Unknown (no access to original source)	Human Serum Albumin from proteins	[66]
2002	Classic 8-zone SMB Cascade (ternary)	Anti-Langmuir	Insulin from a ZnCl and high-molecular weight proteins	[40]
2002	5-zone SMB (ternary)	Bi-Langmuir	dimethyl phthalate, dibutyl phthalate, and dioctyl phthalate	[23]
2005	5-zone SMB (ternary)	Langmuir	enantiomer (RSR)-nadolol from its racemate(a ternary mixture)	[47]
2007	MCSGP (ternary)	Non-linear	Calcitonin from a multi-component polypeptide mixture	[62]
2007	3-zone SE-SMB (binary)	Linear	Bone Morphogenic Protein (BMP) dimers from BMP monomers and HCP impurities	[67]
2008	MCSGP (ternary)	Langmuir	Three monoclonal antibody variants	[68]
2009	SMB 8-zone cascade (ternary)	Langmuir	nucleotides	[69]
2010	Modified Four-Zone SMB (ternary)	Linear	l-methionine, lphenylalanine, and l-tryptophan	[70]
2011	Pseudo-SMB (ternary)	Linear	dihydrocapsaicin from capsaicinoids	[57]
2011	SMB 4-zone with stepwise-elution (binary)	Linear	Streptokinase from HCP impurities	[37]
2012	SMB 8-zone cascade with stepwise-elution (ternary)	Linear	epigallocatechin gallate from tea polyphenols	[71]
2015	Intermittent-SMB 3-zone cascade (isocratic)	Langmuir	Nandolol from racemic mixture	[60]

### 1.3 Adoption of intensified and continuous processes in industry

The majority of downstream bioprocesses currently involve traditional bind-elute batch-chromatography processes. While these polishing chromatography steps are often run productively through the optimization of such variables as column-loading, flow-rate, modulator-gradient, and buffer-composition, there has yet to be large-scale adoption of any of intensified and continuous processes discussed in the previous section. There are at least two reasons that explain this slow adoption rate.

First, it is unclear which of the many possible intensified and continuous chromatographic configurations and operation modes best suits application to industrial bioprocessing. Whilst theoretical and practical comparisons have been performed, the results of these comparisons are often inconsistent (i.e. the relative performance of processes differs between the comparisons), incompatible (because the studies assess for different objective functions, such as optimizing desorbent utilization instead of sorbent productivity), incomplete (because they omit important process benchmarks, such as recycle-batch processes and SE-SMB cascades, from the comparison), or else of questionable relevance to biotechnology applications (where competitive isotherms, slow mass-transfer kinetics, small separation-factors and modulator-controlled binding are common features) [42,45,69,72,73].

Second, there are manufacturing considerations which prevent the fast adoption of any intensified process even once a candidate process has been selected. A significant aspect of these considerations is the need to engineer 'robustness' of a process to minor and major process variances or 'faults'. There are two approaches to the engineering of robustness for many industrial processes. On the one hand, robustness to small-scale faults and deviations may be accounted for in the design of process operation conditions. For example, if a pump flow-rate is accurate to within 5% of the set-point flow-rate value, chromatographic systems can be designed to operate successfully at all expected pump flow rates within this range of accuracy. On the other hand, processes can encounter certain major faults – or very severe variations in control variables – which are either impossible to overcome through robust process design, or else require a very significant trade-off between the robust design of a process and its productivity. For this latter class of process faults, significant intervention in the process may be required. For example, if a pump were to fail completely, a chromatographic process would require a control unit, or human operator, to both detect the fault and fix it.

These two facets of ‘robustness’ of intensified chromatographic systems are discussed in the following two subsections.

### **1.3.1 Robust design of isocratic SMB operations**

A popular method of designing robustness in SMB operations is through the use of the ‘Triangle theory’. Triangle theory delineates a triangular operation window in a two-dimensional  $M_2$ - $M_3$  design space. The ‘M’ axes constitute dimensionless ‘flow-rate ratios’ of a TMB’s separation zones (Z2&Z3); this ratio represents the volumetric ratio between the liquid and solid flow-rates in a hypothetical TMB. A triangular operation space in this flow-rate ratio space is framed by the standard TMB design equations, which are functions of the partition coefficients for the more and less retained species in a binary separation (‘Ka’ and ‘Kb’ in Figure 1-7)[74–76]. ‘Triangle theory’ provides a reliable framework within which isocratic TMB separations of species with low mass-transfer resistance may be designed [75,77]. It is possible to convert a set of operating conditions (designed for an isocratic TMB separation) into a corresponding set of operating conditions for an isocratic SMB separation through the use of well-established transfer functions [2].

Triangle theory permits the design of productive and robust isocratic conditions. By running the system at the vertex of the triangular operation window, at point ‘P’ in Figure 1-7, the feed flow-rate is maximised, because the difference between the Z2 and Z3 flow-rates is largest. For robust operation of an SMB process, an operation point chosen at a ‘safety margin’ distance away from the edges of the operation window (e.g. point ‘R’ in the figure) permits a degree of process resilience to pump flow-rate variation.

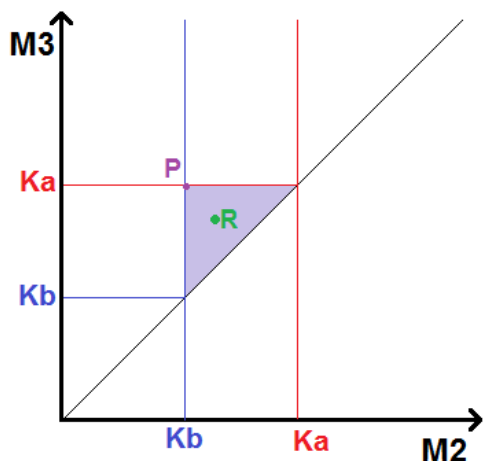


**Figure 1-7 Triangle theory for the design isocratic binary separations**

*The most productive operation point, 'P', is at the edge of the design space, whilst the robust point, 'R', is not. The axes 'M2' and 'M3' represent the liquid–solid flow-rate ratios of the TMB zones adjacent to the feed port (Z2&Z3).*

Triangle theory has been developed to describe the design space for separation problems of both slow and fast mass-transfer, as well as linear and non-linear isotherm behaviour [76,78]. Design of processes robust to the failure-modes of column fouling (which affect mass-transfer resistance) and feed composition changes (which modulate binding behaviour as described by non-linear isotherm) may be achieved in an identical 'safety-margin' manner to that used to design TMB processes for robustness against flow-rate variation.

Whilst the design space of so-called 'solvent gradient-TMB' systems has previously been delineated within the framework of Triangle theory, the modulator-dynamics of SE-SMB systems differ significantly from gradient-TMB systems [79]. Therefore, the successful design of robust and productive SE-SMB systems through a gradient-TMB model can be unreliable [1].

### 1.3.2 Control engineering of intensified processes

A number of approaches to control of isocratic SMB and other intensified chromatographic processes have been proposed and demonstrated. These approaches include the use of PID controllers, feed-forward neural networks, and Model Predictive Control strategies [64,65,80–83].

A common feature of the existing control engineering approaches to SMB systems is the use of on-line or at-line analytical tools for the assessment of the purities of outlet streams. One tool used for monitoring SMB processes is rapid High Performance Liquid Chromatography (HPLC) analysis of outlet samples. Unfortunately, HPLC does not allow for very rapid analysis of the samples

(i.e. the time-frame is in the order of minutes and not seconds). Other, faster, process-monitoring tools include the use of curve-fitting, by computational models, of the SMB outlet concentration profiles. This method relies on the provision of accurate model parameters, but can perform analytical tasks rapidly if not completely reliably. Alternatively, for certain simple separation problems such as the binary separation of nucleosides, online monitoring of SMB outlet streams is possible through spectroscopic measurements at different wavelengths. Unfortunately, a number of spectroscopic methods require some fundamental development before their reliable application as Process Analytic Technologies (PAT) in complex bio-chromatographic separation problems [84].

While these control systems have generally proved successful at maintaining product purity in SMB operations over long periods of time, including in instances of process faults, the root cause of any changes in product purity detected by these control systems is often left undiagnosed. The diagnosis of faults in SMB systems is very challenging due to the fact that there are many different possible faults – and combinations of faults - which can compromise the purity of either (or both) of the extract and raffinate outlet streams [85]. For example, both ligand loss and column fouling can result in raffinate pollution. A method for quickly identifying the root cause of any deviation in SMB performance – without necessitating process interruption – has yet to be made public.

## **1.4 Aims and Organization of Thesis**

The purpose of the preceding literature review was to provide the context for the contemporary industrial interest in continuous and intensified processes. The potential of such processes to improve the performance of chromatography unit operations with respect to separation-resolution, sorbent-specific productivity, and desorbent utilization was noted. Furthermore, the attractiveness of end-to-end continuous bioprocessing – in particular for the bioprocessing challenges in cases of fragile (low-stability) products and low-producer cell lines – was detailed. Various approaches to intensified chromatographic operations were introduced, and key concerns regarding the industrial feasibility of candidate intensified chromatographic processes were reviewed.

The aim of this thesis is to address two significant concerns which deter industrial adoption of SE-SMB chromatography (an intensified and continuous bioseparation process):

First, the design of SE-SMB processes is a much more complex and challenging task than that for the design of traditional single-column batch processes. This design challenge is composed

of the related problems of both defining an efficient and appropriate configuration of an SE-SMB system for bioseparations, and then mapping a design space which facilitates the design of robust and productive chromatographic bioseparations.

Second, the issue of process robustness is of prominent industrial concern, and is a subject of investigation in this thesis. Whilst some process variation may be accounted for in the initial robust design of an SE-SMB process, there remain a number of possible process perturbations for which robust operation design may struggle to safely accommodate. In these cases of significant process variations, additional monitoring and control strategies are required to maintain process performance. Therefore, a second aim of the work presented by this thesis is to propose a set of process monitoring strategies which may aid future efforts in the control engineering of SE-SMB systems.

The organization of this thesis is as follows:

**Chapter 1** provides an introduction to the use of chromatography in bioprocessing, and details some of the challenges facing the adoption of intensified and continuous bioprocesses.

**Chapter 2** details the Materials and Methods used in this thesis.

**Chapter 3**, the first Results chapter, theoretically analyses the modulator dynamics of SE-SMB systems. Consequently, the design of robust and productive binary SE-SMB systems is shown to be possible through a newly-proposed set of design constraints and a new graphical design space.

**Chapter 4**, the second Results chapter, extends the theoretical insights of the first chapter to analyze the construction of optimal ternary SE-SMB systems under the conditions of modulator dynamics, non-linear isotherms, and challenging separation problems. Experimental demonstration of challenging purification tasks by SE-SMB processes is documented, and various processes are compared through computational investigation.

**Chapter 5**, the third Results chapter, investigates how faults in SE-SMB systems may be rapidly identified by human and automated operators. A number of common SE-SMB failure modes are analysed experimentally and computationally, and the results of this analysis inform the development of an initial set of 'rules' which enable fault identification.

**Chapter 6** concludes this thesis with an overview of its findings.



# CHAPTER 2 MATERIALS AND METHODS WITH THEORETICAL CONSIDERATIONS

## 2.1 Computational Methods

### 2.1.1 Modelling of Ideal and Real SMB chromatography

Two computational models were used in SMB simulations: the first model was a solid-phase linear driving force (LDF) lumped mass-transfer model, and the second model was a liquid-phase LDF lumped mass-transfer model.

The equations of the solid-phase LDF lumped mass-transfer model are shown by the following Partial Differential Equations (PDEs).

$$\frac{\partial c_{i,j,x}}{\partial t} = D_i \frac{\partial^2 c_{i,j,x}}{\partial z^2} - \left( \frac{Q_j}{\varepsilon_{T,i} A_c} \right) \cdot \frac{\partial c_{i,j,x}}{\partial z} - \left( \frac{1-\varepsilon_{T,i}}{\varepsilon_{T,i}} \right) \frac{\partial q_{i,j,x}}{\partial t} \quad (1)$$

$$\frac{\partial q_{i,j,x}}{\partial t} = k_{m,i} \cdot (q_{i,j,x}^* - q_{i,j,x}) \quad (2)$$

Where  $k_{m,i}$  is the solid-phase LDF mass-transfer rate coefficient. The equations which describe the liquid-phase mass-transfer model (where the mass-transfer rate coefficient is denoted  $k_{f,i}$ ) are the following:

$$\frac{\partial c_{i,j,x}}{\partial t} = D_i \frac{\partial^2 c_{i,j,x}}{\partial z^2} - \left( \frac{Q_j}{\varepsilon_{T,i} A_c} \right) \cdot \frac{\partial c_{i,j,x}}{\partial z} - \left( \frac{1-\varepsilon_e}{\varepsilon_e} \right) \frac{\partial c_{i,j,x}^p}{\partial t} \quad (3)$$

$$\frac{\partial c_{i,j,x}^p}{\partial t} = \frac{k_{f,i} \alpha}{\varepsilon_{p,i} + (1-\varepsilon_{p,i}) K_{0,i} e^{-S_i C_{M,j,x}}} (C_{i,j,x} - c_{i,j,x}^p) \quad (4)$$

Where  $c_{i,j,x}$  and  $c_{i,j,x}^p$  denote the solute concentration of species 'i' in the bulk liquid and in the particle pores respectively. The particle porosity is denoted by  $\varepsilon_{p,i}$ , the total sorbent porosity available to a feed species is represented by  $\varepsilon_{T,i}$ , the interstitial void fraction is represented by  $\varepsilon_e$ , and  $\alpha$  accounts for the external surface area of the particles per unit volume ( $\alpha=6/d_p$ ). Subscript 'j' represents the zone in which a column is located (j=1,2,3), and subscript 'x' refers to the node number (x=1:n) along the axial distance ('z') of a column.

These two models of chromatography are commonly used to describe the spatio-temporal concentration dynamics of a feed species in a chromatography column; examples of the application of these models may be found in the following references [2,86,87]. The solution of these models

was found through numeric methods. One-dimensional finite-volume discretization of the convective terms ( $\frac{\partial c_{i,j,x}}{\partial z}$ ) was performed using a first-order upwind-differencing method as described in the following reference [88]. A first-order central-differencing method was used for finite-volume discretization of the axial dispersion term ( $D_i \frac{\partial^2 c_{i,j,x}}{\partial z^2}$ ) [88]. Matlab's ode15s solver was then used to find numerical solutions to the system of ordinary differential equations. The number of nodes per column varied between the simulations; this information is detailed for each simulation in the relevant results tables.

To build an SMB simulator, a set of Differential Algebraic Equations (DAE) were constructed. Since the discretized PDEs listed above describe the concentration profile in a single SMB column, the set of columns used in SMB required simultaneous solution of a set of PDEs. These 'sets' of PDEs were linked by algebraic equations that relate the outlet concentration of one column to the inlet concentration of the following column, or else used algebraic equations to account for the feed input at the junction between Zones 2 and 3.

The mass balances for the liquid phase in a three-zone SMB system are listed below.

$$Q_1 = Q_D \quad (5)$$

$$Q_2 = Q_D - Q_E \quad (6)$$

$$Q_3 = Q_2 + Q_F \quad (7)$$

The boundary conditions at the feed point (inlet to first column of Z3) were as follows:

$$c_{i,3,1} = \frac{Q_F}{Q_3} \cdot F_i + \frac{Q_2}{Q_3} \cdot C_{i,2,n} \quad (8)$$

$$c_{M,3,1} = \frac{Q_F}{Q_3} \cdot C_F + \frac{Q_2}{Q_3} \cdot C_{M,2,n} \quad (9)$$

The boundary conditions at the desorbent point (inlet of first column in Z1) were as follows:

$$c_{i,1,1} = 0 \quad (10)$$

$$c_{M,1,1} = C_D \quad (11)$$

The modulator was treated as an un-retained component. In real SE-SMB models, its concentration profile is dynamic and thus subject to description by a DAE equation. However, for the

ideal SE-SMB model, the modulator concentration was set as a fixed parameter in each zone. The theory underlying the difference between these two models is presented in detail by the first results chapters.

Port-switching in the computational model was simulated by solving the DAE for each switching period, and then shifting the final concentration profile by one column's distance in the feed flow's direction around the SMB, such that this shifted concentration profile constituted the initial conditions for the DAE solver for the following port-switching period. This is a common method used to model SMB dynamics; examples of its use can be found in the following references [32,34].

Initial conditions were as follows for the first switching interval:

$$t = 0: c_{i,j,x} = q_{i,j,x} = 10^{-5}; c_{C_M,j,x} = C_D; q_{C_M,j,x} = 0 \quad (12)$$

The relative and absolute tolerances of the ODE solver were both set to 1e-9.

In simulations which modelled chromatographic behaviour through use of the linear isotherm, the relationship between the equilibrium concentration of a species in the solid phase ( $q_{i,j,x}^*$ ) and the modulator concentration ( $C_M$ ) was described for proteinaceous ion-exchange chromatography by the following formulation:

$$q_{i,j,x}^* = c_{i,j,x} \cdot K_{0,i} e^{-S_i \cdot C_{M,j,x}} \quad (13)$$

This relation of an exponential dependency between protein binding and modulator concentration was first proposed in the following reference for linear and non-linear isotherms [89]. Simulations that investigated chromatography operated under high feed-loading conditions - the body of work in this thesis' second Results chapter - were described by a competitive langmuirian isotherms where binding was also exponentially sensitive to modulator concentration. The isotherm equations models used for the ternary non-linear model systems were as follows:

$$q_{i,j,x}^* = \frac{c_{i,j,x} \cdot \lambda_i \cdot K_{0,i} e^{-S_i \cdot C_{M,j,x}}}{1 + c_{a,j,x} \cdot K_{0,a} e^{-S_a \cdot C_{M,j,x}} + c_{b,j,x} \cdot K_{0,b} e^{-S_b \cdot C_{M,j,x}} + c_{c,j,x} \cdot K_{0,c} e^{-S_c \cdot C_{M,j,x}}} \quad (14)$$

The parameters used in the binary and ternary non-linear isotherm SMB simulations are listed in Table 2-1.

**Table 2-1 Model Parameters for Competitive Langmuirian Isotherm Simulations**

Model parameter	Value
$\lambda_a$	50
$\lambda_b$	50
$\lambda_c$ (only used in ternary simulations)	50
$K_{0,a}$	3.92
$K_{0,b}$	2.8
$K_{0,c}$ (only used in ternary simulations)	2
$S_a$	14
$S_b$	17
$S_c$ (only used in ternary simulations)	20
$\varepsilon_{T,i}$	0.5
$\varepsilon_{T,Cm}$	0.5
Column dimensions (cm)	2.5 x 1.4(i.d.)
Maximum liquid flow-rate across column (mLmin <sup>-1</sup> )	10
SMB cascade's second-train column dimensions (cm)	2.5 x 3(i.d.)
SMB cascade's second-train maximum liquid flow-rate across column (mLmin <sup>-1</sup> )	20
SMB column configuration (binary separation experiments for asymmetric productivity)*	1;2-2
SMB column configuration (ternary SAW)	1-3-2-2
SMB column configuration (ternary T1)*	1;3-3
SMB column configuration (ternary T2)*	1;2-3
Maximum liquid flow-rate of feed (mLmin <sup>-1</sup> )	10
Ternary mixture feed composition ('Weak' Contaminant :Product: 'Strong' Contaminant)	0.333:0.666:0.333
Solid-phase mass transfer co-efficient, min <sup>-1</sup>	20
*use of detached Z1, see Results Chapter 2 or [46]	

Additional details of simulation parameters used in computational experiments, such as column configurations, modulator concentrations, isotherm and void-fraction parameters, feed concentrations, and liquid flow rates, are displayed within the relevant Results sections.

A set of simulations were carried out to validate the experimentally-obtained results in the first Results' chapter. These simulations used experimentally determined isotherm parameters, as well as estimates of the axial dispersion and liquid-phase mass-transfer coefficients. These estimates of parameters were found by using standard correlations: the Chung and Wen correlation was used to find the lumped axial diffusion term, the Wilson-Geankopolis correlation was used to find the external-film mass transfer coefficients, and the Young correlation was used to find the diffusivity of the proteins [90–92]. Table 2-2 details the parameters used for this set of simulations.

**Table 2-2** Properties of model system used in laboratory SMB experiments

Parameter	Parameter value
$k'_{a,0}$ (lysozyme)	1.75e4
$S_a$ (lysozyme)	14.2
$\varepsilon_{T,a}$ (total void fraction available to lysozyme)	0.54
Lysozyme diffusivity, $\text{cm}^2\text{s}^{-1}$	1.03e-6
Tortuosity factor for lysozyme on SP FF resin according to [93]	1.8
Pore diffusion of lysozyme, $\text{cm}^2\text{s}^{-1}$	9.77e-8
$k_{f,a}$ (lumped mass transfer rate of lysozyme), $\text{s}^{-1}$	6e-3
$D_a$ (axial dispersion coefficient of lysozyme), $\text{cm}^2\text{min}^{-1}$	0.171
$k'_{b,0}$ ( $\beta$ -Lactoglobulin)	8e4
$S_b$ ( $\beta$ -Lactoglobulin)	22.6
$\varepsilon_{T,b}$ (total void fraction available to $\beta$ -Lactoglobulin)	0.52
$\beta$ -Lactoglobulin diffusivity, $\text{cm}^2\text{s}^{-1}$	7.52e-7
Tortuosity factor (conservative estimate for $\beta$ -Lactoglobulin)	5
Pore diffusion of $\beta$ -Lactoglobulin, $\text{cm}^2\text{s}^{-1}$	2.13e-8
$k_{f,b}$ (lumped mass transfer rate of $\beta$ -Lactoglobulin), $\text{s}^{-1}$	1.3e-3
$D_b$ (axial dispersion coefficient of $\beta$ -Lactoglobulin), $\text{cm}^2\text{min}^{-1}$	0.171
$\varepsilon_{T,C_M}$ (total void fraction available to modulator)	0.86
$V_{lag}$ (lag time for step in salt concentration to reach end of column compared with plug-flow ideal), mL	0.4
Individual column dimensions, cm	2.5 x 0.7 i.d.
$\varepsilon_e$ (interstitial void fraction as found by [94])	0.35
$d_p$ , cm	1e-4
Maximum liquid flow rate across column, $\text{mLmin}^{-1}$	4

### 2.1.2 Modelling of SMB failure modes

For this thesis' third results chapter, failure-modes (included fouling, column degradation, ligand loss, a valve leak, and pump flow-rate variation) were simulated in MATLAB. These were modelled in the following ways:

1) Ligand loss was modelled as a reduction in the binding capacity of a column, which – for the linear isotherm relation described by equation (13) – was simulated as a reduction in the  $K_{0,i}$  parameter. This is a common method to simulate ligand loss; an example of its prior use may be found in the following reference [95].

2) Fouling was modelled by a reduction in the mass-transfer rate coefficient; this method of modelling fouling has been previously described in the following reference [96].

3) Pump variation was modelled as a stable change in flow-rate affecting any of the desorbent, extract or feed pumps. This flow-rate change was simulated to affect all columns downstream of the faulty pump's inlet or outlet port in the SMB column series.

4) A type of column 'degradation' was modelled by a change in the void fraction  $\varepsilon_{T,i}$ ; this affected the phase ratio ( $\phi$ ) of a faulty column.

5) A valve block leak was modelled as a variable outlet flow-rate. Unlike the outflow from the extract pump, which always withdraws liquid from between Z1 and Z2, the point at which the leak withdrew liquid from the SMB column series was static with respect to the valve block's reference frame. Therefore, the position of the leak was cycled between column zones during the course of a simulated process run, as would be the case for an experimental system's valve-block leak. All columns down-stream of the leak were simulated to experience a reduction in flow-rate such that the liquid mass balances of the simulated system remained closed.

The leak flow-rate was thought to vary depending on its zonal position. The experimental failure-mode model of a valve-leak fault provided results which showed that most volumetric outflow from the leak occurs when a leak is positioned in Z1. Therefore, the computational model also simulated a constant leak flow-rate for when the leak is positioned in Z1. This leak flow-rate applied to switching intervals including those in which the leak valve was coincident with the extract port at the junction between Z1 and Z2, but not when it was simulated to lie between the desorbent inlet and the first column of Z1.

Failure modes were simulated to occur in two different SMB pump configurations. The first was a conventional 3 zone SMB system, where the flow-path connection between Z1 and Z2 was orthogonally connected to an extract pump. The second configuration made use of a so-called 'Z2 pump'; this pump takes fluid from the outlet of Z1 and directs it into the inlet of Z2. The difference between the Z1 liquid flow rate and the Z2 liquid flow rate exits the SMB system through an outlet flow path connected to the Z1 column outlet; flow through this 'extract' flow path is not mediated by any pump. The Z2 pump configuration was invented by the Wang group and is detailed in the following reference [97].

For the final results chapter, Table 2-3 provides details of the failure-mode simulations performed. All failure-mode simulations used 40 nodes per column. The choice of simulated parameters was, in some cases, deliberately extreme (e.g. 50% ligand loss from a column) such that trends and patterns in the simulated outlet signals could be identified as well as visually recognized.

**Table 2-3** Simulation parameters used to investigate failure mode signal patterns

	Ligand loss failure experiments (% $K_{0,i}$ reduction)	Column fouling failure (% $k_{m,i}$ reduction)	Column degradation failure (% $\varepsilon_{T,i}$ reduction)	Leak Failure (% flow rate diversion through faulty valve)	Pump variability failure (% pump flow rate change)
<b>Simulated parameters in individual experiments</b>	5%; 10%, 25%; 35%; 50%	10%; 25%; 35%; 50%; 70%	2% ; 5%; 8%; 10%; 13%	10%; 15%; 20%; 25%; 30%	D: $\pm 5$ , $\pm 50\%$ E: $\pm 5$ , $\pm 50\%$ F: $\pm 5$ , $\pm 50\%$
<b>General Simulation parameters</b>	$Q_D$ : 4 mLmin <sup>-1</sup> ; $Q_E$ : 2.5 mLmin <sup>-1</sup> ; $Q_F$ : 1 mLmin <sup>-1</sup> ; Column configuration in 3-Zone SE-SMB: 4-2-2; $C_D$ : 0.53M; $C_F$ : 0.35M; $\varepsilon_{T,a}$ : 0.54; $\varepsilon_{T,b}$ : 0.52; $\varepsilon_{T,C_M}$ : 0.86; $K_a$ : 2.05e4; $S_a$ : 14.2; $K_b$ : 8.67e4; $S_b$ : 22.6; Switching Time: 2.5 minutes; $k_{m,a}$ : 3 min <sup>-1</sup> ; $k_{m,b}$ : 1.5 min <sup>-1</sup> ; $D_{L,a}$ : 0.171 cm <sup>2</sup> min <sup>-1</sup> ; $D_{L,b}$ : 0.171 cm <sup>2</sup> min <sup>-1</sup> ; $D_{L,C_M}$ : 1 cm <sup>2</sup> min <sup>-1</sup>				

### 2.1.3 Multi-Objective Optimization (MOO) methods

Optimization was performed using the multi-objective genetic algorithm from MATLAB's (2015a) optimization application.

The multi-objective optimization was used to find the Pareto front between a simulated SMB process' yield and productivity, which were defined as follows:

$$Productivity = \frac{[Product\ in\ Outlet] \cdot (Outlet\ flow\ rate)}{(Total\ sorbent\ mass)} \quad (15)$$

$$Yield = \frac{[Product\ in\ Outlet] \cdot (Outlet\ flow\ rate)}{[Product\ in\ feed] \cdot (Feed\ flow\ rate)} \quad (16)$$

The 'options structure' used for the genetic-algorithm multi-objective optimization were as follows: 1) The population size was 50, 2) The cross-over fraction was 60% (the default value), 3) The number of generations was 50, 4) The elite count was 3, and 5) The constraint tolerance was 1e-6. The 'elite count' (the number of individuals guaranteed to survive selection into the next generation) was set as a low number in order to prevent premature convergence of the algorithm on local minima [98]. For a number of simulations, the Pareto curve was found only for separations which purified a product in excess of 95% purity. This purity constraint was enforced by modifying the objective function of the SMB model to penalize any individuals which failed the purity criteria at cyclic steady state. In the simulation experiments which aimed to show 'asymmetric productivity' of SMB separations, the final populations of extract- and raffinate-product experiments were combined into an initial population for additional testing – over 15 generations - of the optimality of each port

product's Pareto curve. More details on these asymmetry experiments may be found in the second results chapter. The stopping criteria of the non-linear isotherm SMB simulator was defined by the time needed for the simulator's inlet/outlet mass balance to close to within 5% accuracy, in addition to one further cycle time period of run time.

The following constraints applied to the MOO of binary and ternary SE-SMB separations in the classical 3 zone configuration:

$$1 - \frac{Q_1 \cdot t_s}{V_{a,c_D}} < 0 \quad (17)$$

$$\frac{Q_2 \cdot t_s}{V_{a,c_D}} - 1 < 0 \quad (18)$$

$$\frac{Q_3 \cdot t_s}{V_{a,c_3}} - 1 < 0 \quad (19)$$

$$\Psi - 1 < 0 \quad (20)$$

For the Wang SMB configuration, where the first zone is routinely detached and eluted with a separate buffer [46], the above constraint structure was modified such that only constraints (18-20) were applied.

These constraints were constructed on the basis that the slowest migration velocity possible for a feed species in a non-linear SMB system would be that determined by the linear isotherm SMT equations. The full set of constraints needed for design (and constrained optimization) of non-linear SE-SMB systems have yet to be elucidated, so the above constraints were used to prevent the genetic algorithm's consideration of known infeasible operating conditions, rather than to define a design space of successful operating conditions.

For the first separation train of a ternary SMB cascade, both the product and either one of the 'strong' or 'weak' impurities were classed as 'product' for the purpose of defining a separation's purity, but the productivity and yield were defined only by the actual product (the intermediate-eluting compound).

Ternary SE-SMB cascade separations were optimized through the following approach. First, the first train of a ternary SMB cascade was subject to a MOO such as that described above for binary separations. The optimization function was subject to a constraint such that the objective function would only be returned for simulated separations which purified the product and either the

Strong or Weak contaminant (depending on inter-train coupling configuration) if the purity exceeded 95%. After a Pareto curve was found from this optimization procedure, selected points from across the Pareto curve were used to provide fixed parameters for the second SMB separation train in the cascade. These parameters for the second separation train were 1) Product concentration in the feed from the first separation train, 2) Strong contaminant concentration from the first separation train, 3) Weak contaminant concentration from the first separation train, and 4) Modulator concentration of the outlet stream from the first separation train. Subsequently, a second (manual) optimization was performed to find the productivity-yield Pareto-curve of separations which separated the product to a final purity greater than 95%.

The SAW ternary separation was subject to a genetic algorithm MOO which used the following constraints:

$$\frac{Q_1 \cdot t_s}{V_{a,C_D}} - 1 < 0 \quad (21)$$

$$\frac{Q_2 \cdot t_s}{V_{b,C_D}} - 1 < 0 \quad (22)$$

$$\frac{Q_3 \cdot t_s}{V_{b,C_3}} - 1 < 0 \quad (23)$$

$$\Psi - 1 < 0 \quad (24)$$

Where  $Q_1$  refers to the desorbent flow-rate,  $Q_2$  refers to the Z2 flow rate, and  $Q_3$  refers to the Z3 flow-rate. Similar to the constraint equations (17-20), these equations prevent the genetic algorithm from exploring operating conditions which are obviously infeasible for successful operation under non-linear and linear isotherm conditions.

#### 2.1.4 Modelling of single-column batch and recycle-batch chromatography

A simple bind-elute batch-gradient process simulation was constructed based upon the solid-phase LDF lumped mass-transfer model equations described above. The following degrees of freedom in the process' operation were included in this model: 1) initial salt concentration of salt-gradient, 2) final salt concentration of salt-gradient, 3) gradient length, 4) Column loading (units: g/L). For this batch-process simulation, the modulator was treated in the same un-retained 'third component' manner as in the SE-SMB simulations.

Multi-objective optimisation of the batch chromatography simulator was performed with use of the following objective functions.

$$Productivity = \frac{[Product\ mass\ in\ collected\ fraction]}{(Total\ sorbent\ mass) \cdot (processing\ time)} \quad (25)$$

$$Yield = \frac{(Product\ mass\ in\ collected\ fraction)}{(Product\ mass\ loaded\ on\ column)} \quad (26)$$

Where the following constraints applied to the batch simulations: 1) the final concentration of the salt gradient must be equal to, or greater than, the initial concentration of salt gradient, 2) the salt gradient must span less than 25 column volumes, and 3) the choice of salt concentrations may span the range of 0M to 1M [NaCl].

For both the batch and recycle-batch simulators, product purity was specified as a parameter ( $\geq 95\%$ ). This purity requirement was used to inform fraction collection from the simulated column-outlet concentration profile: only the ‘fractions’ (defined as volume eluted between the individual time-steps taken by the PDE solver), greater or equal to the chosen threshold purity were ‘collected’. These ‘collected’ fractions were then assessed for their sum mass of product, thus allowing yield and productivity of individual processes to be calculated.

For the recycle-batch chromatography experiments, the batch chromatography simulator was adapted in a manner similar to that used by the following reference for their so-called ‘recycle-recycle’ simulator [12]. The input parameters for this simulator were as follows: 1) batch chromatography initial salt concentration of salt-gradient, 2) batch chromatography final salt concentration of salt-gradient, 3) batch chromatography gradient length, 4) batch chromatography column loading (units: g/L), 5) number of batch chromatography runs before the recycle batch method is used to separate the impure fractions, 6) recycle batch chromatography initial salt concentration of salt-gradient, 7) recycle batch chromatography final salt concentration of salt-gradient, 8) recycle batch chromatography gradient length.

The recycle chromatography simulator used the following objective functions:

$$Productivity = \frac{[Product\ mass\ in\ collected\ fractions]}{(Column\ sorbent\ mass) \cdot (processing\ time\ for\ batch\ runs\ and\ recycle\ run)} \quad (27)$$

$$Yield = \frac{(Product\ mass\ in\ batch\ and\ recycle\ batch\ collected\ fractions)}{(Product\ mass\ loaded\ per\ batch\ run) \cdot (Number\ of\ batch\ runs\ before\ recycle\ batch\ step)} \quad (28)$$

## 2.2 Experimental Methods

### 2.2.1 SMB and single-column batch chromatography experiments

All protein ternary model-mixture separations (lysozyme, alpha-chymotrypsinogen and  $\beta$ -Lactoglobulin A&B) used a 25mM solution of citric acid-sodium citrate buffer at pH 3.8. Experiments which separated various hen egg albumin (hereafter termed 'ovalbumin') variants used a 50mM solution of tris buffer, pH 9.0. Sodium chloride was added appropriately to control salt concentration for both tris and citric acid-sodium citrate buffers. All buffer materials were purchased from Sigma-Aldrich UK.

Ovalbumin (9006-59-1), lysozyme (12650-88-3), alpha-chymotrypsinogen (9035-75-0), and  $\beta$ -Lactoglobulin A&B (9045-23-2) were purchased from Sigma Aldrich UK. Purities of certain proteins were assessed by either PAGE or agarose-gel electrophoresis and were estimated by the manufacturer to be as follows: Ovalbumin (>90% agarose gel electrophoresis), lysozyme (>90% PAGE),  $\beta$ -Lactoglobulin A&B (>90% PAGE). For the model ternary mixture separation, the feed solution contained 1mg/ml Lysozyme, 1mg/ml alpha-chymotrypsinogen and 3mg/ml of the  $\beta$ -Lactoglobulins. HiTrap SP FF 1mL (2.5cm x 0.7cm i.d.) cation exchange columns, from G.E., were used for the model mixture separations (with the citric acid-sodium citrate buffer). Note that under acidic buffer conditions (around pH 3.8),  $\beta$ -Lactoglobulin A&B dimerize to produce a feed species that may be treated as one component in CEX chromatography [99]. HiTrap Q HP 1mL (2.5cm x 0.7cm i.d.) anion exchange columns, also from G.E., were used for ovalbumin separations (with the tris buffer).

An Octave SMB device, purchased from Semba Biosciences (Wisconsin, USA), was used in all SMB experiments. To monitor outlet concentration profiles, an Agilent multi-cell spectrometer was used to measure UV280nm absorbance with one flow-cell connected to each of the SE-SMB extract and raffinate ports respectively. Additionally, a spectrometer purchased from Semba was used to measure an outlet's UV280nm absorbance in certain experiments.

Details of experimental conditions used in various experiments, including parameters such as column configuration, desorbent modulator concentration, feed modulator concentration, switching time, feed protein concentrations, and liquid flow rates, are displayed within the relevant results tables.

## 2.2.2 Isotherm determination

Isotherm determination of the three CEX model proteins (lysozyme,  $\beta$ -Lactoglobulin, and  $\alpha$ -chymotrypsinogen) was performed according to the isocratic-elution retention-time method [2]. The retention time of the proteins was measured by the time taken between the elution of the top of the retained peak ( $t_R$ ) and the elution time of an unretained peak ( $t_0$ ). Loading was performed through emptying the contents of a 100 $\mu$ L sample loop (containing approximately 1mg of protein) on to a 4ml HiTrap SPFF column (10 x 0.7cm i.d.) at a flow-rate of 2mLmin<sup>-1</sup>. An AKTA PURE system from G.E. was used in all isotherm determination experiments. Equilibration, loading and elution of the column were conducted at a constant modulator concentration for each isocratic elution experiment.

The total void fraction available to protein species ( $\varepsilon_{T,i}$ ) was found by measuring the elution time of the species under un-retained conditions ( $t_0$ ). This was achieved by isocratic elution at 1M NaCl; this method has been used previously in other isotherm-determination studies [34].

The isotherm coefficients were determined with use of the following equations:

$$k'_i = \frac{t_R - t_0}{t_0} \quad (29)$$

$$k'_i = \varphi \cdot K_i \quad (30)$$

Where:

$$\varphi = \left( \frac{1 - \varepsilon_{T,i}}{\varepsilon_{T,i}} \right) \quad (31)$$

After a set of data for  $K_i$  values obtained at various isocratic modulator concentrations was collected, Matlab's curve-fitting application was used for the fitting of the following relation between modulator concentration ( $C_M$ ) and  $K_i$  [89].

$$K_i = K_{0,i} \cdot e^{S_i \cdot C_M} \quad (32)$$

Parameter estimation of both  $V_{lag}$  (defined as the elution volume between 50% and 100% conductivity breakthrough for a modulator step to reach the end of one SMB column), and the total void fraction available to both the modulator ( $\varepsilon_{T,C_M}$ ), was conducted with a 10ml (25cm by 0.7cm

i.d.) HiTrap SPFF column at a flow rate of  $2\text{mLmin}^{-1}$ . A modulator step between 0 to 1M NaCl was used for estimation of  $V_{lag}$ .

### 2.2.3 Construction of failure-mode experimental models

Three experimental SMB failure modes models were constructed for laboratory investigation of SMB failure modes.

First, a model of column fouling was made by subjecting a single 1mL HiTrap SPFF column to washing with a cyanobacterial extract. About 3 column volumes of the extract were washed through the column, which was subsequently washed with buffer and 20% ethanol solution. The column was visibly fouled by this procedure, as the sorbent retained the blue-green colour of the cyanobacterial extract.

The cyanobacterial extract was made by mixing a 1g dried sample of cyanobacteria (*Spirulina platensis*) with 500mL water, and then subjecting the mixture to 4 cycles of freeze-thawing. After filtration to remove solids with a stericup ( $20\mu\text{m}$  pore-size), proteins in 100mL of the filtrate were precipitated with 50% w/v ammonium sulphate. The supernatant was then decanted, and the precipitate was re-suspended in citric acid-sodium citrate buffer for subsequent de-salting through use of a dialysis membrane in 10L de-ionized water. This phycocyanin extraction and purification procedure was very similar to that used in the following reference [100].

The second experimental model of an SMB failure modes constructed was that of a valve leak. In this experimental failure mode, an SMB operation was programmed to keep a single valve open throughout the SMB run. This valve, which was orthogonally connected to the flow path between the fifth and sixth SMB columns, was connected to an outlet flow path capped by a 40psi back-pressure regulator. The motivation of applying a back pressure regulator to this valve-leak model system was to more closely mimic small, low flow-rate leaks instead of the kind of high flow-rate leaks caused by completely open valves. In industrial SMB operation, it is thought that small scale leaks from partially-stuck valves are more likely to occur, harder to detect, and thus more threatening to a process than valves which aberrantly stay open.

The third experimental model of an SMB column failure constructed was that of 'material loss' from a column, which also may be termed 'column degradation'. This failure mode was modelled by emptying a column of roughly half of its sorbent; this was done mechanically through use of a syringe and needle.

#### 2.2.4 Analytical chromatography methods for purity assessment

The AKTA PURE system from G.E. was used to analyze the outlet purities from the SMB model mixture separations. A 2ml SP HP column (5 x 0.7cm i.d.) was used. The column was equilibrated at 375mM NaCl, 0.5ml of an SMB outlet sample was loaded onto the column, and then a gradient was applied from 375 to 700mM NaCl over 8 column volumes. This was done separately for each of the raffinate, extract 1 and extract 2 outlet streams.

For certain poor-quality separations in the first Result's chapter, an additional purity-assessment method was employed to support the results of the analytical batch-chromatography method detailed above. Some SMB experiments were subject to linear-isotherm conditions (i.e. <5mg/mL loading), thus it was possible to investigate the behaviour of single feed components in the SMB by performing single-component runs. To assess purity, the partitioning of individual feed species between the different outlet ports was found by comparing the absorbance of collected outlet samples once cyclic steady state had been reached.

HPLC with a bia monolith (BIA Separations, Mirce 21, 5270 Ajdovscina Slovenia) for anion exchange (CIMac™ QA analytical column) was used to analyze the Ovalbumin variant samples. A linear modulator gradient between 0mM and 300mM over 35 minutes at a flow-rate of 0.5ml/min was used. Dilution of the wash outlet stream (dilution factor 1:2) was performed with tris buffer (0mM NaCl) so as to ensure retention on the column during feed-loading. 100 microliters of sample (post-dilution) were loaded onto the monolith column. An Agilent 1100 HPLC (Santa Clara, CA 95051, United States) was used for all experiments with the monolith column.

The analytical chromatograms generated from the monolith and SP-HP column experiments were normalised to control for dilution and outlet flow-rates. Normalising chromatograms with respect to the SMB outlet flow-rates involved scaling the amplitude of each of the chromatogram (e.g. extract, wash, raffinate) with a fraction consisting of the relevant outlet port's flow-rate divided by the fastest outlet flow-rate (the raffinate); this permitted accurate comparison between the chromatograms because it represents mass-outflow from each port rather than outlet concentration.

## 2.3 Analytical Methods

### 2.3.1 Failure-mode signal-analysis methods

As detailed by the theory section of the final Results chapter, SMB outlet concentration patterns may be analysed through defined features of outlet signals produced either during a switching time, or signals produced during a complete SMB cycle. These features are termed ‘column-signal’ and ‘cycle-signal’ features, respectively, and Table 2-4 lists the signal features analysed. Certain features were normalized with respect to a baseline (no-failure) value, for example: the extract peak area of a failure mode’s column signal was converted to a fraction of the baseline column-signal extract peak’s area.

Conditional formatting (‘heat maps’) in Microsoft Excel was used to look for unique features, and unique combinations of features, within the data produced by failure mode simulations. Data describing cycle- and column-signal features for each simulated failure-mode signal was exported from Matlab 2015 in to an Excel spreadsheet for heat map analysis. Additionally, experimental results were observed for unique features of different failure modes; this method also aided the construction of fault-classification decision trees.

A set of Matlab scripts were programmed to classify failure modes based upon cycle-signal and column-signal data generated by the simulations. These scripts were also used to investigate the parsimony and accuracy of proposed decision trees.

Table 2-4 Signal Feature Analysis

Feature Number, (Code)	Feature Description	Cycle/ column signal?	Normalized w.r.t Baseline signal? (Y/N)
Feature 1 (F1)	Intra-minima raffinate signal gradient (concentration change per port-switching period)	Column	N
Feature 2 (F2)	Intra-minima extract signal gradient (concentration change per port-switching period)	Column	N
Feature 3 (F3)	Inter-maxima raffinate signal gradient (concentration change per port-switching period) (w.r.t. preceding column signal)	Column	N
Feature 4 (F4)	Inter- maxima extract signal gradient (concentration change per port-switching period) (w.r.t. preceding column signal)	Column	N
Feature 5 (F5)	Raffinate signal area (mg·ts/ml)	Column	Y

Feature 6 (F6)	Extract signal area(mg-ts/ml)	Column	Y
Feature 7 (F7)	Raffinate peak retention time (% of switch time)	Column	Y
Feature 8 (F8)	Extract peak retention time (% of switch time)	Column	Y
Feature 9 (F9)	Raffinate band broadening at 90% of peak height	Column	Y
Feature 10 (F10)	Extract band broadening at 90% of peak height	Column	Y
Feature 11 (F11)	Raffinate Peak maximum's amplitude	Column	Y
Feature 12 (F12)	Extract Peak maximum's amplitude	Column	Y
Feature 13 (F13)	Raffinate post-peak minimum's amplitude	Column	Y
Feature 14 (F14)	Extract post-peak minimum's amplitude	Column	Y
Feature 15 (F15)	Raffinate MP duration (% of switch time)	Column	Y
Feature 16 (F16)	Raffinate conductivity post MP-pulse (% of post MP modulator concentration)	Cycle& Column	Y
Feature 17 (F17)	Max extract signal peak co-incident with min-raffinate signal peak, or within range of one switching period.	Cycle	N.A.
Feature 18 (F18)	Max extract signal peak co-incident with max-raffinate signal peak	Cycle	N.A.
Feature 19 (F19)	Some/all column-signal extract minima below baseline extract column-signal minima	Cycle	N.A.
Feature 20 (F20)	Change in sum of raffinate and extract mass outflow w.r.t baseline	Cycle	Y
Feature 21 (F21)	Reduction in extract mass-flow rate w.r.t baseline	Cycle	Y
Feature 22 (F22)	Extract post-peak minima amplitude	Cycle	Y
Feature 23 (F23)	Raffinate MP duration consistent?	Cycle	N.A.
Feature 24 (F24)	Cyclic patterning of outlet feed-species chromatograms?	Cycle	N.A.

# CHAPTER 3 ROBUST AND PRODUCTIVE DESIGN OF STEPWISE-ELUTION SMB BINARY SEPARATIONS

## 3.1 Introduction

### 3.1.1 Design of isocratic SMB systems

Since the original conception of SMB chromatography, a number of process-design methods have been proposed. Particularly well-known examples of these design methods include Standing Wave Analysis (SWA) and Triangle theory [75,87]. Both SWA and Triangle theory have been successfully used to design SMB processes under linear-isotherm and isocratic conditions with either low or high mass-transfer resistances [76,87]. Furthermore, SWA has been adapted for design of SMB systems under non-linear isotherm conditions [101]. By contrast, Triangle theory has been extended to facilitate design of non-linear isotherm TMB systems [77].

Underlying all existing SMB design methods are a set of common design constraints. These design constraints may be derived by various means, one of which is through a ‘standing wave’ concept of SMB operation. In this understanding, the net velocity of a feed species in an SMB zone is determined by the difference between the feed species’ velocity and the port-switching velocity ( $v_{ps}$ ). The port-switching velocity, a function of the length of a column ( $L$ ) and the port-switching frequency ( $\omega$ ), is given by the following expression:

$$v_{ps} = \omega \cdot L \quad (1)$$

Where the port-switching frequency is defined:

$$\omega = \frac{1}{t_s} \quad (2)$$

On the other hand, the zonal velocity of a feed species ( $v_{i,j}$ , for the ‘i’-th feed species in the ‘j’-th zone) is defined by Solute Movement Theory (SMT) as a function of the zonal liquid flow-rate ( $Q_j$ ), the  $k'_i$  value of the feed species, and the total void fraction of the column available to the feed species ( $\varepsilon_{T,i}$ ) [102]. This SMT expression is written as follows for species subject to linear isotherm conditions:

$$v_{i,j} = \frac{Q_j}{\varepsilon_{T,i} A_c (1+k'_i)} \quad (3)$$

In the standing-wave analysis of SMB, a set of isocratic operation conditions – comprising the switching time and the zonal liquid flow rate – exist such that the port-switching velocity and the feed species' velocity are equal within a zone:

$$v_{i,j} = v_{ps} \quad (4)$$

Under operation conditions where the above equality holds, and under linear-isotherm conditions, a feed species in an SMB zone will remain 'trapped'; it will neither elute from the zone into the raffinate nor extract no matter how many port switches occur, and is therefore said to constitute a 'standing wave'. Since the purpose of SMB separations is to elute different feed components from separate outlet ports, the design constraints for each of the SMB operation zones are written as a set of inequalities which prevent standing waves from occurring. These standard design constraints ensure feed species are eluted from either the extract or the raffinate, and are listed below:

$$v_{a,1} > v_{ps} \quad (5)$$

$$v_{b,2} > v_{ps} > v_{a,2} \quad (6)$$

$$v_{b,3} > v_{ps} > v_{a,3} \quad (7)$$

$$v_{b,4} < v_{ps} \quad (8)$$

Where subscript 'a' refers to the More-Retained Component (MRC), which should be purified in the extract outlet, and subscript 'b' refers to the Less Retained Component (LRC), which should be purified in the raffinate outlet. As illustrated by Figure 3-1, the above design inequalities ensure that:

- 1) The MRC and LRC move faster than the port-switching velocity in Z1, and thus the sorbent in Z1 is regenerated.
- 2) The MRC in Z2 moves more slowly than the port switching velocity, and thus migrates to the extract port over time. By contrast, the LRC moves faster than the port switching velocity in Z2, and therefore should not contaminate the extract port.
- 3) The MRC in Z3 moves more slowly than the port switching velocity, and thus migrates to the extract port (away from the raffinate port) over time. By contrast, the LRC moves faster than the port switching velocity in Z2, and therefore is collected by the raffinate outlet stream.

- 4) The MRC and LRC move more slowly than the port-switching velocity in Z4, and thus the desorbent in Z4 is regenerated.

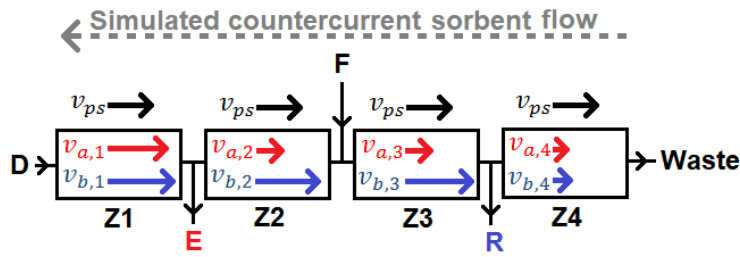


**Figure 3-1 Standing Waves in SMB separation**

Differences between port-switching ( $v_{ps}$ ) and species' velocities ( $v_{i,j}$ ) in SE-SMB zones (Z1, Z2, Z3, Z4) facilitate continuous binary separation and sorbent regeneration. The 'Waste' outlet can be connected to the desorbent inlet in order to recycle some of the system's mobile phase. Letters F, D, E, and R refer to the Feed, Desorbent, Extract and Raffinate ports respectively. Arrow length represents migration velocity of feed species and ports. Figure adapted from [1] with permission.

### 3.1.2 Design of non-isocratic countercurrent systems

Apart from the design method proposed by the author in the following reference [1], there are two methods for design of step-gradient countercurrent chromatography systems. One of these methods is an adaptation of Triangle Theory, and the other method is named 'Separation Volume Design' [103–105]. Triangle theory is based upon a TMB model of SE-SMB system, whilst Separation Volume Design is based upon non-generalizable (i.e. separation-specific) experimental results of single-column batch chromatography studies.

One aspect of SE-SMB systems, for which Triangle Theory and Separation Volume Design methods fail to account, are Modulator Perturbations (MPs). MPs are periodically generated variations in the Zone 3 (Z3) modulator concentration profile, and have been previously noted by a number of investigators [106,107]. MPs may explain instances of disappointing experimental SE-SMB separation results in the literature, which have occurred despite complete fulfilment of solvent-gradient TMB-based design criteria [37].

### 3.1.3 Motivation for Chapter 3

This chapter has the following aims:

- 1) To make the case for a new graphical design space for SE-SMB systems,
- 2) To describe and analyze modulator dynamics in SE-SMB systems,

- 3) To present new design constraints which account for modulator dynamics in experimental SE-SMB systems,
- 4) To demonstrate the new design constraints are experimentally meaningful,
- 5) To demonstrate how robust and productive SE-SMB may be designed in the frame of the new graphical design space bounded by the new design constraints.

This chapter will consider the design of binary SE-SMB separations of linear-isotherm, fast-mass transfer systems subject to a modulator which is un-retained by the sorbent. Analysis of SE-SMB operation at this level is a necessary prelude to the analysis of more complex (and more industrially-relevant) SE-SMB operations; the next chapter will build on the theory and results presented in this chapter to investigate the design of SE-SMB ternary separations under non-linear isotherm conditions.

Some components of this chapter's contents relate to work previously published by the author in the following reference [1].

## **3.2 Theory**

### **3.2.1 A new 3D design space for SE-SMB systems**

Of the three SE-SMB control variables which determine a feed species' migration velocity in an SE-SMB zone, it is often the modulator concentration to which a species' migration velocity is most sensitive. The other SE-SMB control variables, zonal liquid flow-rates and port switching frequency, do not define the design space for productive and robust SE-SMB systems in the exclusive manner that they do for isocratic SMB separations. Therefore, it is arguable that Triangle Theory's flow-rate ratio design space is more suited to design of isocratic SMB systems than for design of SE-SMB systems.

It is suggested that a comprehensive design space for SE-SMB systems should display all possible combinations of switching frequency ( $\omega$ ), zonal liquid flow-rate ( $Q_j$ ) and zonal modulator concentration ( $C_j$ ) choices. Therefore, a three dimensional design space in each of the three SMB zonal control variables has been proposed by the author [1]. The following section defines how this 3D design space may be used to design ideal SE-SMB systems.

### 3.2.2 Design of ideal SE-SMB systems

Ideal SE-SMB systems are defined as systems in which MPs do not occur. Therefore, the modulator concentration profile across ideal SE-SMB systems is consistently identical to that of step-gradient TMB systems. The purpose of this section is to detail how ideal SE-SMB processes may be designed through use of the newly-proposed 3D design space.

SWA-type design constraints apply to both isocratic SMB and ideal SE-SMB systems. However, these design constraints need to be re-written for ideal SE-SMB systems to explicitly account for zonal differences in modulator concentration. The modulator concentration of an SMB zone significantly influences the migration velocity of a feed species; this effect may be modelled by expressing the  $k'_i$  value in the SMT equation as a function of zonal modulator concentration ( $C_j$ ) [89].

$$k'_{i,C_j} = \varphi_i \cdot K_{0,i} \cdot e^{-S_i \cdot C_j} = k'_{i,0} \cdot e^{-S_i \cdot C_j} \quad (9)$$

Thus, the standing wave condition may be derived for SE-SMB zones by including this relation between modulator concentration and protein binding; this is shown below:

$$v_{ps} = v_{i,j} \quad (10)$$

$$\frac{L}{t_s} = \frac{Q_j}{\varepsilon_{T,i} \cdot A_c \cdot (1 + k'_{i,C_j})} \quad (11)$$

$$\omega = \frac{Q_j}{\varepsilon_{T,i} \cdot V \cdot (1 + k'_{i,C_j})} = \frac{Q_j}{V_{i,C_j}} \quad (12)$$

The SWA design inequalities may thus be written for SE-SMB systems as functions of switching frequency, liquid flow-rate and retention volume.

$$\frac{Q_1}{V_{a,C_1}} > \omega \quad (13)$$

$$\frac{Q_2}{V_{b,C_2}} > \omega > \frac{Q_2}{V_{a,C_2}} \quad (14)$$

$$\frac{Q_3}{V_{b,C_3}} > \omega > \frac{Q_3}{V_{a,C_3}} \quad (15)$$

$$\frac{Q_4}{V_{b,C_4}} < \omega \quad (16)$$

In SE-SMB systems, the modulator concentration is identical between Z1 and Z2, and also between Z3 and Z4. A difference between the desorbent and feed modulator concentrations creates the modulator step at the feed point between Z2 and Z3 [30]. In 'step-down' SE-SMB systems, the modulator concentration of the post-feed port zones (Z3&Z4) is lower than that of the preceding zones. Given that the feed modulator concentration ( $C_F$ ) cannot be less than zero, and that pressure-drop constraints limit the maximum liquid flow-rate through SMB columns, there is a maximum modulator step-size for all 'step-down' SE-SMB systems; this can be found from the solvent mass-balance equation of SE-SMB systems:

$$Q_3 \cdot C_3 = Q_2 \cdot C_D + Q_F \cdot C_F \quad (17)$$

where:

$$Q_F = Q_3 - Q_2 \quad (18)$$

$$C_D > C_F \geq 0 \quad (19)$$

$$Q_{max} \leq Q_2 + Q_F \quad (20)$$

$$Q_F > 0 \quad (21)$$

$$Q_2 > 0 \quad (22)$$

$$Q_3 > 0 \quad (23)$$

Note that for SE-SMB separations in which the modulator concentration is increased downstream of the feed point, a maximum modulator-step size also exists due to the liquid flow-rate constraints and the upper bound of the feed modulator concentration.

In summary, design of ideal SE-SMB systems must fulfil the four classical inequalities (Equations 13-16) whilst ensuring the modulator step-size is physically feasible. This is a non-trivial design problem, because definition of the feasible range for a modulator step may only occur given prior choice on at least two of the following SMB operation variables:

- 1)  $Q_2$
- 2)  $Q_3$
- 3)  $C_D$
- 4)  $C_F$

This design problem forces the SE-SMB designer to take a sequential approach to operation design, as the experimental feasibility of certain proposed operating conditions (e.g.  $Q_2$  &  $Q_3$ ) may only be established once the solution to the remaining variables in the solvent mass-balance equation (e.g.  $C_D$  &  $C_F$ ) are shown to respect the constraints (19-23).

Previously, for a gradient TMB system, the Morbidelli group has proposed that pre-selection of the desorbent and feed modulator concentrations should be used to define the flow-rate ratio design space [103,104]. It is arguable that an alternative sequential design process from that of Triangle Theory's may permit the SE-SMB designer better flexibility in choosing optimal zonal operating conditions, and thus enable the design of more productive and robust systems. It has previously been proposed (by the author) that the sequential design process should begin with a choice of the Z2 operating conditions, followed by choice of the Z3 operating conditions [1]. Approaching the sequential design of SE-SMB systems in this manner, as opposed to the Morbidelli approach of  $C_D$  &  $C_F$  pre-selection followed by Z2 & Z3 flow-rate-ratio selection, presents a number of advantages which will be covered in the discussion section of this chapter.

The 3D SE-SMB operation space is defined in the dimensions of zonal modulator, zonal liquid flow-rate, and switching frequency. For a four zone SE-SMB system, each zone has an operating condition which may be represented by an individual co-ordinate in the 3D operation space; therefore, four points may be plotted within this 3D operation space to describe such an SE-SMB system. Figure 3-2D shows such a set of four points, where each point represents operating conditions for one of the four SE-SMB zones, graphed onto a two-dimensional cross-section of the three dimensional design space (i.e. at a single switching frequency). The complete selection of all four SE-SMB operating points is the final stage in this proposed SE-SMB design process; the earlier stages in the design process are illustrated in Figure 3-2 and are also explained in the text which follows below.

For an operator to select appropriate operation points in the course of a graphical design process, the SWA-type constraints and solvent mass-balance constraints need to be mapped into the 3D operation space so as to define a design space for each SE-SMB zone. Such a graphical representation of the SWA constraints may be achieved through simply graphing a surface into the design space which delineates the operation conditions which produce a standing wave. These surfaces in the 3D design space, shown by Figure 3-2A, are termed 'stationary surfaces', because zonal operating conditions which lie on a stationary surface result in a feed species being 'trapped'

(or stationary) within a zone. Since the standing wave operating conditions bound the inequality-type design constraints in the ideal SE-SMB design equations, their representation as stationary surfaces in graphical space likewise define zonal design regions in the 3D design space.

The stationary surfaces in the 3D operation space thus enclose the zonal design spaces as follows:

- The Z1 design space is 'beneath' the MRC stationary surface (i.e. lower in any  $\omega/C_j/Q_j$  dimension to the closest point in the stationary surface). This ensures that species in Z1 migrate faster than that of the port-switching velocity, so the sorbent is regenerated.
- The Z2 and Z3 operating conditions must lie within the MRC and LRC stationary surfaces, because successful operation of these zones requires simultaneous movement of the LRC species to be faster than the port switching velocity, as well the MRC species migration to be slower than the port switching velocity, in order that separation is achieved.
- The Z4 design space is 'above' the LRC stationary surface (i.e. superior in any  $\omega/C_j/Q_j$  dimension to the closest point in the stationary surface), such that feed species migrate more slowly than the port switching in Z4 and the desorbent is regenerated.

Design of an ideal binary SE-SMB system under linear isotherm, fast-mass transfer conditions may therefore be carried out as follows:

1. Select a switching frequency with reference to the 3D design space. For the separation system represented by Figure 3-2A, it is efficient for the operator to choose a low switching frequency. This is because the stationary surfaces enclose a larger range of liquid flow-rates at lower switching frequencies than is the case for higher switching frequencies; this difference in range may be seen from the example of two switching frequency planes in Figure 3-2B. Lower switching frequencies permits the use of larger feed flow-rates for this particular separation system.
2. The selection of a port-switching frequency permits simplification of the design space by representing it in a 2D  $C_j/Q_j$  space. This is possible because the switching frequency applies to all zones of an SMB, and thus all four zonal operation points may be plotted on a single switching-frequency plane in the 3D space.
3. Once a port-switching frequency has been chosen, selection of the Z2 operation point may proceed. This Z2 operation must be chosen to lie between the MRC and LRC stationary

curves, which in Figure 3-2C are shown as red and blue curves respectively. To facilitate maximisation of the feed flow rate, which is the difference between the Z2&Z3 operation points' liquid flow-rates, a minimal liquid flow-rate should be chosen for the Z2 operation point. For this Z2 operation point to be operationally robust, it should not lie so close to the stationary curves such that small modulator or flow-rate variations may cause it to trespass either of the stationary curves.

4. The selection of the Z2 operation point permits the use of the solvent mass balance equation, in conjunction with the flow-rate and feed modulator-concentration constraints, to define a physically feasible operation region for the Z3 operation point in the SE-SMB system. This physically feasible region is shown by the cyan space in Figure 3-2C. It is noteworthy that this physically feasible Z3 region covers the entirety of the Z3 design space enclosed by the stationary curves; for this system, therefore, the modulator-step-size constraints will not determine a designer's choice of the Z3 operating point.
5. The selection of an efficient Z3 operation point is now possible. This operation point must lie between the stationary curves and within the physically-feasible cyan space. It may be seen from Figure 3-2C that a modulator step between the Z2 and Z3 operation points is necessary to maximise the feed flow-rate; if the Z3 point were chosen to be isocratic to that of the Z2 operation point, the feed flow rate would be very small, and the system would thus be unproductive.
6. After selection of the Z2 and Z3 operation points, the Z1 and Z4 operation points may be chosen at modulator concentrations isocratic to the Z2&Z3 operation points respectively. The Z1 design constraints requires that both species move faster than the port switching velocity, so the Z1 point must be selected to lie above the MRC stationary curve. For the Z4 operation point, desorbent regeneration is produced by ensuring feed species move more slowly than the port switching velocity, so the Z4 operation point must be chosen to lie beneath the LRC stationary curve.
7. The final plot of each of the four SE-SMB operation points may be joined together by lines in the order of the Z1→Z2→Z3→Z4 operation points to reveal an 'N' shaped structure. This structure provides a simple and helpful means to visualize the flow-rate and modulator differences between sequential operation zones at a glance. This 'N' structure is shown by Figure 3-2D.

It is also possible to design an ideal SE-SMB system starting from choice of the Z3 operation point, which may then used to define the physically-feasible region available to the Z2 operation point. However, for real SE-SMB systems, design from the Z2 operation point is often more convenient when begun from the 3D design space; the reason for this is presented at the end of section 3.2.4.

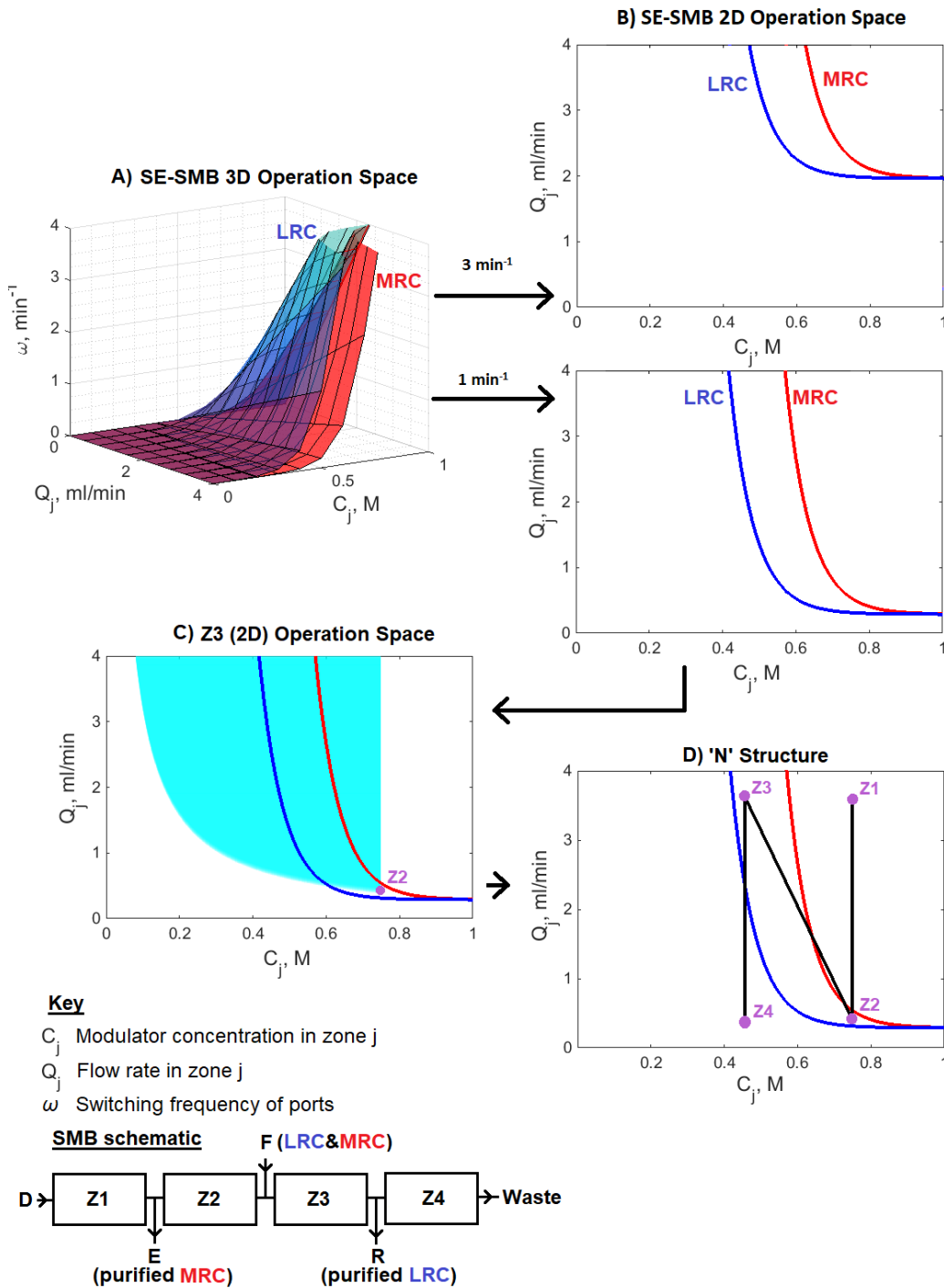


**Figure 3-2 SE-SMB design within 3D design space**

**A)** 3D SE-SMB operation design space with stationary surfaces defining the MRC and LRC standing wave conditions, where the set of feasible Z2&Z3 operation conditions are enclosed between the two stationary surfaces (blue and red), **B)** Stationary curves on two switching frequency planes of the 3D design space, which shows how the span of the Z2 design space (enclosed by the MRC and LRC stationary curves) is modified by the selection of the port-switching frequency, **C)** Solvent mass-balance constraints define the physically feasible region (cyan) for the Z3 operation point once the switching frequency and Z2 operation point (purple point) have been selected, **D)** 'N' structure formed by joining the four chosen operation points sequentially.

### 3.2.3 The Modulator Perturbation (MP) problem in real SE-SMB systems

In real SE-SMB systems, MPs occur. These MPs are generated by the periodic dislocation between the feed port and the modulator step position. Whilst in ideal SE-SMB and step-gradient TMB systems, the location of the feed port and modulator step position are fixed at one position, in real SE-SMB systems, periodic port switching disrupts this overlap. As shown in Figure 3-3B, port-switching instantaneously shuffles the modulator profile in an SE-SMB system, and therefore temporarily disjoins the feed port and modulator step positions. Subsequently (as shown by the modulator-profile snapshots in the second, third and fourth rows of Figure 3-3B), a modulator perturbation (shown as a light-blue 'plug' in the Figure) is generated as the liquid in the pre-feed port column is 'over-diluted' by its mixing with the feed stream. For SE-SMB systems which are designed to have a lower modulator concentration in the post-feed zones compared to that of the desorbent modulator concentration, 'over-dilution' is defined as the generation of a modulator concentration which is lower than that of the ideal SE-SMB's Z3 modulator concentration.

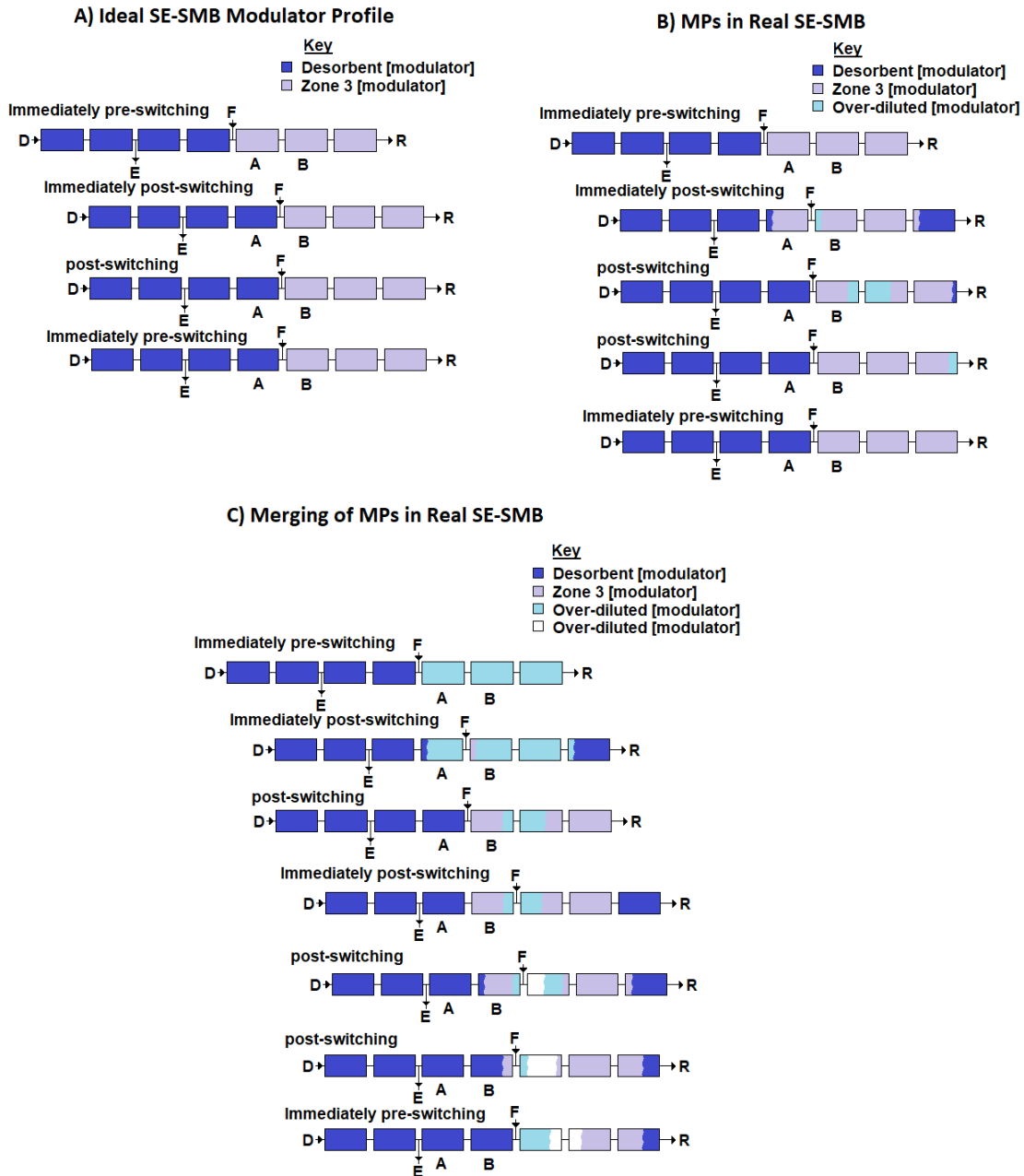


**Figure 3-3 Transient modulator profiles in SE-SMB systems**

**A)** Ideal SE-SMB transient profiles **B)** Transient modulator profiles showing how MPs are generated in real SE-SMB, **C)** Transient modulator profiles showing how MPs merge under certain SE-SMB operation conditions. **For all diagrams:** SMB ports are represented by letters 'D', 'E', 'F' and 'R' for Desorbent, Extract, Feed and Raffinate ports respectively, each row represents a 'snapshot' of the modulator profile across the SMB column series as time progresses, and letters 'A' and 'B' identify two columns that are transported between zones because of port-switching.

MPs distort the modulator concentration profile that is assumed by existing ideal SE-SMB (or 'gradient TMB') design methods. Therefore, MPs make the existing design constraints - detailed for ideal SE-SMB systems in the previous section - unreliable.

### 3.2.4 Design of real SE-SMB systems with account of MPs: the $\Psi$ constraint

The modulator concentration profile in three zones of real SE-SMB systems differs from that of the corresponding ideal SE-SMB modulator profile; these three zones are Z2, Z3 and Z4. It follows that real SE-SMB design constraints should look to correct and regularize the movement of feed species within these three zones, whilst the ideal SE-SMB constraints should hold for Z1 design of real-SE-SMB systems because MPs do not disturb the modulator concentration profile in this zone.

First, consider the situation in an SE-SMB which is shown by the second line of Figure 3-3B. Here, immediately post port-switching, a column equilibrated at the Z3 modulator has been shifted into Z2. In order that the next port-switch does not allow the Z3 modulator concentration to reach further into Z2 (and thus eventually reach the extract port), a constraint is needed to ensure that the Z2 modulator concentration is re-equilibrated to that of the desorbent concentration before the next switch occurs. This constraint may be simply formulated by ensuring that the re-equilibration time of the pre-feed column in Z2 ( $t_2$ ) is less than that of the switching time, and is written as follows:

$$t_2 < t_s \quad (24)$$

where:

$$t_2 = \frac{V_{Eq}}{Q_2} \quad (25)$$

$$V_{Eq} = \varepsilon_{T,cm} \cdot V + V_{lag} \quad (26)$$

Here, the equilibration volume of a column ( $V_{Eq}$ ) is written as the sum of the column's void fraction available to the modulator ( $\varepsilon_{T,cm} \cdot V$ ) in addition to an extra volumetric parameter ( $V_{lag}$ ) which accounts for the non-plug flow behaviour of the modulator front. For a theoretical column and modulator which did not have any axial dispersion phenomena, the equilibration volume would be equal to the void volume of the column alone, as the  $V_{lag}$  term would be equal to zero.

Respecting the constraint in equation (24) makes the Z2 SWA-type design constraint (equation 14) from the ideal SE-SMB system hold for the design of Z2 conditions in a real SE-SMB system. This is due to the fact that a feed species bound to the furthest end from the feed port of the pre-feed column in Z2 will experience identical conditions of liquid flow-rate and modulator concentration in either the real or ideal SE-SMB processes. Given that the ideal SE-SMB conditions ensures that this most-unfavourably (i.e. distantly) placed LRC feed species in the pre-feed column migrates faster than the port-switching velocity, it follows that all other LRC species bound at various other axial distances in the in the pre-feed column will migrate past the feed port before the next port switching.

While the constraint in equation (24) establishes consistent re-equilibration of the Z2 modulator concentration to that of the desorbent, and thus allows the application of the ideal SE-SMB Z2 design constraint to Z2 of real SE-SMB systems, it does not ensure the Z3 modulator profile is even transiently identical to that of the ideal SE-SMB's Z3 modulator profile. The reason for this is that the modulator perturbations can, under certain conditions of flow-rates and switching times, 'merge'. This occurs when a modulator perturbation has yet to clear the end of the first post-feed column in Z3 before the next port-switching, as illustrated by Figure 3-3C. When modulator perturbations 're-insert' themselves into subsequently-generated modulator perturbations in this manner, further over-dilution of previous MPs occurs - in addition to constitutive expansion of the MP 'footprint' in Z3. This phenomenon is here termed 'constitutive over-dilution' for the case of step-down SE-SMB systems. Eventually, this constitutive over-dilution process is predicted to result in a stable and isocratic modulator concentration, equivalent to that of the feed modulator concentration, being established around the feed port. This would make the modulator profile in the real SE-SMB consistently different from that of the ideal SE-SMB equivalent.

The constraint in equation (24) may be modified to ensure that the process of MPs being 're-inserted' into subsequent MPs, as illustrated by Figure 3-3C, does not occur. This outcome may be avoided by requiring that each MP is cleared from the end of the post-feed column in advance of the next port-switching. Since the time taken for re-equilibration of the post-feed column at the ideal Z3 SE-SMB modulator concentration is the sum of the re-equilibration time of the pre-feed column ( $t_2$ ) and the post-feed column ( $t_3$ ), a constraint which ensures Z3 is subject to some liquid flow at a modulator concentration equivalent to the ideal SE-SMB's Z3 modulator may be derived as follows:

$$t_3 = \frac{V_{Eq}}{Q_3} \quad (27)$$

$$t_2 + t_3 < t_S \quad (28)$$

$$\frac{V_{Eq}}{Q_2} + \frac{V_{Eq}}{Q_3} < t_S \quad (29)$$

Equation (29) may be re-written in the form of a dimensionless number,  $\Psi$ , as is detailed below:

$$\frac{1}{t_S} \left( \frac{V_{Eq}}{Q_2} + \frac{V_{Eq}}{Q_3} \right) < 1 \quad (30)$$

$$\frac{V_{Eq}}{t_S} \left( \frac{1}{Q_2} + \frac{1}{Q_3} \right) < 1 \quad (31)$$

$$\Psi = \frac{V_{Eq}}{t_S} \left( \frac{1}{Q_2} + \frac{1}{Q_3} \right) \quad (32)$$

$$\Psi < 1 \quad (33)$$

Given that there is a maximum liquid flow rate (as a result of pressure drop constraints) across SMB zones ( $Q_{max}$ ), and an efficiently-designed SMB process would maximise the feed flow rate with respect to this maximum liquid flow rate through Z3, it is possible to formulate an explicit boundary on the Z2 flow rate from the dimensionless number constraint (equation 33) which ensures the  $\Psi$  constraint is respected; the derivation of this Z2 flow-rate constraint is shown below:

$$\Psi = \frac{V_{Eq}}{t_S} \left( \frac{1}{Q_2} + \frac{1}{Q_3} \right) < 1 \quad (34)$$

$$\left( \frac{1}{Q_2} + \frac{1}{Q_3} \right) < \frac{t_S}{V_{Eq}} \quad (35)$$

$$\frac{1}{Q_2} < \frac{t_S}{V_{Eq}} - \frac{1}{Q_3} \quad (36)$$

$$\frac{1}{Q_2} < \frac{Q_3 t_S - V_{Eq}}{V_{Eq} Q_3} \quad (37)$$

$$Q_2 > \frac{V_{Eq} Q_3}{Q_3 t_S - V_{Eq}} \quad (38)$$

$$\because Q_3 \leq Q_{max} \quad (39)$$

$$Q_2 > \frac{V_{Eq} \cdot Q_{max}}{Q_{max} \cdot t_S - V_{Eq}} \quad (40)$$

The Z2 liquid flow-rate constraint defined by equation (40) can usefully restrict consideration of feasible Z2 operating conditions in the 3D design space. As shown by the RHS of Figure 3-4, using the inequality in equation (40) can significantly curtail the real SE-SMB Z2 design space with respect to the ideal SE-SMB design space (shown by the LHS of Figure 3-4). This presents the designer with a fully-defined Z2 design space, and thus suits the Z2→Z3 sequential design process more than the Z3→Z2 sequential design process.

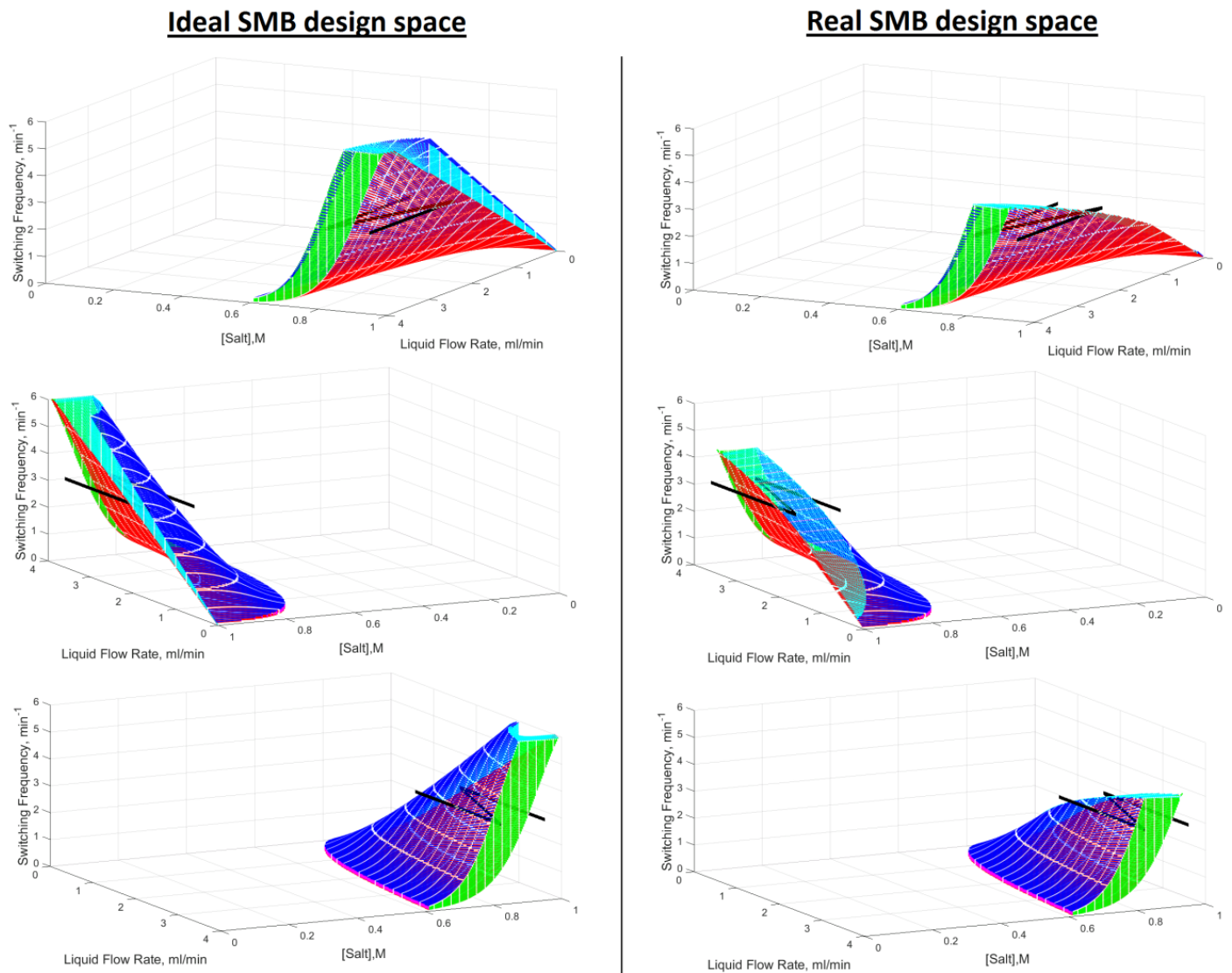


**Figure 3-4 Differences between the Real and Ideal SE-SMB operation spaces**  
**RHS) Ideal SE-SMB Z2 design space, LHS) Real SE-SMB Z2 design space as bounded by the  $Q_2(\Psi, Q_{max})$  constraint, which results in a significantly curtailed design space compared to that of the ideal design space.**

### 3.2.5 Design of real SE-SMB systems with account of MPs: the $\Omega$ constraint

While the  $\Psi$  number may ensure that: 1) the ideal SE-SMB Z2 constraints apply to real SE-SMB systems, and 2) Z3 experiences some exposure to a modulator concentration identical to that of the ideal SE-SMB system's Z3, the  $\Psi$  number cannot ensure that correct migration of feed species in Z3 takes place in the presence of MPs. The ideal SE-SMB design constraints for Z3 (equation 15) are similarly unable to ensure appropriate migration of feed species in Z3 given their assumption of no modulator perturbations. Therefore, a new design constraint for Z3 needs to be derived that accounts for the effects of modulator perturbations on the feed species' migration within Z3.

The migration distance of a feed species in Z3 may be found, approximately, by assuming that there are only two modulator concentrations to which the species is exposed: these are the modulator concentration of the MP ( $C_{\ddagger}$ ) and the modulator concentration of the ideal Z3 ( $C_3$ ). This assumption is based on the simplifying assumption that a MP travels as a square wave, and in an SE-SMB operation where the  $\Psi$  constraint is satisfied. These assumptions will be discussed later in this section.

From SMT, and the square-wave approximation of the MP, the distance in which a feed species travels in Z3 during one switching period ( $x_i$ ) may be derived as the sum of the distance it travels under sequential exposure to liquid flow at both the  $C_3$  and  $C_{\ddagger}$  modulator concentrations:

$$C_{\ddagger} = \frac{Q_2 \cdot C_3 + (Q_3 - Q_2) \cdot Q_2 \cdot C_F}{Q_3} \quad (41)$$

$$x_i = (t_S - t_2) \left( \frac{Q_3}{\varepsilon_{T,i} \cdot A_c \cdot (1 + k'_{i,C_3})} \right) + t_2 \left( \frac{Q_3}{\varepsilon_{T,i} \cdot A_c \cdot (1 + k'_{i,C_{\ddagger}})} \right) \quad (42)$$

Since the Z3 SWA-type design constraints require the MRC and LRC species to travel less than, and more than, the distance of one column's length ( $L$ ) during the course of a single switching-period respectively, the Z3 constraint for real SE-SMB systems may be derived as follows:

$$\left( \frac{(t_S - t_2) \cdot Q_3}{\varepsilon_{T,a} \cdot A_c \cdot (1 + k'_{a,C_3})} \right) + \left( \frac{t_2 \cdot Q_3}{\varepsilon_{T,a} \cdot A_c \cdot (1 + k'_{a,C_{\ddagger}})} \right) < L < \left( \frac{(t_S - t_2) \cdot Q_3}{\varepsilon_{T,b} \cdot A_c \cdot (1 + k'_{b,C_3})} \right) + \left( \frac{t_2 \cdot Q_3}{\varepsilon_{T,b} \cdot A_c \cdot (1 + k'_{b,C_{\ddagger}})} \right) \quad (43)$$

Equation (43) may be simplified with the use of two new dimensionless numbers ( $\Omega_a$  &  $\Omega_b$ ) to the following:

$$\Omega_b < 1 < \Omega_a \quad (44)$$

where:

$$\Omega_b = \frac{Q_2}{Q_3} \left( \frac{V_{b,C_3} \cdot V_{b,C_{\ddagger}}}{(Q_2 \cdot t_s - V_{Eq}) \cdot V_{b,C_{\ddagger}} + V_{b,C_3} \cdot V_{Eq}} \right) \quad (45)$$

$$\Omega_a = \left( \frac{Q_3}{Q_2} \right) \left( \frac{(t_s \cdot Q_2 - V_{Eq}) \cdot V_{a,C_3} + V_{Eq} \cdot V_{a,C_{\ddagger}}}{V_{a,C_{\ddagger}} \cdot V_{a,C_3}} \right) \quad (46)$$

Equation (44) should thus replace the SWA-type design inequalities for Z3 of ideal SE-SMB systems. Likewise, for a four zone SE-SMB, the Z4 design constraints must also acknowledge the effects of MPs. Given that – in the presence of MPs - the migration velocity of the LRC must be slower than that of the port-switching velocity in Z4 such that the desorbent may be re-generated, the following design constraint may be derived for the final zone in a four-zone SE-SMB:

$$\left( \frac{(t_s - t_2) \cdot Q_4}{\varepsilon_{T,b} \cdot A_c \cdot (1 + k'_{b,C_4})} \right) + \left( \frac{t_2 \cdot Q_4}{\varepsilon_{T,b} \cdot A_c \cdot (1 + k'_{b,C_{\ddagger}})} \right) < L \quad (47)$$

This may be simplified to the following constraint:

$$Q_4 \left( \frac{(V_{b,C_{\ddagger}}(t_s - t_2) + t_2 \cdot V_{b,C_3})}{V_{b,C_3} \cdot V_{b,C_{\ddagger}}} \right) < 1 \quad (48)$$

Therefore, for four-zone SE-SMB systems which has an un-retained modulator, linear isotherm binding behaviour, and low mass-transfer resistances, the comprehensive set of design constraints is as follows:

$$\frac{Q_1 \cdot t_s}{V_{a,C_1}} > 1 \quad (49)$$

$$\frac{Q_2 \cdot t_s}{V_{a,C_2}} < 1 < \frac{Q_2 \cdot t_s}{V_{b,C_2}} \quad (50)$$

$$\Psi < 1 \quad (51)$$

$$\Omega_b < 1 < \Omega_a \quad (52)$$

$$Q_4 \left( \frac{(V_{b,C_{\ddagger}}(t_s - t_2) + t_2 \cdot V_{b,C_3})}{V_{b,C_3} \cdot V_{b,C_{\ddagger}}} \right) < 1 \quad (53)$$

There are two simplifying assumptions which enabled the construction of the above algebraic SE-SMB design constraints. These assumptions are the ‘square-wave’ simplification of MP

profiles, and the  $V_{lag}$  simplification which accounts for axial dispersion in the migration of modulator fronts. Figure 3-5 illustrates how these assumptions simplify experimentally-relevant MP profiles.

It may be seen from Figure 3-5 that this theory's approximation of the MP profile to a square-wave perturbation includes a  $V_{lag}$  term to account for the effects of axial dispersion of the modulator front. The  $V_{lag}$  term applies only to one 'step' in the modulator perturbation; this is because the 'tailing-step' of the MP's modulator front is subject to axial-dispersive effects by its migration through a Z2 column. By contrast, the 'front-step' of the MP is formed instantaneously after port-switching, thus axial-dispersive effects are unlikely to destabilize the shape of the modulator 'front-step' (from the reference point of feed species located at the feed-port end of Z3).

The theory's simplifying assumptions of a 'square wave' MP, adjusted by the  $V_{lag}$  term, is a conservative approximation of the MP profile. This assumption is conservative because any discrepancy between the theory's assumed modulator profile and that generated experimentally is likely to result in the LRC being less retained in Z3 than theoretically predicted. In this way, these simplifying assumptions create a slightly more strict ( $\Omega_b$ ) design constraint on the Z3 SE-SMB operation conditions than necessary. It follows that the Z4 design constraint presented in this chapter is also slightly more strict than needed.

On the other hand, the MP simplifying assumptions also under-estimate the retention of the MRC in Z3, thus making the  $\Omega_a$  design constraint slightly looser than that required for ensuring a pure raffinate stream. However, it is arguable that this slackness in the  $\Omega_a$  constraint should not be of concern to SE-SMB process designers. This is because operation conditions which risk raffinate pollution are very unlikely to be intentionally chosen by a process designer. This argument is best understood through examination of the hypothetical design space on the LHS of Figure 3-5A, which shows the Z3 cyan design space over-stepping the MRC stationary curve (red) due to the definition of the  $\Omega_a$  design constraint. Given that the MRC stationary curve is an overly strict constraint on the SE-SMB Z3 design space (since it ignores modulator perturbations), and given that the  $\Omega_a$ -defined boundary outside the MRC stationary curve is too-slack a constraint on the SE-SMB Z3 design space (due to the theoretical MP assumptions), the section of the Z3 cyan operation space which risks raffinate pollution is bounded by the MRC stationary curve and the  $\Omega_a$ -defined boundary. A designer's choosing of a Z3 operational point in this region of the design space would mean choosing a very small modulator step within the SE-SMB system, which would undermine any motivation by

the designer to construct a non-isocratic SMB system, and is thus unlikely. Indeed, a large modulator step size is recommended for efficient SE-SMB design of experimental systems (see discussion).

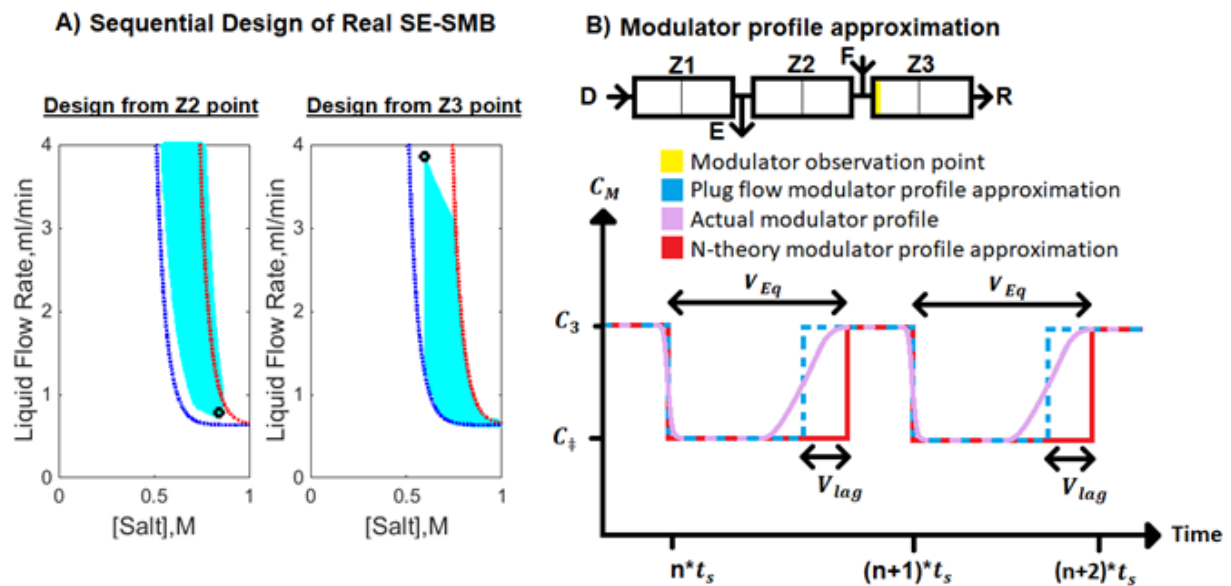


**Figure 3-5 Sequential design and theoretical approximations of theory**

**A)** Sequential design of SE-SMB systems by either  $Z2 \rightarrow Z3$  or  $Z3 \rightarrow Z2$  operation points shows different design constraints (forming cyan design space) apply to Z2 and Z3 in real SE-SMB systems **B)** The theoretical approximation of MPs by a square-wave. Figure adapted from [1] with permission.

### 3.2.5 Robust design of SE-SMB systems

Of the various failure modes which can disturb satisfactory SE-SMB operation, there are two classes of failure for which robust design within the new design space is easily pursued.

First, robust SE-SMB systems may be designed to protect operation from variation in the pump flow-rates. In SE-SMB systems, unlike isocratic SMB systems, pump flow-rate variations are often accompanied by significant changes to the modulator concentration profile of the SE-SMB given the modulator-dependence of Z3&Z4 on pump flow rates. Small changes in modulator concentration can have very large effects on the retention of feed species in SE-SMB separations, thus sensitivity of SE-SMB system to pump variation can be disproportionately larger than that of isocratic SMB systems. As will be demonstrated in the results section of this chapter, the new design space's independent modulator and liquid flow-rate axes permit a designer to easily evaluate the robustness of proposed operational conditions to the effects of pump flow rate variation as well as modulator concentration variation.

Second, ligand loss from columns is a common failure mode in SMB systems. It is arguable that this may be modelled as a virtual decrease in the port switching frequency. This is because ligand loss generally decreases the retention of feed species within a column, and thus favours migration of species in the liquid flow's direction. A decrease in port switching frequency also favours migration of species in the liquid flow's direction, and is thus hypothesised to simulate the effects of ligand loss. Therefore, given that the port-switching frequency dimension exists in the new design space, a process' robustness to ligand loss may be inferred from the distance that a set of operation conditions may be displaced towards the zero end of the switching-frequency axis before the operation points cross any of the stationary surfaces. This hypothesis is tested in the results section, and a system robust to ligand loss is demonstrated.

### 3.3 Results

#### 3.3.1 Testing integrity of newly-proposed design constraints

The isotherm parameters for two protein feed species were determined from a set of isocratic elution experiments with lysozyme and the  $\beta$ -Lactoglobulin dimers. Additionally, void fraction and modulator parameters were determined in the course of these experiments. These results, and the isotherm parameters subsequently derived from them, are detailed in the table below.

**Table 3-1** Isotherm and void fraction parameter determination

Experiment number	1	2	3	4	5
Lysozyme isocratic elution salt concentration, M	0.55	0.50	0.45	0.60	1.00
Lysozyme peak retention volumes (mL)	12.20	20.20	42.06	7.85	2.16
$\beta$ -Lactoglobulin dimers isocratic elution salt concentration, M	0.400	0.425	0.450	1.000	
$\beta$ -Lactoglobulin dimers peak retention volumes (mL)	24.56	14.99	9.20	2.08	
Parameters	Values				
$k'_{a,0}$ (lysozyme)	1.75e4				
$S_a$ (lysozyme)	14.2				
$\epsilon_{T,a}$	0.54				
$k'_{b,0}$ ( $\beta$ -Lactoglobulin)	8e4				
$S_b$ ( $\beta$ -Lactoglobulin)	22.6				
$\epsilon_{T,b}$	0.52				
$\epsilon_{T,C_M}$	0.86				
$V_{lag}$ , mL	0.40				

Experimental investigation of the  $\Psi$  number was performed by operating an SE-SMB system under two operating conditions. The first experiment satisfied the  $\Psi$  modulator constraint, whilst the second experiment violated this constraint. These two experiments are represented graphically by Figure 3-6A. The left-hand side (LHS) of the figure shows a SE-SMB operation which is in violation of the  $\Psi$  modulator constraint; this constraint is graphed as a horizontal solid-black line, and is expressed in terms of a lower limit on the Z2 flow rate (which is possible because the modulator number can be expressed as a constraint on the Z2 flow rate:  $Q_2(\Psi)$ ). The right hand-side (RHS) of Figure 3-6A is a graphical representation of experimental operating conditions which satisfied the  $Q_2(\Psi)$  constraint; this is shown by the Z2 operation point being placed at a higher liquid flow-rate than the flow-rate threshold defined by the  $Q_2(\Psi)$  constraint line. These results of these two experiments are listed in Table 3-2, where it may be seen that – for this experimental system – violation of the  $\Psi$  number constraint was paired with compromised extract purity.

Also demonstrated by the experiments graphed in Figure 3-6A is the importance of the  $V_{lag}$  approximation to account for non-idealities in the modulator front's migration. The horizontal dotted-black lines in the figure represent the  $Q_2(\Psi)$  constraint for the case of no axial dispersion ( $V_{lag}=0$ ). Both separation systems in Figure 3-6A satisfied this idealised plug-flow version of the  $Q_2(\Psi)$  constraint, as both systems used Z2 operating conditions at liquid flow-rates in excess of the threshold defined by the dotted black lines. However, only one of the two separation experiments produced a successful separation, which indicates the poor predictive power of the plug-flow ( $V_{lag}=0$ ) approximation for this particular system.

**Table 3-2** Experiment to demonstrate N-theory first MP constraint

Parameter	Experiment 1 (Figure 3-6A left) Violation of first MP constraint (magenta system)	Experiment 2 (Figure 3-6A right) Parameter value System robust to first MP constraint (green system)
Extract Purity	~50%	>98%
Raffinate Purity	>98%*	>98%
$\Psi$	1.06	0.70
$\Omega_b$	0.37	0.27
$\Omega_a$	0.47	0.53
$Q_E$ , mL/min	1.54	1.26
Fixed Parameters	$Q_D$ , 2.1mL/min; $Q_F$ : 2.8mL/min; $C_D$ : 0.56M; $C_F$ : 0.42M; Column configuration: 3-2-3 ; $t_s$ : 2.5 minutes; Feed components: 1 mg/mL lysozyme & 1 mg/mL $\beta$ -Lactoglobulins	
*Significantly reduced yield of raffinate product		

Computational simulations were used to investigate the integrity of the  $\Omega_b$  constraint. The details and results of these simulations are graphed in Figure 3-6B and listed in Table 3-3. SE-SMB operation conditions which satisfied the  $\Omega_b$  number (formulated as constraint on the Z2 liquid flow rate,  $Q_2(\Omega_b)$ ), and displayed as a curved black line bounding the cyan Z2 design space in the figure) were simulated to produce pure separations at cyclic-steady state. For SE-SMB operation conditions which violated the  $Q_2(\Omega_b)$  constraint, shown as magenta systems in Figure 3-6B, cyclic steady state was not reached and simulations predicted that the LRC would accumulate around the feed port in the column series during the course of the run. These simulations were repeated with an 'ideal' SE-SMB simulator; as predicted, the ideal SE-SMB simulations all reached cyclic steady state.

Experimental investigation of the  $\Omega_b$  constraint was also performed. As shown by Figure 3-6C and detailed by Table 3-4, various Z3 operating conditions were used to test the integrity of the  $Q_3(\Omega_b)$  boundary in the design space. This design space is shown by a cyan block in the figure, and it was found that only Z3 operation points which lay within this design space (green systems) were capable of pure binary SE-SMB separation.

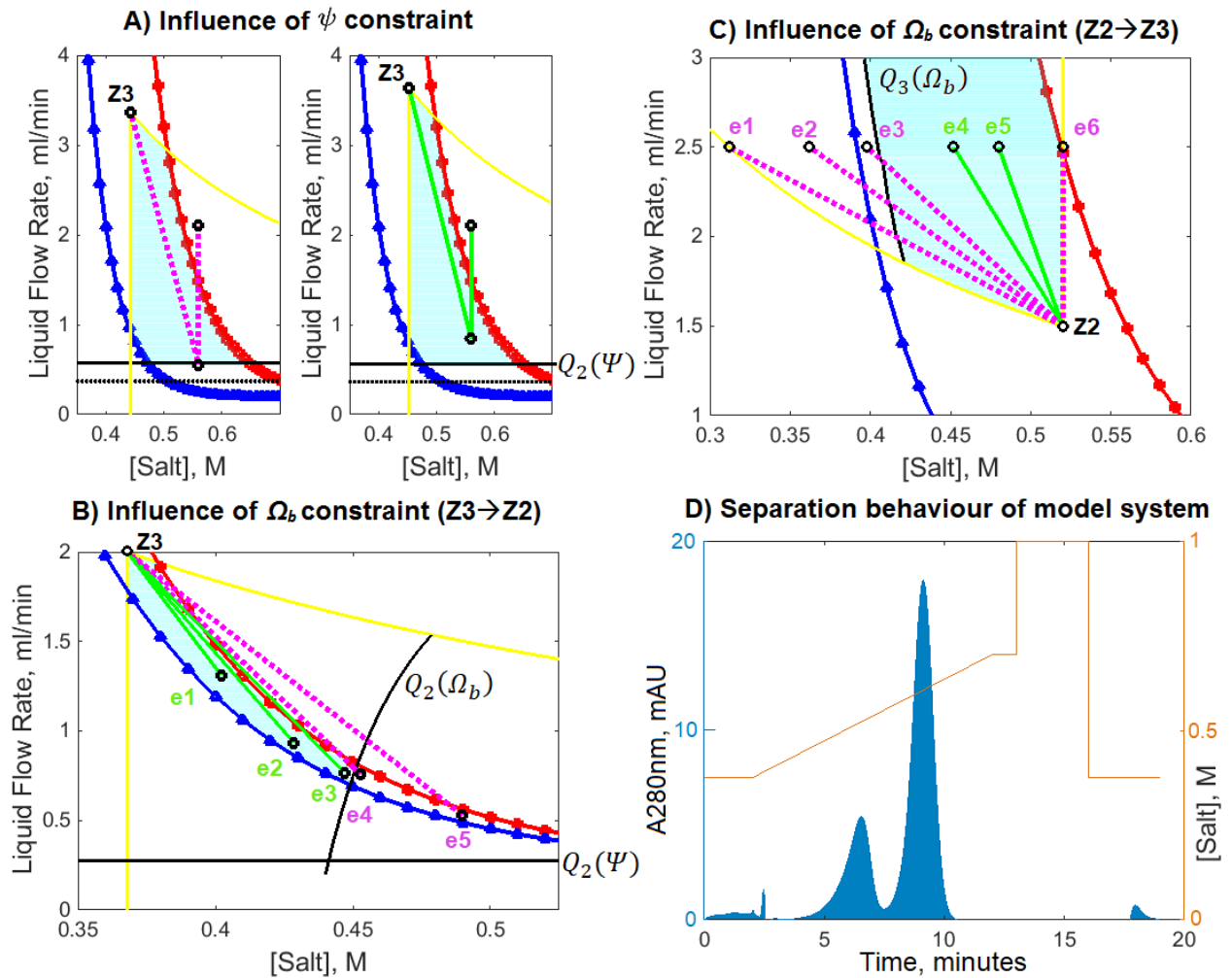


**Figure 3-6 Experiments and simulations to test theory**

**A)** Experiments to test the integrity of the  $Q_2(\Psi)$  constraint (solid black line). Z2 operation points were chosen at liquid flow-rate values superior (RHS) and inferior (LHS) to the  $Q_2(\Psi)$  constraint; only the RHS - which satisfied the  $Q_2(\Psi)$  constraint – produced a successful separation. **B)** Computational simulations to test the  $Q_2(\Omega_b)$  constraint integrity, shown by a curved black line. Only the experiments which satisfied the  $Q_2(\Omega_b)$  constraint (e1-3, superior to the constraint curve), produced successful separations. **C)** Experimental testing of the Z3 design space (cyan) as determined by the  $\Omega_i$  constraints. Only experimental Z3 operation points which fulfilled the  $\Omega_i$  constraints (e4&e5) produced successful separations, whilst e3 failed despite fulfilling all ideal SE-SMB constraints. **D)** Example analytical chromatogram of binary protein mixture used in SE-SMB experiments. **ALL)** Red curve/surface is the MRC stationary curve/surface, blue curve/surface is the LRC stationary curve/surface, straight black line is the  $Q_2(\Psi)$  constraint, yellow lines delineate physically feasible Z2 or Z3 design spaces as determined by the solvent mass-balance equation and the relevant modulator concentration/flow-rate constraints, the cyan ‘blocks’ are the Z2 or Z3 design space, the green systems produced successful separations, and the magenta systems failed by either producing impure separations or were incapable of reaching cyclic steady state. Figure adapted from [1] with permission.

**Table 3-3** Properties of simulated system used to demonstrate N-theory second MP constraint

Parameter	Experiment 1	Experiment 2	Experiment 3	Experiment 4	Experiment 5
System position in Figure 3-6B	Left-most	2 <sup>nd</sup> from left	3 <sup>rd</sup> from left	2 <sup>nd</sup> from right	Right-most
Inside/Outside Real SE-SMB design space?	In	In	In	Out	Out
Inside/Outside Ideal SE-SMB design space?	In	In	In	In	In
Reached Steady State? (Y/N)	Y	Y	Y	N	N
$\Omega_b$	0.9361	0.9703	0.9959	1.0030	1.0598
$\Psi$	0.2083	0.2928	0.3570	0.3598	0.5144
$C_F$ , M	0.3027	0.3148	0.3188	0.3159	0.3239
$C_D$ , M	0.4021	0.4286	0.4471	0.4528	0.4897
$Q_F$ , mL/min	0.6877	1.0661	1.2342	1.2402	1.4685
$Q_E$ , mL/min	0.6877	1.0661	1.2342	1.2402	1.4685
Fixed Parameters	$Q_D$ : 2mL/min; Maximum $Q_D$ : 2mL/min; Column configuration: 2-4-2; Mass transfer rate: 20s <sup>-1</sup> ; $V_{lag}$ : 0mL; $D_i=0$ m <sup>2</sup> /s; Individual column dimensions: 2.5 x 0.7 i.d. cm; $K_{0,a}$ (MRC): 2.08e3; Sa (MRC): 15; $K_{0,b}$ (LRC): 1.6e3; Sb (LRC): 15; $t_s$ : 2 minutes; $\epsilon_{T,a}=\epsilon_{T,b}=\epsilon_T=0.5$ ; Simulated run time: 24 hours; 90 nodes per column.				

Analysis of experimental SE-SMB outlet purities separation was performed through use of a batch-gradient protocol. A chromatogram generated by analysis of the SMB experiments' feed mixture is given in Figure 3-6D. This chromatogram is included to show that the model protein separation is not of trivial ease; both protein species in the binary feed mixture are retained.

**Table 3-4** Operation conditions used to demonstrate N-theory operation window boundaries

Parameter	Experiment 1	Experiment 2	Experiment 3	Experiment 4	Experiment 5	Experiment 6
System position in Figure 3-6C	Left-most	2 <sup>nd</sup> from left	3 <sup>rd</sup> from left	3 <sup>rd</sup> from right	2 <sup>nd</sup> from right	Right-most
Inside/outside real SE-SMB design space?	Out	Out	Out	In	In	Out
Extract Purity	~50%	~70%	~80%	>98%	>98%	>98%*
Raffinate Purity	>98%*	>98%*	>98%*	>98%	>98%	~50%
$\Omega_b$	8.22	2.66	1.19	0.38	0.23	0.13
$\Omega_a$	0.03	0.06	0.11	0.29	0.49	1.01
$\Psi$	0.42	0.42	0.42	0.42	0.42	0.42
$C_F, M$	0	0.125	0.215	0.35	0.42	0.52
Fixed parameters	$t_s$ : 2.5 mins; Column configuration: 4-2-2; $Q_D$ : 4mL/min; $Q_E$ : 2.5mL/min; $Q_F$ : 1mL/min; $C_D$ :0.52, M					
*Reduced yield from outlet port						

### 3.3.3 Experiments to demonstrate robust and productive design

To investigate the hypothesis that ligand loss may be modelled by a virtual decrease in the switching frequency an SMB separation is subject to, a set of computational simulations were performed. In these simulations, out of a set of eight columns in an SE-SMB system, three consecutive columns were simulated to have lost 33% of their ligand. Instead of investigating more realistic expectations of experimental ligand loss severity, this harsh scenario was chosen to robustly test the predictive power of the just-stated hypothesis. Ligand loss was modelled by a 33% decrease in the  $K_{0,i}$  value which applied to feed species passing through these columns; this is an established approach to model ligand loss [95,96]. A pair of operation conditions was chosen to fulfil all SE-SMB design constraints at a chosen switching frequency under the assumption that no ligand loss occurred. These two operating sets are represented by green and magenta lines (between the Z2 and Z3 operation points) in the upper side (w.r.t. the switching frequency axis) of Figure 3-7A. These two operation constraints are also re-drawn on a lower switching frequency plane of Figure 3-7A, at a switching frequency which is 33% less than that of the original pair. The two operational sets were chosen such that one is robust to ligand loss (i.e. the green system's Z3 operation points stay within the stationary curves and modulator constraint limits on the reduced switching frequency plane), whilst the other operation set (magenta) was chosen such that it's displacement to the lower switching frequency plane would place it's operation points outside of the stationary curves which apply to it at the lower switching frequency.

The simulation results, detailed in Table 3-5, showed that the magenta system from Figure 3-7A suffered periodic raffinate pollution during the course of a simulated process run, whilst the robustly-designed system (green in the figure) did not produce any raffinate pollution.

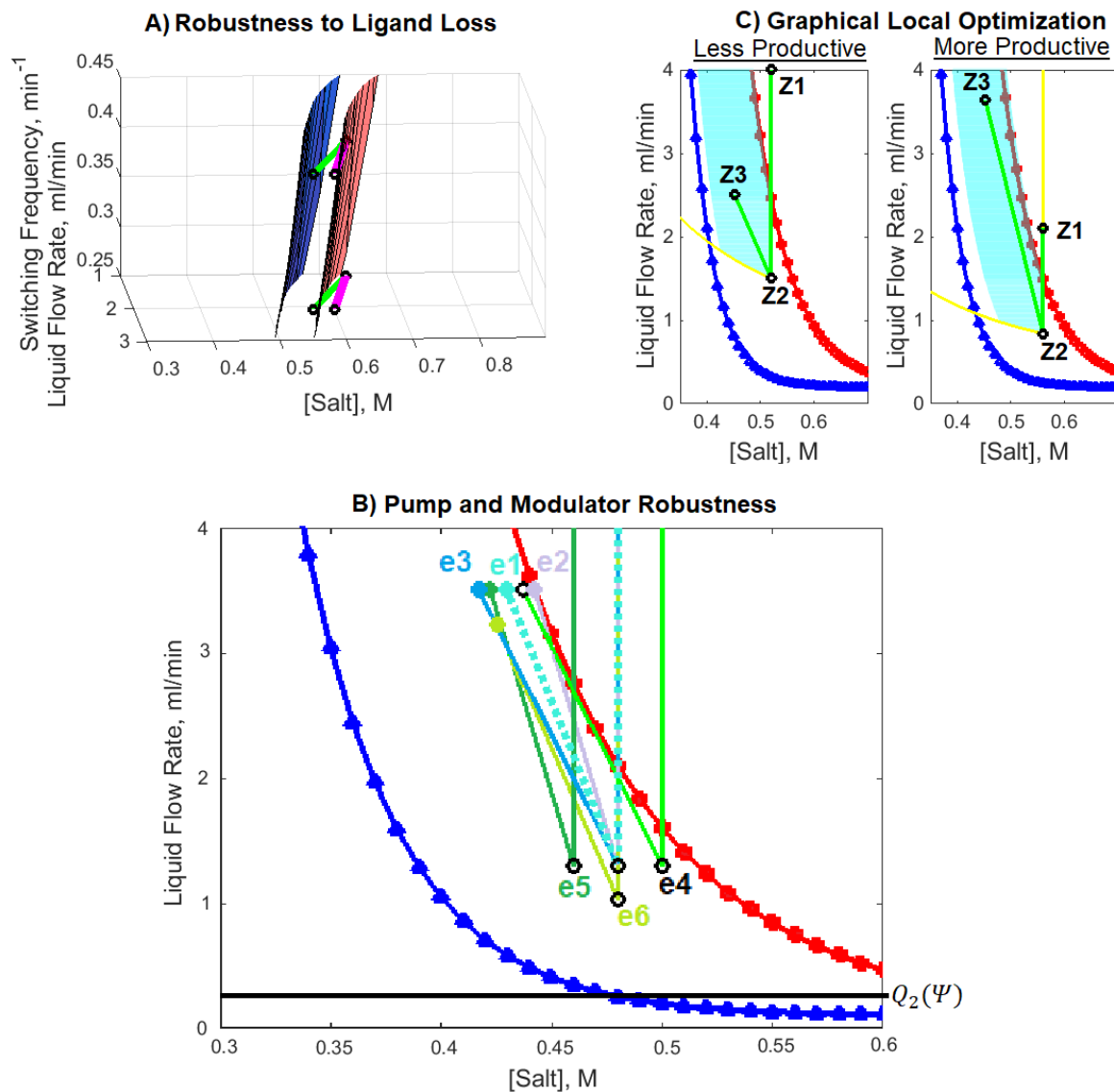


**Figure 3-7 Experiments and simulations to demonstrate application of theory for robust and productive SE-SMB design**

**A)** Ligand loss modelled as a translocation of an SE-SMB operation points to a lower switching frequency plane, where the green system – but not the magenta system - was robust to ligand loss. **B)** Robust design of an SE-SMB system against pump and conductivity variances: The dotted cyan system is the set-point system, and the solid-lined systems are selected worst-case scenario modulator and flow-rate perturbations of this set-point system which - despite experiencing the operating perturbations – all produced pure separations, **C)** Efficient design of SE-SMB systems through increasing the feed flow-rate, LHS: Original system, RHS: System of improved productivity with increased feed flow-rate (as represented by the increased vertical (flow-rate) distance between the Z2&Z3 operation points. **ALL)** Red curve/surface is the MRC stationary curve/surface, blue curve/surface is the LRC stationary curve/surface, straight black line is the  $Q_2(\Psi)$  constraint, yellow

lines delineate physically feasible Z2 or Z3 design spaces as determined by the solvent mass-balance equation and the relevant modulator concentration/flow-rate constraints, the cyan 'blocks' are the Z3 design space.

**Table 3-5** Properties of simulated system used to demonstrate N-theory design of robustness to ligand loss

Parameter	Experiment 1	Experiment 2	Experiment 3	Experiment 4
System in Figure 3-7A (Green/Magenta)	Green	Green	Magenta	Magenta
Simulated Conditions (Normal/Ligand Loss)	Normal	Ligand Loss	Normal	Ligand Loss
Raffinate Purity, %	99.9%	99.9%	99.9%	96.6%
$C_F$ , M	0.456		0.537	
Fixed Parameters	$Q_D$ : 4mL/min; $Q_F$ : 2.5mL/min; $Q_E$ : 1mL/min; Maximum $Q_j$ : 4mL/min; Column configuration: 3-2-3; Mass transfer rate: 20s <sup>-1</sup> ; $V_{lag}$ : 0mL; Individual column dimensions: 2.5 x 0.7 i.d. cm; $k'_{0,a}$ (MRC): 8.16e4; $k'_{0,a}$ (MRC in failed columns): 5.51e4; $S_a$ (MRC): 16; $k'_{0,b}$ (LRC): 3.27e4; $k'_{0,b}$ (LRC in failed columns): 2.38e4; $S_b$ (LRC): 16; $t_s$ : 2.5 mins; $C_D$ : 0.629M; $D_i=0$ m <sup>2</sup> /s; modulator is unretained. 30 nodes per column.			

The potential for robust design against flow-rate variation and modulator concentration variation in the frame of the new design space was investigated experimentally. As shown by Figure 3-7B, various three-zone SE-SMB operation sets (shown as 'V's) may be drawn in the 2D design space. In this manner, an SE-SMB designer may explore the consequences of deviation from the initial set-point operation conditions (shown as the dotted cyan 'V' operation set).

The set-point operation conditions were designed for robustness by initially choosing a low switching-frequency to minimize the effects of modulator perturbations. After this switching frequency was selected, a Z3 operation point (blue point in Figure 3-7B) was chosen to be the point which would only be experienced by the system in the case of the most unfavourable pump/modulator variation possible. Given that the design of the set-point operating conditions also attempted to define a productive process, it was assumed that the feed flow-rate would be greater than that of the Z2 flow-rate, and thus the Z3 modulator conditions would be more sensitive to variations in the feed modulator concentration than to other possible variations in operation conditions. Therefore, the chosen 'most unfavourable' Z3 operation point (blue point in the figure) defined the operation conditions experienced by the system in the instance of a decrease in feed modulator concentration. The corollary scenario of an increase in feed modulator concentration was accounted for by plotting a Z3 operation point just inside of the MRC stationary curve at the same

liquid flow rate as that of the blue scatter point. These two Z3 operation points bound the entire range of modulator variations in Z3 to which the set-point system is designed to be robust. The set-point Z3 operation point was thus selected to be equidistant between the two feed-modulator failure-mode Z3 operation points. The Z2 operation point was then chosen to be inside the Z2 design space as defined by the ‘most unfavourable’ Z3 operation point (blue scatter). Thus the robust set-point operation conditions were found, and various operating conditions – constituting perturbations from this set-point system - were experimentally tested. The results of this set of experiments to test the robustness of the set-point operating conditions are detailed in Table 3-6, and the operating conditions of all experiments are graphed in Figure 3-7B. As may be seen from the figure, all perturbed operation conditions maintained placement of Z2 and Z3 within the stationary curves and within the MP constraints defined by the ‘most unfavourable’ Z3 operation point, and therefore were all experiments were predicted to produce successful separations. This was indeed the case: all separations achieved purities of at least 90%.

**Table 3-6** Experimental operation conditions used to demonstrate N-theory robust design

Parameter	Experiment 1 (set-point)	Experiment 2	Experiment 3	Experiment 4	Experiment 5	Experiment 6
$\Delta C_F$ , mM	0	+20	-20	0	0	0
$\Delta C_D$ , mM	0	0	0	+20	-20	0
$\Delta Q_E$ , %	0	0	0	0	0	-10
Extract Purity (lysozyme)	>98%	>98%	>98%	>98%	>98%	>98%
Raffinate Purity ('Lacs)	>98%	>90%	>98%	>90%	>98%	>98%
$\Omega_b$	0.18	0.14	0.23	0.16	0.20	0.15
$\Psi$	0.21	0.21	0.21	0.21	0.21	0.17
Fixed Parameters	$t_s$ : 5 mins; Column configuration: 2-3-3; Set-point $Q_D$ : 4mL/min; Set-point $C_D$ : 0.48M; Set-point $Q_E$ : 2.7mL/min; Set-point $Q_F$ : 2.2mL/min; Set-point $C_F$ : 0.4M; Feed components: 1 mg/mL lysozyme & 1 mg/mL $\beta$ -Lactoglobulins;					

For linear isotherm SE-SMB systems, productive design generally involves maximisation of the feed flow-rate. The new design space facilitates feed flow-rate maximization by clearly delineating the modulator and liquid flow-rate conditions which bound the feasible Z3 design space. To demonstrate efficient design of an SE-SMB, two separation systems are presented in Figure 3-7C. The LHS of Figure 3-7C shows an un-optimized separation designed from pre-selection of the Z2 operation point; here, the Z3 operation point has been poorly chosen because a much larger feed flow-rate could have been achieved while retaining the Z3 operation point within the cyan Z3 design

space. The RHS of the figure shows a more productive set of operating conditions in comparison to the original set; the RHS system's feed flow-rate has been significantly increased by selection of a smaller Z2 flow-rate and a larger Z3 flow-rate. Furthermore, the desorbent flow rate has been reduced in the RHS system such that the Z1 operation point lies just outside the stationary curve; this satisfies the design constraint on the Z1 operation point, whilst also reducing the buffer consumption of the process, and thus increases the desorbent-utilization of the system. The results of these experimental demonstrations of efficient SE-SMB design are detailed in Table 7.

**Table 3-7** Operation conditions used to demonstrate N-theory design of productive separations

Parameter	Original System (Fig.3-6G left)	Improved design (Fig. 3-6G right)
Extract Purity (lysozyme)	>98%	>98%
Raffinate Purity ( $\beta$ -Lactoglobulins, product)	>98%	>98%
Product-specific Sorbent Productivity, g/L/hour	7.5	20.6
Desorbent Utilization ( $Q_F/Q_D$ )	0.25	1.33
$Q_D$ , mL/min	4	2.1
$Q_E$ , mL/min	2.5	1.26
$Q_F$ , mL/min	1	2.8
$C_D$ , M	0.52	0.56
$C_F$ , M	0.35	0.42
$\Omega_b$	0.14	0.10
$\Psi$	0.19	0.33
Fixed Parameters	$t_s$ : 5 mins; Column configuration: 3-2-3; Feed components: 1 mg/mL lysozyme & 1 mg/mL $\beta$ -Lactoglobulins	

Additional simulation experiments were used to confirm that the high-purity separations achieved experimentally in this Results chapter were not otherwise explainable through slow mass-transfer phenomena. These simulations employed a linear-isotherm liquid-phase lumped mass-transfer model which modelled the mass-transfer rates of the feed species by use of standard correlations (see details in Materials and Methods section). Two sets of mass-transfer rates were investigated – one set was found from standard correlations, and the other was defined as a 'fast' rate of  $20s^{-1}$ . It was found that there was complete agreement between the experimental results and their simulation counterparts for both rates of the mass transfer coefficient parameter employed.

### 3.4 Discussion

This chapter has presented a set of design constraints in the form of the dimensionless numbers,  $\Psi$  and  $\Omega$ , which enable successful design of linear-isotherm, fast mass-transfer SE-SMB separations through accounting for the effects of modulator perturbations. Furthermore, a new 3D operation space has been shown to facilitate the use of the new modulator constraints for graphical design of robust and productive SE-SMB systems. The collection of ideas presented in this chapter, which pertain to the effects of modulator dynamics on the design and operation of SE-SMB systems, are hereafter termed ‘N-theory’ for convenience. N-theory may be modified for different models of modulator-dependent binding, such as the  $k'_{i,C_j} = k'_{i,0} \cdot C_j^{S_i}$  relation common to mass-action formulations and other more complex formulations [108,109]. Furthermore, different SE-SMB systems - such as those using H.I.C or mixed-mode resins - should also be amenable to description in the same design space and through the same derivation of dimensionless numbers as described in this chapter.

It is arguable that the N-theory approach to design of SE-SMB systems is better to the alternative Triangle Theory approach, even if consideration is only given to the design of ideal SE-SMB systems. There are certain advantages to designing systems within a 3D space as opposed to a 2D space. One aspect of the 3D design space is that the designer is able to straight-forwardly design systems explicitly robust to either ligand loss, flow rate variation, or modulator deviation. Such robust design in the Triangle Theory design space is complicated by the fact that the switching frequency and flow-rate control variables are collapsed into dimensionless ‘flow-rate ratio’ axes; therefore, the consequences of either flow-rate variation or ligand loss may only be foreseen once potential deviant operating conditions are converted into a ‘safety margin’ of flow-rate ratios. Another aspect of N-theory design is that the sequential design process begins at the Z2 operation point, which – for productive separations involving large modulator steps – is also generally the least robust operation point given its proximity to the stationary curves at high modulator concentrations. The N-theory design method endows the designer with more flexibility to manage the tradeoffs between productive and robust design of this sensitive operation point in comparison to triangle theory, because selection of the Z2 operating point through the N-theory design method does not require pre-selection of any modulator concentrations or liquid flow rates.

However, there are a couple of issues with N-theory which prevent its immediate application to the design of certain industrial applications:

First, the theory presented in this chapter will need modification for other modulators which interact with sorbents. For example, certain organic solvents are retained by SMB sorbents, and their binding behaviour is described by non-linear isotherms [33,106,110]. Currently, no framework exists for the design of such separations apart from iterative computational modelling or experimental optimization.

Second, the design space for separation of feed species which have slow mass-transfer – such as large biological macromolecules – will differ from that determined only by equilibrium-controlled separations. Future work is needed to adapt N-theory to describe systems of slow mass-transfer.

Third, competitive non-linear isotherm behaviour is a common feature of productive industrial separations, thus a design framework based upon the assumption of linear isotherms will not accurately inform SE-SMB design under overload conditions. Non-linear isotherm behaviour makes inapplicable both the SWA-type design constraints as well as the  $\Omega$ -type design constraints presented in this chapter. However, modulator perturbations will still affect non-linear SE-SMB systems.

Experienced SMB operators will know that a common ‘rule of thumb’ for efficient SMB design under non-linear condition is for the designer to employ high switching frequencies [2]. For SE-SMB systems, both a large modulator step and a high switching-frequency serve to linearize the isotherms, but the pairing of these two operation conditions is accompanied by the generation of significant modulator perturbations. The  $\Psi$  constraint is thus very likely to influence the design of SE-SMB systems under non-linear conditions, because – unlike the  $\Omega$  constraints – the  $\Psi$  constraint is concerned with stabilizing the size and position of the modulator step in an SE-SMB system rather than describing the migration behaviour of feed species. Describing the migration of feed species under competitive non-linear isotherm conditions in SE-SMB systems is deferred to future work, but the topic of applying stepwise-elution schemes to non-linear ternary separation is the subject of the next chapter.

# CHAPTER 4 STEPWISE-ELUTION SMB SYSTEMS FOR NON-LINEAR TERNARY BIOSEPARATIONS

## 4.1 Introduction

The previous chapter investigated the modulator dynamics of SE-SMB systems under linear isotherm conditions, and described how such modulator dynamics pertain to the design of robust and productive binary SE-SMB separations. This chapter seeks to extend these insights to inform design of productive ternary SE-SMB systems under high feed-loading conditions.

Furthermore, this chapter addresses the question of whether ternary SE-SMB systems, if appropriately-designed to operate productively under overload conditions, are competitive with other approaches to down-stream bio-process intensification. Various means to achieve process-intensification of preparative chromatography have been proposed in recent years, including: Recycle batch chromatography, SMB chromatography, MCSGP, Pseudo-SMB chromatography, and various types of hybrid SMB-batch chromatography[11,18,19,32,42,49,52,59,105,111–118]. It is an open question as to which method best suits industrial downstream bioprocessing.

One reason why there is no favoured approach to process-intensification of polishing chromatography is that proper theoretical comparison between different operating modes involves very challenging multi-dimensional optimization problems. Also, a fair comparison is difficult to design or achieve when the subjects of comparison differ in so many aspects. An example of this problem may be seen in the comparison between an optimized batch and an SMB process; here, the batch column length parameter can arguably be chosen to equal the length of either: 1) an individual SMB column, or 2) an SMB zone, or 3) the two SMB zones which flank the feed port, or 4) the entire SMB column series. For a comprehensive comparison between many intensified processes, such considerations multiply in both complexity and number.

In spite of the optimisation and fair-comparison difficulties, useful and informative attempts have been made to compare different intensified processes [69,72,116,119,120]. However, these previous studies have often not concerned themselves with comparing process performance on the types of separation problems relevant to the bioprocessing industry, which simultaneously involves features such as: small separation factors, non-linear isotherms, high mass-transfer resistances, and centre-cut (non-binary) separations from multi-component mixtures. Despite the lack of comparison studies relevant to industrial bioseparations, given the historic employment of SMB systems for the

industrial separation of challenging small-molecule mixtures, there is reason to believe that SMB-type separations can out-perform batch and recycle-batch processes (in terms of productivity, yield and separation resolving-power) for many bio-separation problems [69].

Another problem with the task of comparing different intensified processes is the very large size of the SMB family of processes. There are many different SMB configurations and operation modes which have been proposed, demonstrated, and compared [18,45,72,121]. Of this family, it is not clear all are equally suited for application to bioprocessing problems. It is also unclear whether the traditional isocratic operation mode for SMB processes has unduly restricted previous attempts to explore the suitability of SMB for biological separations problems, given that non-isocratic SMB operations are rarely reported in the literature.

It is unfortunate that SE-SMB schemes have received less attention than isocratic SMB separation schemes and other intensified batch-type separation processes. SE-SMB schemes are comparatively simple to operate in comparison to many other intensified-processing approaches, and they are also particularly adept for the separation of biological macromolecules. This latter point derives from the fact that what is true for single column batch chromatography is also true for SMB chromatography: modulator steps can significantly improve process productivity, separation resolution, and eluted-product concentration[1,30]. It could be the case that SE-SMB separations are under-investigated in part due to the fact that important design constraints required for their successful operation were only recently formally proposed [1].

Unlike SE-SMB, a great deal of work has already been performed on various systems which apply linear modulator-gradients to 'SMB-type' systems [64,68,112]. The advantages of this approach (MCSGP) to challenging bioseparations problems, in comparison with other approaches (SMB, SE-SMB, common recycle-batch chromatography techniques) has yet to be demonstrated.

#### **4.1.1 Motivation for Chapter 4**

The purpose of this chapter is to define and investigate SE-SMB operational modes for application to the type of challenging, non-linear, centre-cut separations which are industrially-relevant. These operational modes – one of which is presented here for the first time – are demonstrated experimentally. Furthermore, a comparison is made between various popular batch, intensified-batch and SE-SMB operation modes through a computational optimization. The computational comparison method is informed by the theory supplied by both this chapter and that

of the previous chapter. The comparison should therefore provide more relevant results for the bioprocess industry with respect to the existing literature.

## 4.2 Theory

While SMB is often used for industrial separations of binary enantiomeric mixtures, it may also be applied to preparative, ternary, bio-separation problems. Ternary separations involve the separation of two groups of contaminating species from a protein product. These contaminating species may be conceptually grouped into 'strong' (S) and 'weak' (W) sets of impurities which flank either side of the intermediately-retained product (P) in a batch-elution chromatogram. Because the intermediately retained species is the target for separation, purification of such 'ternary' mixtures are often referred to as 'centre-cut' SMB bio-separations.

Two simple approaches have traditionally been used to adapt binary SMB systems for isocratic ternary separations. The first is an SMB 'cascade', and the second is an 'integrated' or 'single-train' separation scheme. (Note that some nomenclature differences exist in the literature for various configurations.)

Since SMB has historically been applied to binary separations, it follows that a popular means of performing ternary separations is to use a 'cascade' of binary separation trains. In such a system, the first binary separation train removes one feed species from the other two. Subsequently, a binary SMB separation is performed on the two remaining species, thus purifying the centre-cut product.

Another approach to centre-cut SMB separations is through an 'integrated' SMB configuration. Integrated SMB schemes perform centre-cut separations through use of a single separation train; an example of a five zone integrated SMB configuration is shown by Figure 4-1A. In integrated systems, perfect separation of three species is possible; the S impurity is collected from outlet 'E1', the centre-cut product is collected from the 'E2' outlet, and the W impurity from the Raffinate outlet. Such 'perfect' separation is achievable because SMB, unlike True Moving Bed (TMB) chromatography, does not entail inevitable pollution of the centre-cut fraction by the strong impurity [44,47,48,51,53].

Though SMB is often operated isocratically, the separation performance of biological macromolecules by SMB may be greatly improved with modulator stepwise-elution schemes. The

following theory sections will introduce new considerations which influence the design and relative desirability of various integrated and cascade stepwise-elution SMB schemes.

#### **4.2.1 Optimal approaches to integrated stepwise elution centre-cut SMB separations**

There are at least two features of traditional integrated SMB schemes which frustrate non-isocratic separations of challenging multi-component mixtures.

The first problem of applying stepwise-elution schemes to integrated SMB systems is the generation of modulator perturbations from multiple loci. As detailed in the previous results chapter, Modulator Perturbations (MPs) are generated in SMB systems through port-switches which periodically dislocate the alignment between the feed port and the modulator step position. This does not occur in TMB systems, where the feed port and modulator-step point are fixed to one location. Because of modulator perturbations, more process design-constraints apply to SE-SMB than to isocratic SMB systems; these constraints stabilize the periodic modulator profile and ensure feed species exit the system through the correct outlet port [1]. For integrated SE-SMB schemes, such as the 5-zone integrated SE-SMB, MPs are periodically generated at both the feed port and at the second desorbent port (See Figure 4-1A). Because of these MPs in integrated SE-SMB schemes, successful separation performance requires compliance with modulator-related design constraints. These modulator constraints for integrated SE-SMB schemes (which are adaptations of the  $\Omega$  and  $\Psi$  constraints presented in [1] for binary SE-SMB) frame a much smaller design space compared to that of corresponding TMB (or ideal SMB) models which do not account for modulator perturbations.

Another drawback to traditional integrated SE-SMB schemes is that for mixtures which require a large concentration range of modulator for product separation and sorbent regeneration, the modulator concentration's zero-lower bound (ZLB) can severely constrain the modulator step sizes in the integrated stepwise-elution train. This is because flow rate (i.e. pressure drop) constraints apply to the columns used in SMB; in addition to the fact that the modulator concentration in the second desorbent stream and the feed stream cannot be below zero, these constraints can make design of an efficient integrated process challenging.

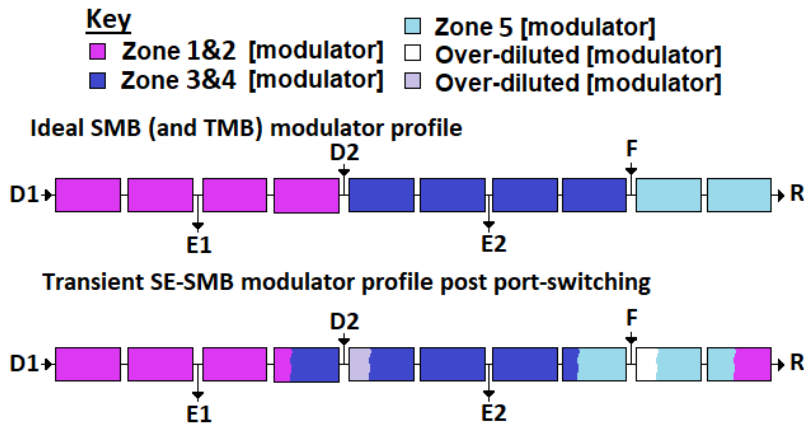
Here, a new integrated SE-SMB process design which can overcome these two design constraints common to most other integrated SE-SMB schemes, is presented.

The Wang research group have previously patented a configuration of SMB for binary-separations which improves sorbent-utilization through reducing Zone 1 (Z1) to a single column [46].

This column is detached from the SMB column series, and its contents (the more-retained component in a binary separation) may be eluted through use of a pump and buffer independent to that of the desorbent. This approach to binary separations (involving detachment of a single Z1 column) has subsequently found application to isocratic ternary separation problems, and has been named as 'Three-Fraction SMB' (3F-SMB) by the Morbidelli group [51,122]. In 3F-SMB, the S impurity is eluted from the detached Z1, the product is eluted from the extract port, and the W impurity is eluted from the raffinate port.

As reported here, aspects of the Wang and Morbidelli groups' inventions may be combined to construct an integrated ternary SE-SMB scheme. A stepwise-elution scheme is used to increase productivity in the new integrated SMB configuration, and a 'Wash' buffer – independent to that of the desorbent - is used to elute the S impurity as well as regenerate the Z1 column. This new separation configuration is named the Step And Wash (SAW) SMB scheme for convenience, and is illustrated by Figure 4-1B. It has the advantage of a larger design space compared to traditional integrated SE-SMB schemes such as that in Figure 4-1A, since 1) modulator perturbations are only generated from one locus, and 2) the desorbent input does not need to step the modulator concentration from the wash buffer, so the ZLB of the modulator concentration does not constrain the design space of the Zone 1&2 modulator concentration.

### A) MPs in integrated SE-SMB



### B) Step And Wash (SAW) configuration

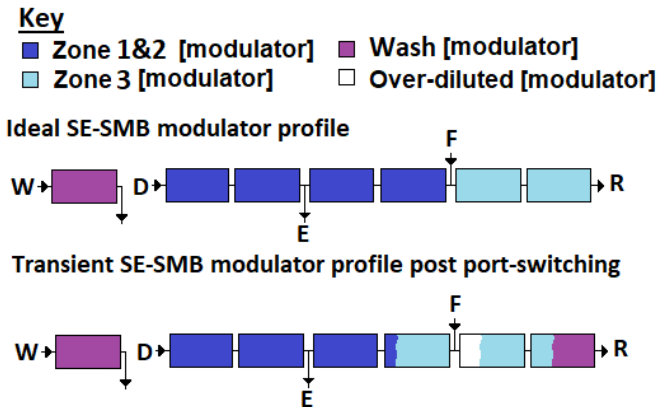


**Figure 4-1 Integrated ternary SE-SMB schemes.**

**A)** A five-zone integrated SE-SMB generates modulator perturbations (shown as plugs of ‘over-diluted modulator’) from multiple loci, as do other classical integrated SE-SMB schemes **B)** The Step and Wash (SAW) SMB configuration generates only one modulator perturbation per port-switch.

#### 4.2.2 Optimal approaches to cascade centre-cut SE-SMB separations

This section considers four theoretical considerations which may influence the design of optimally productive SMB cascades; these considerations are: 1) The impact of MPs on inter-train cascade-coupling, 2) The impact of non-linear conditions on optimal inter-train cascade coupling mode, 3) The impact of Z3 length on optimal cascade productivity, and 4) The productivity gain from adoption of the ‘Wang configuration’ for Z1 in each binary separation train of a cascade.

The first design consideration for SE-SMB cascades involves accounting for modulator perturbations. Since MPs only register in the raffinate outlet, but not the extract outlet, raffinate-coupled SE-SMB cascades can benefit from a mixing tank to intermediate liquid flow between the cascade’s separation trains (shown by Figure 4-2). This mixing tank should smooth-out MPs, and thus

prevent additional modulator-related design constraints from further confining the design space of the second separation train. The mixing tank arrangement means that only the established binary SE-SMB modulator constraints (which are  $\Psi$ , and also  $\Omega$  for linear isotherm conditions as defined in the previous chapter) must be satisfied for successful SE-SMB separations in both trains.

#### A) Six-Zone SE-SMB Cascade

##### Key

- T1 Zone 1&2 [modulator]    ■ T2 Zone 1&2 [modulator]
- T1 Zone 3 [modulator]      ■ T2 Zone 3 [modulator]

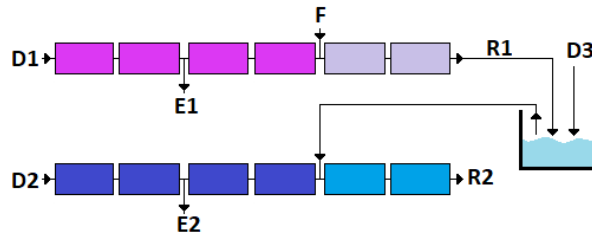


**Figure 4-2 A centre-cut separation of a ternary mixture through a raffinate-coupled SE-SMB 6-zone cascade configuration with intermediary buffer tank**

The cascade's ideal SE-SMB modulator profile is shown by different colours. Symbols:  $D_1$ ,  $D_2$ ,  $D_3$ , refer to the first train's desorbent, the second train's desorbent, and the dilution stream into the intermediary mixing tank respectively. The symbols 'E', 'F', and 'R' refer to extract, feed and raffinate streams; 'T1' and 'T2' refer to the first and second separation trains respectively.

The second and third design considerations concern the optimal zone lengths and coupling between separation trains under non-linear conditions. Given that extract-coupling between the two separation trains in an SMB cascade does not require additional downstream (second train) design-consideration of MPs, or an intermediary buffer tank, it may appear that extract-coupled cascades are preferable to raffinate-coupled cascades. Indeed, since previous studies comparing raffinate- and extract-coupled isocratic cascade configurations have shown no difference in (sorbent-specific) productivity, much complexity in the design and operation of SE-SMB cascades could be avoided by extract-coupling without compromising productivity [42,119]. However, these studies which compared raffinate- and extract-coupled cascades were based on linear isotherm conditions; efficient industrial bioprocessing with SE-SMB cascades will most-likely not operate within the linear-isotherm range. The author is not aware of studies which compare the coupling of SMB cascades under non-linear conditions, and thus cannot assume that productive equivalence exists between the coupling alternatives. Consequently, it has yet to be shown that the complexity of raffinate-coupling is sufficient to justify universal extract-coupling in cascade design.

It is hypothesised here that binary SMB separations are actually ‘asymmetrically productive’ when run under non-linear conditions, for reasons explained in the next paragraph. ‘Asymmetric productivity’ is defined as the existence of a difference between the maximum production rate of a feed component (units: grams/hour) from the extract port, as opposed to the maximum production rate of the counterpart feed component from the raffinate port, normalized with respect to the initial feed composition. This asymmetry hypothesis is pertinent to the design of SMB cascades, because – if it is assumed that the column dimensions, sorbent packing, and zone lengths are comparable between the separation trains (i.e. the dimensions in the first separation train are not larger than in the second separation train) – ternary cascades will feature more non-linear behaviour in the first separation train than in the second. This is because the rate of feed-delivery (in units of grams per hour) into the second SMB train is less than that for the first separation train, as 1) removal of one from three feed species should have occurred, and 2) the mass-balance ensures that the rate of feed-delivery for the two remaining feed components must equal (and not exceed) the rate of feed delivery in the first SMB separation train. Therefore, if binary SMB separations are indeed asymmetrically productive under non-linear conditions, the productivity-equivalence between extract- or raffinate-coupled cascades will not hold.

It is believed that binary SMB configurations may be asymmetrically productive due to the fact that different SMB control variables limit the maximum mass flow-rate of the extract and raffinate streams. First, consider the extract productivity: the extract mass-flow rate is determined by a combination of the rate at which columns are switched into Z1, and the saturation capacity (of sorbent and solvent) of each column being switched into Z1. Both the saturation capacities of columns, and the port-switching frequency, have upper limits. The upper limit of a column’s saturation capacity is determined by physiochemical characteristics such as column dimensions, void fraction and ligand density. For port-switching, the switching frequency is limited by the maximum flow rate (or pressure drop) of columns which may be exploited in order to fulfil the separation’s design constraints (which are the  $\Psi < 1$  constraint and the  $Q_2 > \varepsilon \cdot V \cdot \omega$  constraint for SE-SMB systems in the most-favourable case of an unretained LRC in Z2). Given that the port switching frequency and the column saturation capacity both have upper limits, it follows that there is a theoretical maximum extract mass flow-rate for any SMB system. However, the maximum raffinate mass flow-rate is controlled by different factors from that of the extract. In the case of the raffinate, the mass flow-rate of the LRC is dependent on the liquid flow-rate in Z3 and the saturation limit of the LRC feed species in the liquid. The other factors which control the maximum extract mass-flow

rate – switching time and column saturation capacity – do not affect the raffinate product's theoretical maximum mass-flow rate, though they do influence raffinate product purity and yield.

The idea that SMB binary separation trains are asymmetrically productive at the raffinate and extract outlets should not be particularly controversial for the aforementioned reasons. More controversially, it is hypothesised that SMB binary separations will be asymmetrically productive even under stringent purity constraints for either the extract or raffinate product streams. This hypothesis is based upon the observation that, as different SMB operation variables control the productivity of the extract and raffinate products, so too do different SMB operation variables control the purity of the extract and raffinate product streams.

For the extract product stream, purity depends on the ability of the SMB operating conditions in Z2 to carry the LRC in the direction of the liquid flow at a faster velocity than the port switching carries the LRC in the direction of the extract port. Therefore, the SMB operation parameters which control the extract product purity are the Z2 liquid flow rate, the Z2 modulator concentration, the switching frequency, and the feed loading (which influences the competitive binding interactions between LRC and MRC species within Z2). On the other hand, the purity of the raffinate product is controlled by the Z3 liquid flow rate, the Z3 modulator concentration(s), the switching frequency, and the feed loading. It has already been shown for linear isotherm SMB systems, for which the feed loading does not influence the purity or productivity of the extract or raffinate products, that the other SMB control variables in Z2 and Z3 cannot produce asymmetric productivity in a binary separation [42,119]. However, for SMB systems operated under non-linear isotherm conditions, a simple thought experiment suggests that competitive binding behaviour has an asymmetric effect on yield and purity of the extract and raffinate products. In Z2, for a non-azeotropic, fast mass-transfer, competitive Langmuir-isotherm system, increased competitive binding - brought about by increasing feed loading – should always promote improved extract product purity, because the competitive binding will increase the LRC migration velocity in Z2 with respect to the port-switching velocity and the MRC velocity. However, given the previously-hypothesised upper limit to extract outlet productivity, the improvement to extract product purity wrought by increased feed-loading of SMB systems will, above a certain feed-loading threshold, be marred by a loss of extract product yield; the MRC in such a system will pollute the raffinate outlet once the maximum extract-outlet productivity level is met.

A different set of factors apply to influence the maximum productivity of the raffinate outlet under the conditions of high feed-loading. In Z3, competitive binding interactions are also favourable to promoting a faster migration velocity of the LRC with respect to the MRC migration velocity and port-switching velocity. However, by contrast to the situation in Z2, the purity of the raffinate should be controlled by the saturation capacity of the entire set of columns in Z3. For a simple fast-mass transfer binary separation in which – even under non-linear conditions - the MRC is strongly retained in Z3, this hypothesis stems from the idea that complete binding-site saturation of all post-feed columns with the MRC species must occur before the MRC can contaminate the raffinate. Therefore, an increase in the number of columns in Z3 is hypothesised to increase the feed-loading range of an SMB system without concomitant compromise of raffinate purity. Conversely, it is hypothesised that increasing the number of columns in Z2 will not facilitate any improvement in SMB productivity for fast-mass transfer systems; this hypothesis should hold for either extract or raffinate outlet products.

The fourth design consideration also concerns the optimal zone length. Apart from the hypothesised raffinate-product productivity-gains from increasing the Z3 length, there is another zone in ternary SE-SMB cascades which may be straight-forwardly optimized for process productivity. As reviewed by the preceding section, the Wang group's modification of classical binary SMB schemes –which substitute an integrated Z1 with a detached single Z1 column subject to a bespoke pump and buffer – significantly improves the productivity of a binary separation by Z1 length-shortening [46]. In addition to the productivity gain from this configuration, it is also possible to exploit the extra degrees of design freedom to increase the concentration of the extract outlet streams. The design of a concentrated outlet stream is easily achievable by selection of a low flow-rate and high modulator concentration for the Z1 (or Wash) buffer.

It is suggested that the Wang group's binary SMB configuration should be implemented in both separation trains of ternary SE-SMB cascades, as productivity in both cascade sections may be improved through the reduction in sorbent volume. However, if inter-train coupling is mediated through the raffinate outlet of the first train, the Wang configuration may cause a particular problem. As shown by Figure 4-1B, when Z1 columns are switched into Z3, they periodically carry one column-volume of Z1 buffer (which has a high modulator concentration) into Z3. This column volume of high modulator-concentration buffer is subsequently eluted into the raffinate outlet and the buffer mixing tank is required to smooth out all such modulator perturbations in raffinate-coupled cascades (see Figure 4-2). Design of a raffinate-coupled cascade often requires dilution of the feed modulator concentration into the second separations train, since the product (the MRC in the raffinate-coupled

cascade's second separation train) needs to be more retained in the second separation train than it was before its raffinate-elution in the first separation train. This dilution flow rate can cause design problems, because it can force a high feed flow-rate to apply to the second separation train, which in turn can reduce the design space and thus the yield/productivity performance of this second train. However, it is possible to reduce to dilution flow-rate in the intermediating buffer tank if the contribution of high modulator-concentration buffer from the Z1 column is diverted or prevented.

A simple way to prevent this high modulator-concentration from entering the intermediary buffer tank is to introduce a sub-step to each switching period of the first train's operation. After washing the Z1 column with a high modulator-concentration buffer, a sub-step involving quick re-equilibration of this column with a low modulator-concentration buffer before the following port-switching period should reduce the need for a high flow-rate dilution of the second train's feed buffer. In turn, this reduces the necessary flow-rate into the second separation train to fulfil the inter-train mass balance requirements, and thus opens up more design space in Z2 for slower switching frequencies and use of lower second-train desorbent-modulator concentrations.

#### **4.2.3 Performance differences in integrated and cascade centre-cut SE-SMB separations**

Chromatography steps in bioprocess tasks typically involve the purification of a product from a challenging mixture. In this context, a 'challenging mixture' refers to a poorly-resolved multi-component ternary separation problem; examples of this sort of chromatography problem include purification of specific product variants from a mixture of variants (i.e. sialylated mAbs from asialylated mAbs) as well as purification of product from unfavourable host-cell protein profile background.

The strict purity requirements which apply to biopharmaceuticals promote the use of downstream purification processes capable of high-resolution separations. This section will make the universal case that traditional SMB cascades have more resolving power in comparison to single column batch techniques and single-train continuous processes such as the SAW SMB.

As shown by the chromatograms in Figure 4-3, single-train separation processes may be used to collect pure fractions from ternary separations only in cases where the ternary mixture is subject to high separation-resolution. The chromatograms in Figures 4-3B&C illustrate cases of more challenging ternary mixtures where high separation-resolution is unachievable. When separation-resolution is poor, it is impossible to collect fractions of high purity from challenging mixtures due to the overlapping concentration profiles of the product and flanking contaminants.

For poorly-resolved mixtures, pure fractions may instead be collected by transforming the approach to the separation problem from that of a single separation-train process to that of a two separation-train process. An example of a two-train separation process is the SMB cascade, which performs two sequential binary separations on a ternary mixture. This permits collection of a pure product fraction from a challenging ternary mixture, because any separation problem amenable to chromatographic processes must, by definition, be capable of resolving binary mixtures to the extent that pure fractions are collectable.

It is therefore hypothesised that the maximum centre-cut fraction purity achievable through single-train SMB schemes (e.g. MCGSP, SAW SMB, pseudo-SMB) is inversely proportional to a separation's difficulty, or else inversely proportional to a resin's ability to resolve different components. By contrast, as has been well-established for SMB separations, a separation's difficulty does not affect the maximum purity of the centre-cut fraction which may be collected from SMB cascades, although the productivity of such systems is affected by factors such as the separation difficulty[119] .

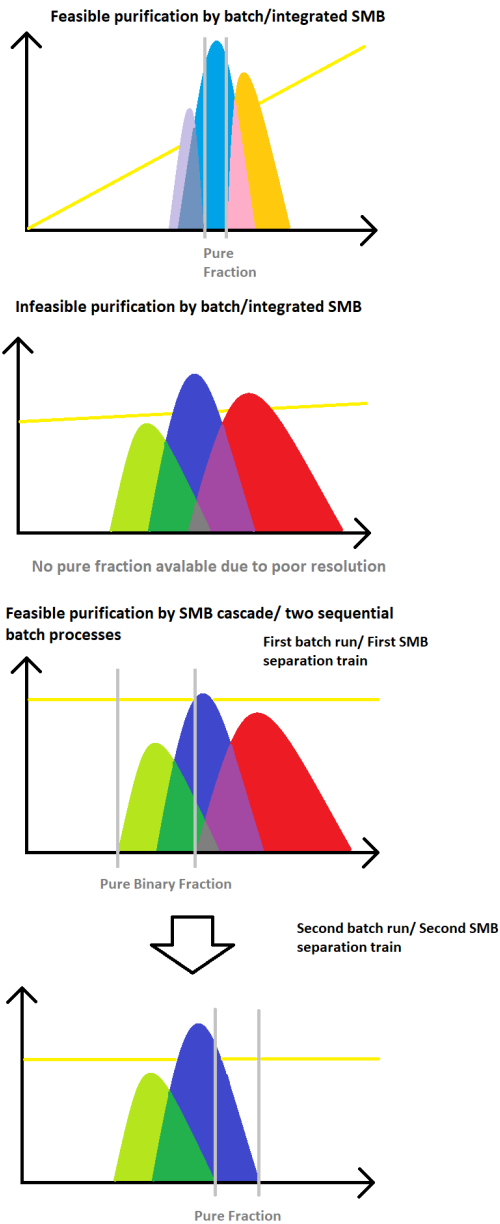


**Figure 4-3 Resolving Power differences between chromatographic processes**

Resolving power differs between single train and cascade (or sequential) separation processes for ternary separation problems where the intermediate component (blue) is the product flanked by contaminants. **A)** A single train purification of a highly-resolved ternary mixture permits collection of a pure fraction, **B)** A single train purification of poorly-resolved mixture does not permit collection of pure fractions, **C)** A cascade SMB, or sequential batch process, permits collection of a pure fraction from a poorly-resolved mixture.

## 4.3 Results and Discussion

### 4.3.1 Experimental batch, SE-SMB cascade, and SAW SMB separation of a model ternary proteinaceous mixture

For the purpose of experimental demonstration, a non-challenging model ternary protein mixture (of composition ratio 1:8:1 for  $\alpha$ -chymotrypsinogen: $\beta$ -Lactoglobulin:Lysozyme proteins) was separated by three different approaches: 1) Single-column batch, 2) SAW SMB, and 3) SE-SMB cascade (raffinate-coupled through intermediary mixing tank).

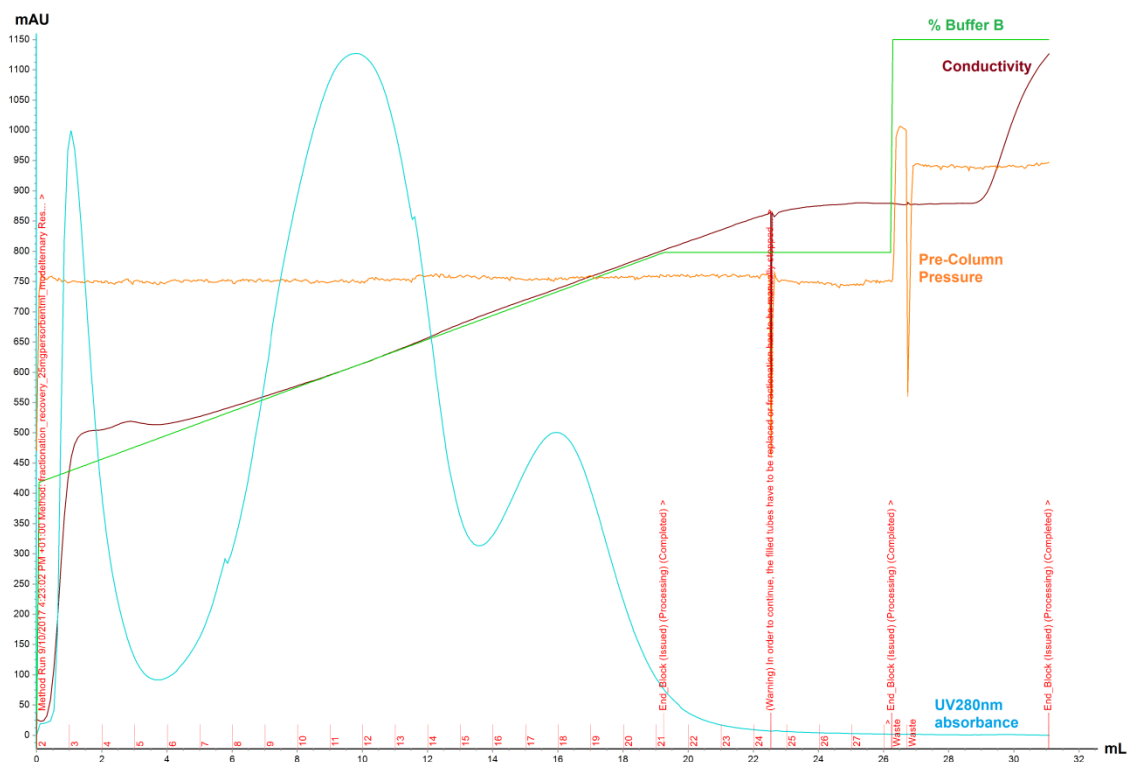


**Figure 4-4 Single column batch chromatogram of model ternary protein separation**

Loading onto the sorbent was 25 g/L; 1mL (0.5 CV) fractions were collected for purity analysis; outlet absorbance was measured at UV280nm.

The results of these laboratory demonstrations, which were not experimentally optimized, are listed in Table 4-1. Experimental details for the three separation modes are listed in Table 4-2.

**Table 4-1 Model ternary mixture separations through various chromatographic approaches**

Process	Product Purity	Yield	Productivity, g/L/hr
Single-Column Batch	>99%	~64%	~38
SAW SMB	>90%	~75%	~23
SE-SMB Cascade	>99%	~70%	~91

\*Calculated by classifying fractions with purities >99% as 'collected' fractions; other fractions were classified as 'waste' fractions and were not subject to any recycle-chromatography steps

Figure 4-4 and Figure 4-5 display some of the experimental chromatograms generated in the model ternary separations.

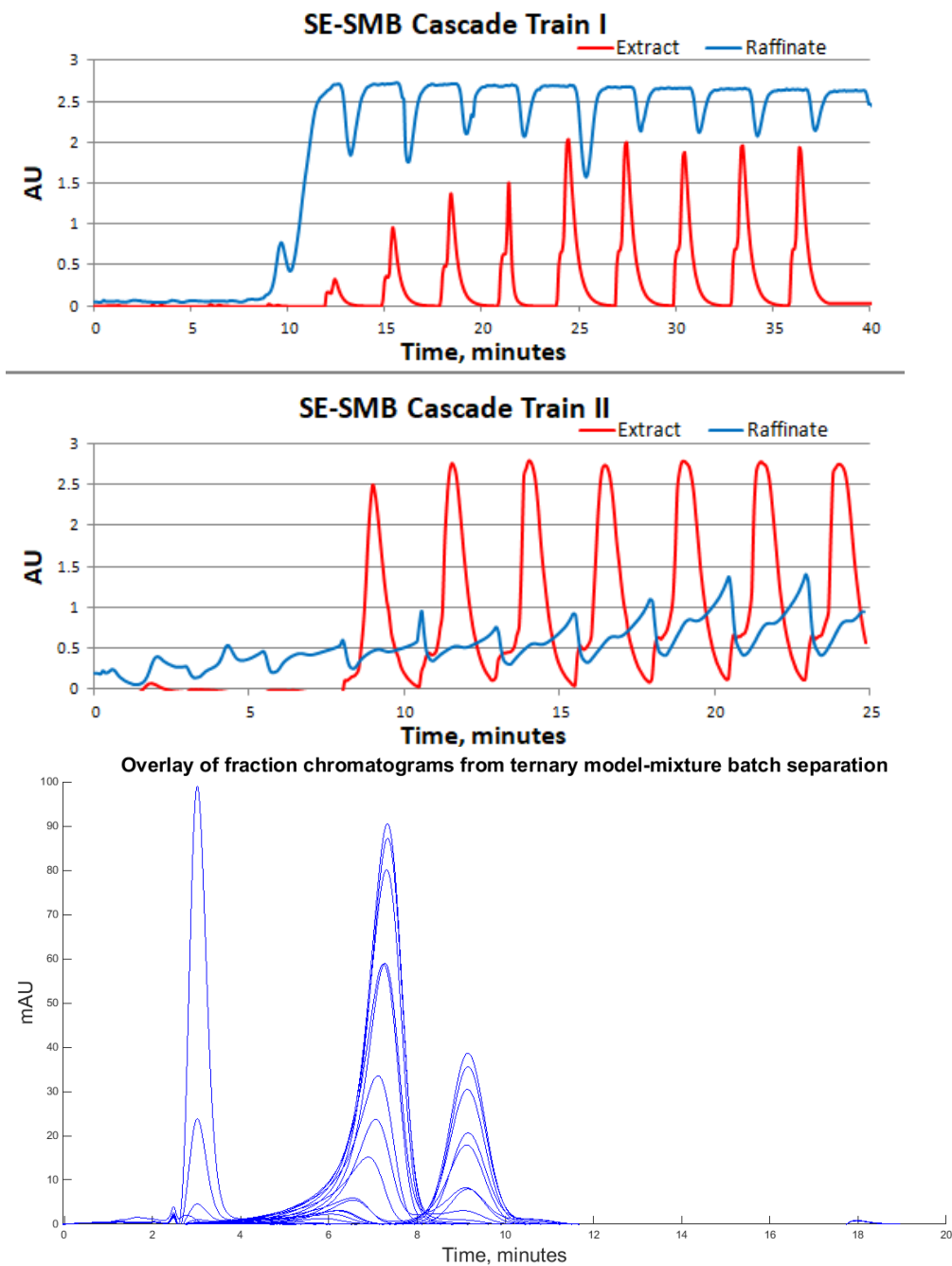


**Figure 4-5 Experimental Separations of Model Ternary Protein Mixture**  
**Top)** Outlet absorbance patterns from first binary separation train (T1) in the SE-SMB cascade  
**Middle)** Outlet absorbance patterns from second binary separation train (T2) in the SE-SMB cascade  
**Bottom)** Overlay of analytical chromatograms from fractions of batch separation

**Table 4-2** Operation conditions of centre-cut experiments

<b>SAW SMB Parameters (Model Mixture)</b>	<b>Values</b>
Wash flow-rate, mL/min	2
Desorbent flow-rate, mL/min	3
Extract flow-rate, mL/min	1.75
Feed flow-rate, mL/min	1.2
Switching time, minutes	5
Wash [NaCl], mM	600
Desorbent [NaCl], mM	430
Feed [NaCl], mM	170
Total feed protein concentration, mg/mL	5
Column configuration	1-3-2-2
Total sorbent volume, mL	8
<b>SMB Cascade Parameters (Model Mixture)</b>	<b>Values</b>
T1 Wash flow-rate, mL/min	2
T1 Desorbent flow-rate, mL/min	1
T1 Feed flow-rate, mL/min	0.7
T1 Switching time, minutes	3
T1 Wash [NaCl], mM	700
T1 Desorbent [NaCl], mM	533
T1 Feed [NaCl], mM	336
Total feed protein concentration, mg/mL	60
T1 Column configuration	1-2-3
Total sorbent volume T1, mL	7
T2 Wash flow-rate, mL/min	4
T2 Desorbent flow-rate, mL/min	1
T2 Overall feed flow-rate, mL/min	3
T2 Dilution flow-rate, mL/min	1.3
T2 Switching time, minutes	2.5
T2 Wash [NaCl], mM	700
T2 Desorbent [NaCl], mM	375
T2 Column configuration	1-2-4
Total sorbent volume T2, mL	7
<b>Batch Parameters (Model Mixture)</b>	<b>Values</b>
Gradient starting [NaCl], mM	375
Gradient final [NaCl], mM	700
Gradient duration, CVs	10
Flow rate, mL/min	1
Total feed loading, mg/mL of sorbent	25
Total processing time per batch run, minutes	20
HiTrap SP HP batch column dimensions, cm	5x0.7(i.d.)
Total sorbent volume, mL	2

#### 4.3.2 Experimental SAW separation of challenging ternary proteinaceous mixture

The SAW SMB was demonstrated with a challenging separation problem through its application to a centre-cut separation of ovalbumin variants. The term ‘ovalbumin variants’ is used to describe the mixture of phospho-, glyco-, sequence-, and quaternary-structure variants that may be found in certain commercially available hen-egg albumin preparations. The three SAW-SMB outlet ovalbumin fractions collected experimentally were compared by the overlaid outlet-fraction analytical chromatograms shown in Figure 4-6. An analytical chromatogram of the ovalbumin feed mixture, used for this SAW SMB separation, is shown by Figure 4-7. These analytical chromatograms were generated through use of an anion-exchange monolith; further relevant experimental details may be found in the Materials and Methods section.

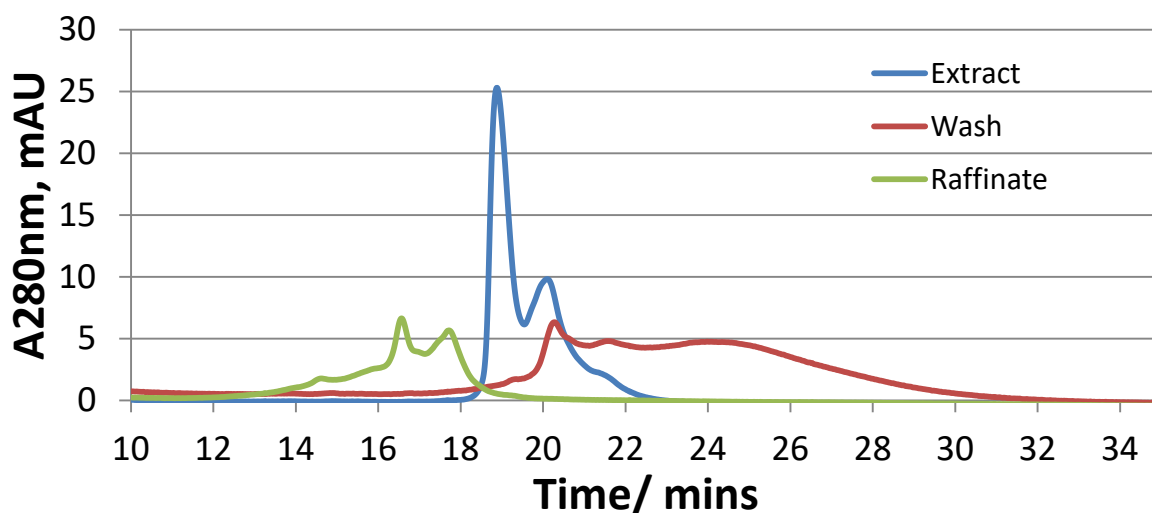


**Figure 4-6 Three fractions (Extract, Wash and Raffinate) of ovalbumin variants (overlaid) from a SAW SMB separation**

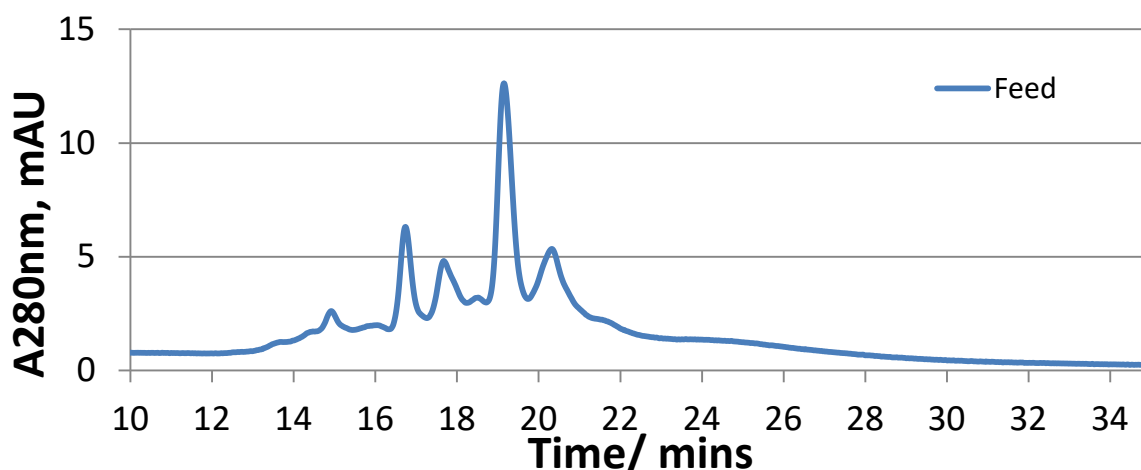


**Figure 4-7 Chromatogram of ovalbumin variants in the SMB feed**  
*(Subject to same analytical chromatography conditions as that used for SAW SMB fraction analysis).*

It is arguable that the purification of ovalbumin variants represents a challenging separation model system, as the separation factors between the variants are small and the collection of variants classed as ‘S’ or ‘W’ impurities have a large weighting in the feed composition. Table 4-3 details the experimental conditions used in the SAW SMB demonstration of a challenging centre-cut separation.

**Table 4-3 Operation conditions of SAW SMB ovalbumin experiment**

Parameter	Value
Wash flow-rate, mL/min	0.375
Desorbent flow-rate, mL/min	1
Extract flow-rate, mL/min	0.5
Feed flow-rate, mL/min	0.25
Switching time, minutes	10
Wash [NaCl], mM	500
Desorbent [NaCl], mM	150
Feed [NaCl], mM	120
Feed protein concentration, mg/ml	5
Column configuration	1-3-2-2

#### 4.3.3 Asymmetry in binary SMB performance under overload conditions

The results of two multi-objective optimizations, which attempted to find the Pareto curve of the yield of an outlet product vs. the SMB’s productivity for its purification to high purity, are shown by Figure 4-8. This optimization was subject to the constraint that the purity of the raffinate or extract product must exceed 95%. This binary optimization was applied to a three-component

feed mixture, where two of the three components were classed as ‘product’ with respect to the remaining component, which was defined as the separation train’s impurity. This definition of ‘product’ in a binary separation of a ternary mixture reflects the optimization objectives of a first separation train in a centre-cut SMB cascade.

For all simulations, 26 nodes per column were used in the finite volume discretization. The use of additional nodes for discretization was thought unnecessary, because the calculated mass balances closed within an error margin of  $\pm 5\%$ , and any ‘numerical dispersion’ caused by use of a rough mesh would be constant across the various systems simulated.

It may be seen from the figure below that SMB binary separations have different Pareto-optimal curves for extract and raffinate products, thus the hypothesis of SMB ‘asymmetric productivity’ is supported.

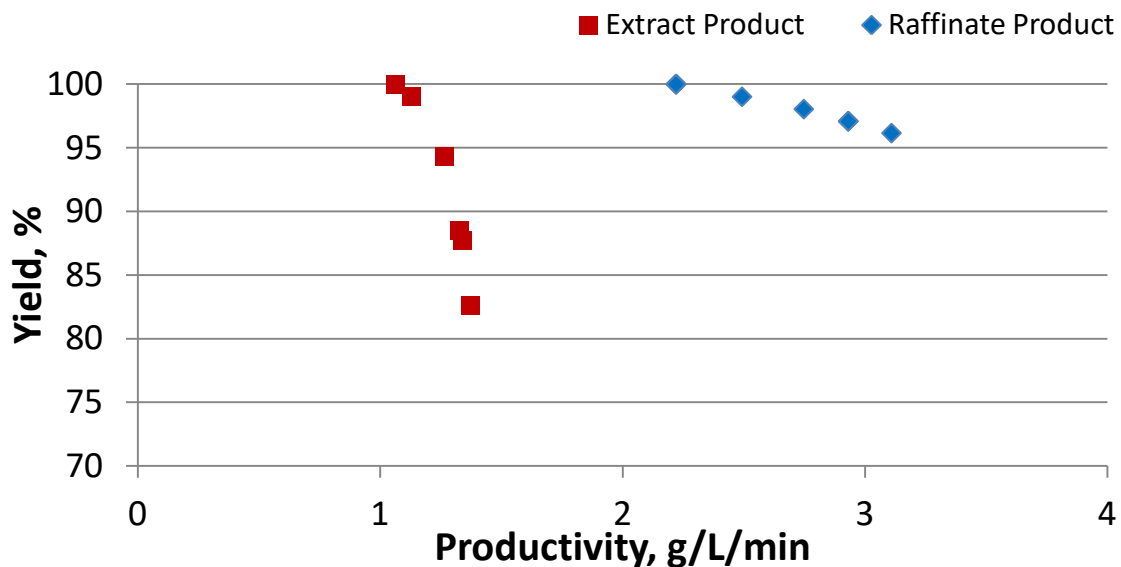


**Figure 4-8 Evidence for ‘asymmetric productivity’ in simulated non-linear system**  
 For a binary SMB system subject to  $>95\%$  purity constraint, ‘asymmetric productivity’ of extract and raffinate products is demonstrated by the offset Pareto-curves from evolutionary MOO of a simulated system.

#### 4.3.4 Effect of Z3 length on binary SMB performance under overload conditions

The results of three multi-objective optimizations, which attempted to find the raffinate product’s purity-productivity Pareto-curve for binary SE-SMB operations with different Z3 lengths, are shown by Figure 4-9. It can be seen from the figure that increasing the Z3 length shifted the

Pareto-optimal curve favourably, as hypothesised. These binary separations were applied to a two-component feed mixture, as detailed in the Materials and Methods. The Z2 length spanned two columns for all simulations.

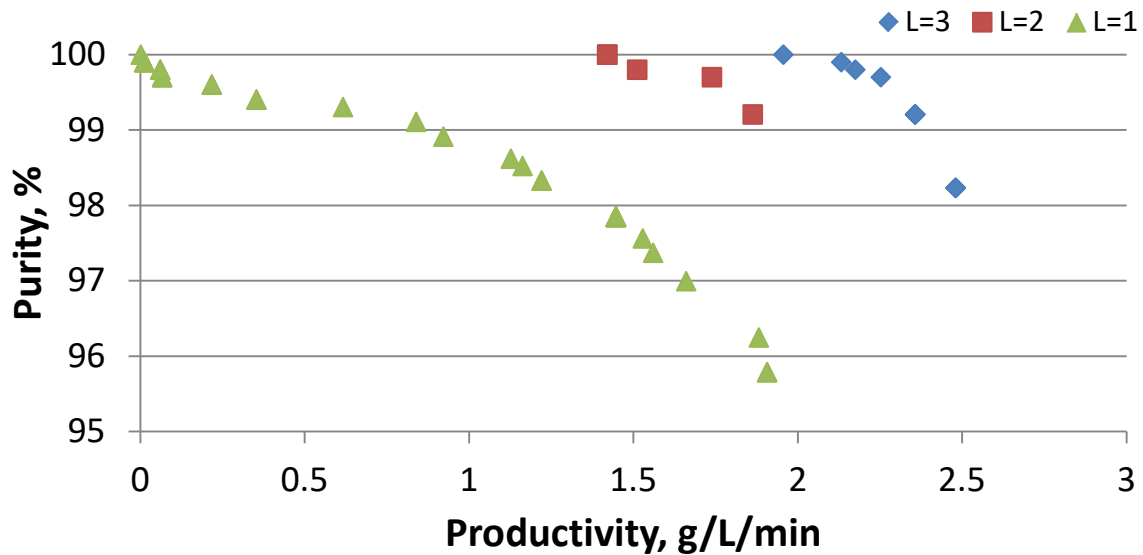


**Figure 4-9 SMB productivity and zone length (Z3) in simulated non-linear system**  
 Pareto purity/productivity curve for SE-SMB operations where the Z3 length is either one column (series L=1), two columns (series L=2), or three columns (series L=3).

#### 4.3.5 Effect of Z2 length on binary SMB performance under overload conditions

The effect of the raffinate-product's purity-productivity Pareto-curves for three different Z2 lengths (2, 3, and 4 columns) was investigated. As may be seen from Figure 4-10, and as hypothesised, no improvement to the Pareto-curve was observed from lengthening Z2. Indeed, the position of the Pareto-curve worsened as extra columns added to the SMB column series reduced the productivity whilst not facilitating any increase in feed loading.

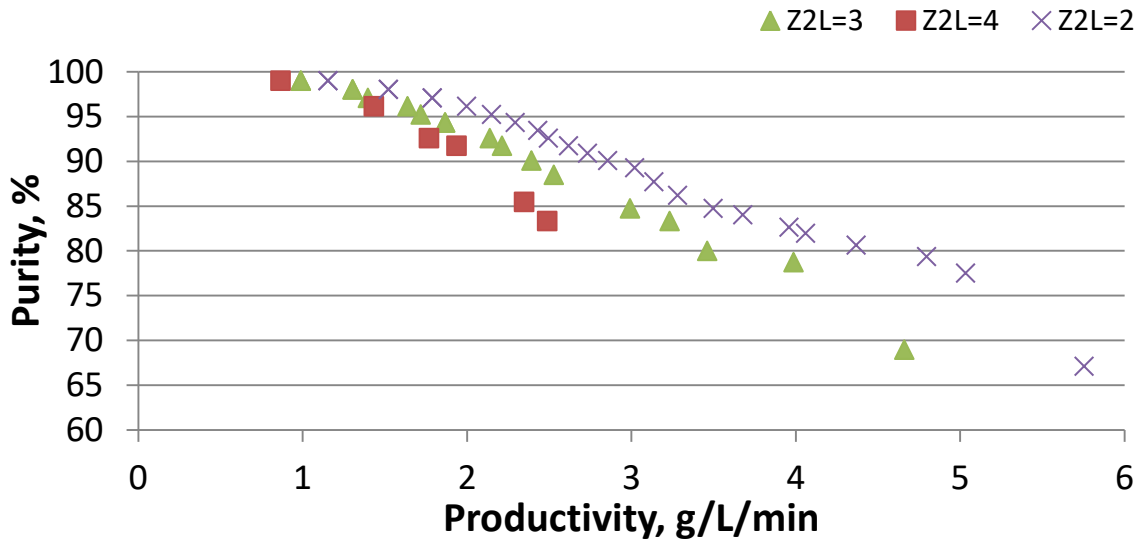


**Figure 4-10 SMB productivity and zone length (Z2) in simulated non-linear system**  
 Raffinate product's Pareto purity/productivity curves for SE-SMB where the Z2 length is either two columns (series Z2L =2), three columns (series Z2L =3), or four columns (series Z2L=4). All configurations simulated to have Z3 length of one column.

#### 4.3.6 Purity limitations of integrated separation schemes

The maximum purity of the centre-cut fraction from the SAW SMB is hypothesised to be dependent on the separation resolution of the feed mixture, hence a purity-productivity Pareto curve was found by MOO through an evolutionary algorithm for a highly chromatographically-resolvable system (with a fast mass-transfer rate) and compared to the Pareto-curve of another system which was less chromatographically-resolvable, but differed from the original system only in the fact that its mass transfer rate was slower. As can be seen from Figure 4-11, the results of the generated Pareto curves suggest a higher maximum centre-cut purity is achievable for the better resolved (fast mass-transfer) system that is possible for the poorly-resolved system in this single-train separation system. As in the other evolutionary optimization experiments, it was not possible to improve on either Pareto curve when an initial population included individuals from the other's final population.

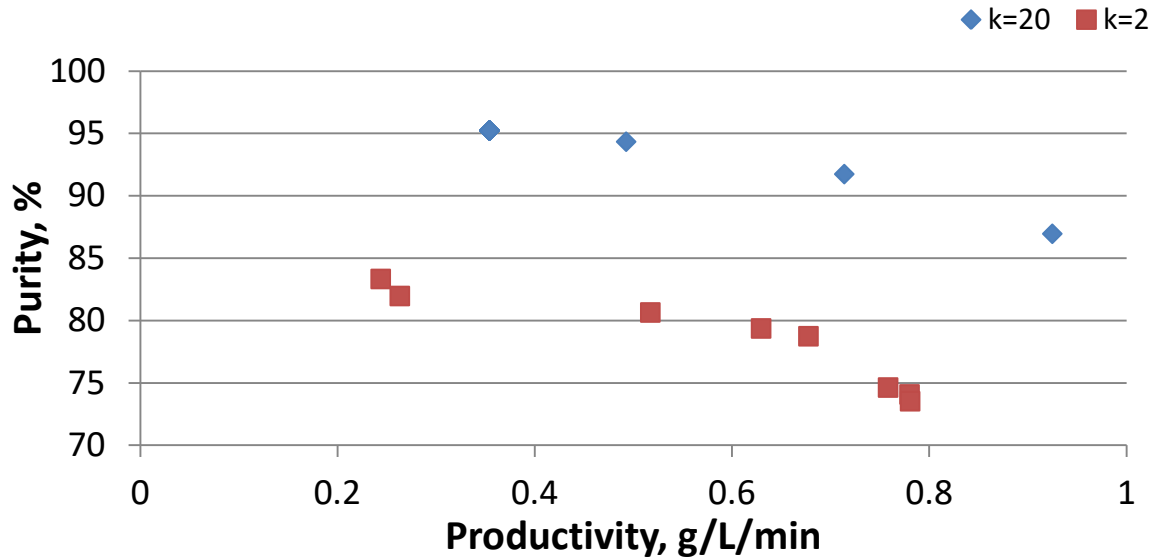


**Figure 4-11 Separation resolution affects single-train SMB performance in simulated non-linear system**

Variation of the mass transfer rate ( $k=2 \text{ min}^{-1}$ ,  $k=20 \text{ min}^{-1}$ ) affects the purity-productivity Pareto curve for SAW SMB separations

#### 4.3.7 Simulated comparison between various intensified approaches to preparative chromatography

Five intensified bioprocess operations were compared by multi-objective optimization for their ability to separate a ternary mixture under non-linear conditions. These operations are: single column batch chromatography, recycle chromatography (using the recycle-recycle method outlined in this reference[12]), SAW SMB chromatography, a raffinate-coupled SE-SMB cascade, and an extract-coupled SE-SMB cascade. The optimization of all processes was subject to the constraint of 95% product purity in the outlet stream or collected fraction. The yield-productivity Pareto-curves for these processes are shown by Figure 4-12. Details of the Pareto conditions found for all simulated processes may be found in the Appendix to this thesis. Simulations used 26 nodes per column in the finite volume discretization; all other model parameters of the simulations (i.e. isotherms, mass-transfer rates, column configurations, e.t.c) are detailed in the Materials and Methods section.

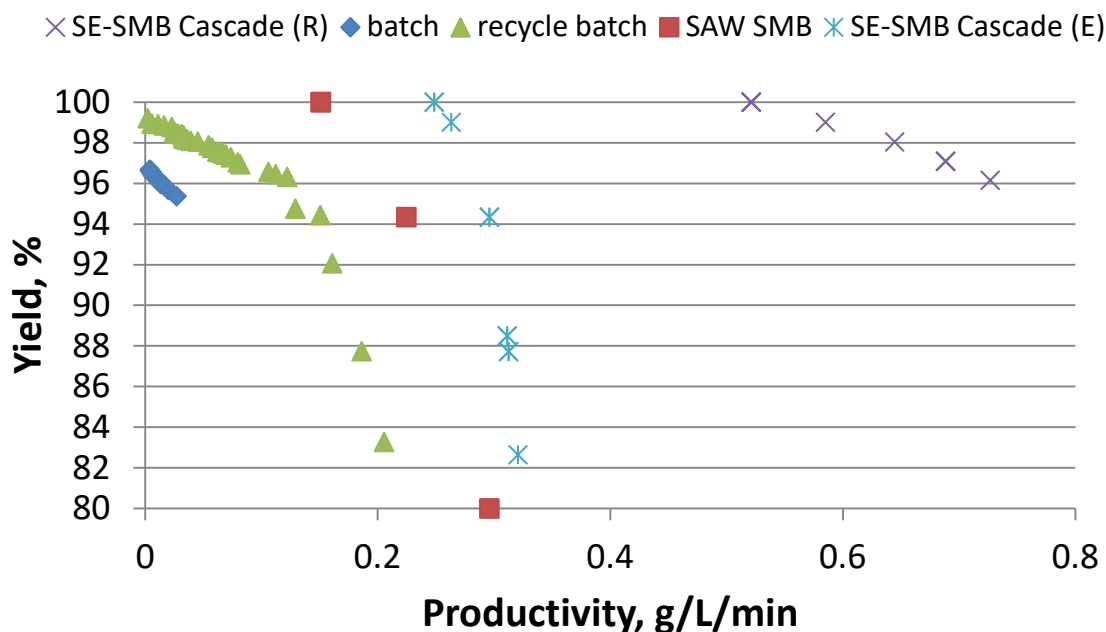


**Figure 4-12 Comparison between intensified processes (purity constrained to >95%) in simulated non-linear system**  
*Pareto sorbent-specific productivity and yield curve for five intensified bioprocess operations.*

This study optimized single-column batch and recycle-batch processes which employed a column simulated to be equivalent in proportion to that of a typical zone in the rival SE-SMB systems (i.e. 2 concatenated SMB columns, thus overall dimensions of 5cm x 0.7cm i.d. for the single batch/recycle-batch column). This batch column length was chosen because the distance a species travels in such a column would be equivalent to the minimum distance any feed species could travel in the rival SMB process (before its elution from the raffinate), and thus this ‘minimum-distance’ parameter was kept constant between rival chromatographic processes. Obviously, since SE-SMB and single-column batch processes differ significantly in their operation and optimization variables, a truly-fair comparison should make use the batch column’s length and diameter as input parameters for global optimization. However, given that column dimensions were not treated as input parameters in the SMB optimizations here – due to limitations of computing power - it was decided to define unoptimized and fixed column sizes for both separation systems. The degree by which optimal column dimensions can affect the Pareto-curves of different processes, even in relation to each other, has yet to be investigated.

The issue of treating column dimensions as an input variable for optimization has consequences for the ‘fair comparison’ problems involved in all studies which compare different

processes (including this study). It is arguable that a fair comparison should be based upon equivalent resin volumes between different processes. However, given that different column dimensions allow for different maximum flow rates as a function of column capacity, placing resin volumetric constraints on a process (e.g. defining the column dimensions of an SE-SMB process such that its total resin volume is exactly equivalent to that of a comparison single-column batch process) may actually distort optimization and comparison results. For example, SMB can often function much more efficiently with the higher flow-rates which are permitted by smaller columns – despite the lower binding capacity of such columns. The trade-off between lower column capacity and higher permissible flow-rates is possibly quite different between SMB-type and batch processes. Therefore, constraining an SMB process to have large columns (so as to replicate the resin volumes used by the rival process-scale batch process) may force the SMB to underperform its potential through unduly limiting the feed flow-rate. Such considerations require further analysis and will be relevant in future attempts at fair comparison between processes.

#### **4.3.8 Towards the global optimization of SE-SMB cascades**

Previously, limited comparison studies between different SMB operation modes for centre-cut separations have been performed [72,119]. As mentioned before, these studies did not consider ternary separations operated productively through stepwise-elution SMB schemes and/or feed overload conditions. Also, several of these comparison studies assumed an SMB would be operated by use of a single column per zone, which – even for linear isotherm separations - is a non-standard and unproductive operation mode for SMB. The results of this chapter suggest that zone length is an important determinant of the productivity of overloaded separations. Therefore, the results of certain existing comparisons involving SMB systems have limited utility.

Results from this chapter suggest that a raffinate-coupled SE-SMB cascade can outperform other bioprocess intensification strategies. Indeed, it is even plausible that the cascade's superiority to the rival processes has been understated here due to the MOO methodology used. This issue arises from the fact that the MOO of the cascade was conducted by a two-step sequential optimization procedure; a MOO was used to find the purity-yield Pareto-curve of the first separation train, and then points on this curve were paired with a set of second-train conditions to facilitate the production of a pure (>95%) product final outlet stream. It is conceivable that this approach could have produced inferior results to one involving global optimization of all operation conditions within the SE-SMB cascade. However, such an optimization was not possible in this (and many other

studies), because it would require very significant computing power given the large number of SE-SMB cascade control variables, which are listed comprehensively below:

- 1) Column dimensions in T1,
- 2) Column dimensions in T2,
- 3) Z2 Column configuration (length) in T1,
- 4) Z2 Column configuration (length) in T2,
- 5) Z3 Column configuration (length) in T1,
- 6) Z3 Column configuration (length) in T2,
- 7) Switching frequency in T1,
- 8) Switching frequency in T2,
- 9) Desorbent modulator concentration in T1,
- 10) Desorbent modulator concentration in T2,
- 11) Desorbent flow-rate in T1,
- 12) Desorbent flow-rate in T2,
- 13) Feed flow-rate in T1,
- 14) Feed modulator concentration in T1,
- 15) Dilution stream's flow-rate between T1 and T2,
- 16) (If extract-coupled process) Wash modulator concentration in Z1 of T1
- 17) (If extract-coupled process) Wash flow-rate in Z1 of T1
- 18) Feed concentration (possible variable only in certain bioprocess)

In the absence of significant computing power and time, an alternative approach to optimization would require the definition of accurate non-linear design-constraints to guide the MOO process. Unfortunately, such non-linear design constraints have yet to be elucidated for SE-SMB systems. However, the doubt concerning the SE-SMB cascade Pareto-curve's global optimality does not undermine the fact that it was found superior to those of the rival processes.

For investigators interested in global optimization of SE-SMB cascades, it may be useful to emphasise the fact that there is no existing, comprehensive theory of cascade coupling to guide cascade optimization. This chapter has investigated the design of efficient raffinate-coupled SE-SMB cascades, as well as argued that raffinate-coupled cascades may often outperform extract-coupled cascades. To reiterate, if it is the case that:

- 1) SMBs are asymmetrically productive under non-linear isotherm conditions,

2) Extension of the Z3 length can increase the relative productive advantage of the T1 raffinate product under non-linear isotherm conditions by permitting higher feed-loading,

3) A cascade's overall productivity is significantly controlled by the feed flow-rate into (or feed-loading of) the first separation train,

4) Identical or larger columns are used in the second separation train with respect to the first separation train, then the degree of nonlinearity of the isotherm will be less in the second separation train because there the separation is binary instead of ternary,

then the logical hypothesis follows that raffinate-coupled cascades will be superior to extract-coupled cascades, due to the fact that a raffinate-configuration enables greater feed loading in the first separation train without sacrificing product yield, whilst the second train will be capable of high-recovery of product from the E2 outlet due to the fact that the non-linearity of the isotherms is reduced, so a greater yield of the extract product in T2 is possible.

However, there are several more considerations which will need investigation before raffinate-coupled cascades may be declared universally superior to the extract-coupled counterparts:

First, for certain centre-cut SE-SMB separations, it is possible that flow-rate constraints in T2 (due to pressure-drop limitations) will create the unavoidable need for larger-diameter columns in T2 if the combined T1 raffinate flow-rate and dilution flow-rate are too high. This can also be the case for extract-coupled systems, where a significant dilution flow-rate of the high modulator-concentration Z1 wash buffer from T1 may be needed in order to create the desired modulator step in T2. It is because of the interaction between pressure-drop constraints and modulator-dilution requirements that column dimensions in T1 and T2 are included in the list of SE-SMB cascade global optimization parameters above. Indeed, the SE-SMB cascade optimization experiments required the use of larger columns in the raffinate-coupled second separation train precisely because of the fact that the second train's input feed flow-rate was too high for use of identical column dimensions to the first train.

Second, it is unclear what sequence of modulator steps is optimal for non-linear SE-SMB cascades. This chapter has investigated systems where the first separation train's modulator levels are higher than that of the second separation train's. It may be the case that a design space exists such that the reverse sequence of modulator steps is possible (modulator levels higher in the second

train) whilst maintaining the order of separation (e.g. a raffinate coupled cascade, where the product is still collected at the extract from the second train). Such an alternative modulator step sequence would require highly competitive binding behaviour in the first separation train to 'simulate' the effects of the high modulator concentration profile in the alternative modulator-step configuration. Therefore, it is possible that that optimal coupling-configuration may be dependent on the non-linear behaviour of any given separation mixture, because 1) If it is indeed the case that inter-cascade modulator concentration/dilution flow-rate constraints factor in controlling a cascade's productivity, as was posited by the previous paragraph, and 2) If the feasible sequence of modulator steps in a cascade is controlled by any given separation's non-linear isotherm behaviour, then there exists an additional mechanism by which non-linear isotherm behaviour could affect a cascade's design space, which in turn broadens the set of operating conditions for consideration in global optimization.

#### **4.3.9 On the utility of Integrated SMB, MCSGP and single-train 'pseudo-SMB' processes for bioprocessing**

It is interesting to note that the SMB cascade configuration out-performed both the SAW SMB configuration as well as the recycle-batch process in this investigation. These results suggest that the superiority of cascade systems over integrated SMB and recycle-batch extends to instances where the processes are run under non-linear conditions; previously, the cascade configuration's comparative superiority has been well-documented only for linear isotherm chromatographic operation. If it is indeed the general case that SE-SMB cascades outperform other intensified processes, there are two important conclusions which may be drawn. Naturally, the first conclusion is that cascade SE-SMB systems merit further investigative attention for their application to bioprocessing.

The second conclusion is that MCSGP-type processes, and certain types of other single-train pseudo-SMB processes, may not offer performance advantages with respect to more traditional SE-SMB cascade approaches. While this chapter has not simulated the two-column MCSGP process for comparison to other processes, due to the optimization problem which derives from the fact that different cycle-by-cycle outlet-fractionation choices can preclude establishment of a generalizable cyclic steady-state for this process, it is arguable that the two-column MCSGP process will – at best – perform similarly to that of either the SAW SMB process (a single train countercurrent ternary separation) or the recycle-batch process (a batch-gradient process involving intermittent fractionation), and will therefore have a (purity-constrained) productivity-yield Pareto-curve inferior

to that of either of the SE-SMB cascade. Therefore, given the fact that the separation-performance of linear modulator gradients are indistinguishable from very finely discretized stepwise-elution schedules, and given that certain optimization studies have found no marginal benefit to increasing the number of 'steps' of a stepwise elution schedule beyond the number of feed components (i.e. three steps optimal for ternary separations) [4,123,124], and in the absence of high-quality comparisons in the literature between SE-SMB processes and the MCSGP, claims of MCSGP productive and/or purification superiority over other intensified processes may be premature.

## **Conclusion**

This chapter introduced a number of theoretical and practical design considerations for SE-SMB operation, which included: 1) Analysis of the effect of MPs on the design of centre-cut separations, 2) Examination of the interaction of non-linear isotherms and zone lengths on SMB productivity, and 3) Proposal of performance differences between extract- and raffinate- coupled SE-SMB cascades operated under overload conditions. This set of considerations informed an attempt to compare different intensified downstream bioprocesses, which suggested that traditional SE-SMB cascade separation schemes are capable of impressive performance in challenging separation tasks with respect to other intensified chromatographic processes.

Besides chromatographic performance indicators such as purity, yield and productivity, other factors feature in the relative attractiveness of various intensifies processes for industrial adoption. These features include capital costs, the chromatographic residence time's impact on protein stability, the ease and simplicity of process operation, and vulnerability to failure modes.

Regarding failure modes, SE-SMB cascades are relatively complex operations with respect to alternative intensified processes, and thus there is greater scope for faults to afflict SE-SMB processes. Indeed, any advantages that SE-SMB cascades offer with respect to other chromatographic processes in terms of productivity and purity may be undermined by such practical issues concerning their implementation in a manufacturing context. It is for this reason that the next chapter seeks to explore failure modes in SE-SMB systems, and proposes methods for rapid on-line detection and diagnosis of faults.

# CHAPTER 5 FAILURE MODE DETECTION AND DIAGNOSIS IN SE-SMB SYSTEMS

## 5.1 Introduction

The previous chapters in this thesis have investigated aspects of the design of robust and productive SE-SMB systems, and have also presented results which suggest cascade SE-SMB systems are attractive alternatives to other intensified chromatographic processes.

Whilst the features of high purity and high productivity make SMB processes attractive for industrial adoption, other engineering considerations are relevant. Of particular concern to the bioprocessing industry is a process' vulnerability to failure modes. In chromatography steps, three distinct risks are posed by process faults. First, high purity requirements are specified by regulation—thus process faults can put the final product at risk of failing regulatory criteria. Second, biological macromolecules are often 'fragile' (i.e. prone to degradation/disassembly/aggregation over time), thus process-interruptions to find and fix faults can result in loss of product quality (i.e. potency). Third, biological macromolecules are high-value products, and thus process faults which result in the discard of contaminated or degraded product can be very costly.

Single-column batch chromatography processes are generally used in industrial bio-chromatography in part because their failure modes are well-understood, easily identifiable, and straightforwardly fixable. For example, a fouled column in an industrial process is often detectable through observation of increased band-broadening of the eluted concentration-signal peaks with respect to those from a non-fouled column. In a bioprocess, such a fouled column may be quickly replaced or repacked, its recent batches of compromised (impure) product discarded, and bioprocessing may promptly resume.

By contrast, intensified and continuous processes, such as SE-SMB chromatography, cannot replicate the versatility of batch processes in the event of failure-mode occurrence. Whilst each type of batch chromatography fault has an SE-SMB failure-mode equivalent (e.g. fouling, ligand loss, leaks), the complexity of SMB processes, and the larger number of interdependent components, make failure modes in SMB systems more consequential than that of isolated batch faults; SMB faults can compromise more product quantity than single column batch faults, but also necessitate longer process down-time for fault identification and fixing. Unlike failure mode diagnosis and repair

in batch systems, SMB fault diagnosis and repair is currently only possible through employment of a human operator's accumulated experience and expertise.

### **5.1.1 Single-column batch chromatography expert systems**

'Expert systems' are automated systems which assimilate the knowledge of human 'experts' to perform classification and control tasks. In the field of batch chromatography, much progress has been achieved over the last few decades in developing such automated systems.

Several approaches to the task of automated chromatographic-fault classification have been investigated previously. One approach employs a so-called 'rules-based system' [125–127]. In a rules-based system, logical tests constitute nodes in a 'decision tree' which categorises faults based upon the answers to a series of questions. The questions posed by decision trees may be simple yes-or-no questions (e.g. 'Is there band-broadening of the chromatographic peak?'), but may also involve more complex questions involving threshold values and logical combinations (e.g. 'Is the peak tailing more than 10% outside the normal range AND is the peak maximum within the normal range?') [128].

Decision tree classifiers have been further developed to improve their accuracy is by constructing a 'random forest' of decision trees. In a random forest, where various decision trees are grown through the random selection of training data for each tree, the random forest's classification decision is made from finding the most common output of the decision trees in the forest [128].

Other methods of automated chromatographic-fault classification exist, such as Artificial Neural Networks (ANNs). However, it is harder for ANNs than decision-tree classifiers to justify their reasoning for classification to a human operator, and ANNs can also be less computationally efficient than decision trees. Nevertheless, ANNs have been successfully used to develop chromatographic expert systems [95,129,130].

### **5.1.2 Countercurrent chromatography expert systems**

Many SMB failure modes, and their process consequences, have been previously investigated; the results of these investigations are summarised in Table 5-1 [1,85,97,131,132].

**Table 5-1** Summary of the effects of various common failure modes on binary SE-SMB processes operated under high feed-loading conditions

Failure Mode	Consequence for Process
Ligand Loss	Raffinate product pollution/ Extract product yield reduction
Column Fouling	Raffinate product pollution/ Extract product yield reduction/ Extract product pollution/ Raffinate product yield reduction
Valve-block leak	Extract product pollution/ Raffinate product yield reduction
Desorbent over-pumping	Raffinate product pollution/ Extract product yield reduction
Extract under-pumping	Raffinate product pollution/ Extract product yield reduction
Desorbent under-pumping	Extract product pollution/ Raffinate product yield reduction
Extract over-pumping	Extract product pollution/ Raffinate product yield reduction
Feed under-pumping	Raffinate product pollution/ Extract product yield reduction
Feed over-pumping	Raffinate product pollution/ Extract product yield reduction

Whilst investigators have developed strategies for detection and diagnosis of certain faults (i.e. pump flow rate variation, ligand loss) in theoretical True Moving Bed (TMB) systems, the development of corresponding systems for SMB processes has yet to be achieved [85,132]. Given the well-known differences between SMB and TMB processes, it is unclear whether previously-proposed TMB fault detection and diagnosis strategies may be straightforwardly applied to SMB processes.

### 5.1.3 Motivation for Chapter 5

While chromatographic expert systems are well-established for single-column batch chromatography, no such system has been developed for SMB chromatography. The purpose of this chapter is to investigate an initial set of decision-tree rules and analytical methods that can inform future development work on industrially-deployable SMB expert systems. This work will focus on classical binary SE-SMBs, because previous chapters have demonstrated that this operation mode is not only efficient for binary separations, but also constitutes an isolatable-stage in highly productive ternary-separation SMB cascades.

This chapter will examine detection and diagnosis of common singular failure modes in SMB systems, including ligand loss from a single column, fouling of a single column, single column degradation through channelling, pump flow-rate variation, and a valve-block leak. Attention will also be given to so-called ‘general failure modes’; examples of this type of failure mode include a general loss of ligand from all columns in an SMB column series, as well as fouling of all columns in the SMB column series.

Informed by the work of other investigators in developing expert systems for chromatography, this chapter documents the investigation of established process-monitoring and analytical methods – such as on-line UV flow-cell spectrometry and chromatographic feature analysis – for their utility in an SMB expert system.

## 5.2 Theory

It is hypothesised that singular failure modes in SMB systems, such as that of ligand loss from a single column, will change the peak shapes of outlet raffinate and extract concentration signals. However, given that singular failure modes travel between different zones during the course of an SMB run (due to the effect of port-switching on shuffling columns'/valve's zonal locations), it is predicted that the shapes of outlet concentration peak shapes will vary 'cyclically'.

In this context, the term 'cyclically' refers to the rotation of SMB ports around the entire column series; therefore, an SMB's 'cycle time' is equal to the number of columns multiplied by the port-switching time. The hypothesis that outlet concentration signals will vary 'cyclically' therefore refers to an idea that outlet concentration patterns will have a repeating 'pattern unit' of duration equal to one 'cycle time'.

It is worthwhile to redefine 'cyclic steady state' in the context of SMB failure modes. Whilst normal (non-faulty) SMB operation is defined as reaching cyclic steady state when the mass balance of the feed's input to the system equals the feed species' outflow from the system, this mass balance is often calculated across a single switching period (given that mass-outflow does not vary in normal SMB systems at cyclic steady state between switching periods). However, under failure mode conditions, the mass-outflow rate is hypothesised to vary between switching times due to the failure mode's switching of zonal locations. Because of this phenomenon, a better definition of 'cyclic steady state' in a faulty SMB system would require the closure of the mass balance over a cycle period, rather than a switching period. This requirement on the closure of mass balance over a cycle-period is applicable to both non-faulty and faulty SMB systems.

At cyclic steady state, given the hypothesis that singular failure modes will result in cyclical modulation of the extract and raffinate concentration signals (such as the column ligand loss scenario illustrated by Figure 5-1), it follows that these concentration signals will provide a means of assessing the nature and location of an SMB's faults. In this chapter, with regard to the biotechnological interest in SE-SMB fault detection methods, outlet concentration monitoring

through use of UV280nm flow-cell spectrometry will be investigated for its ability to detect and diagnose such faults.

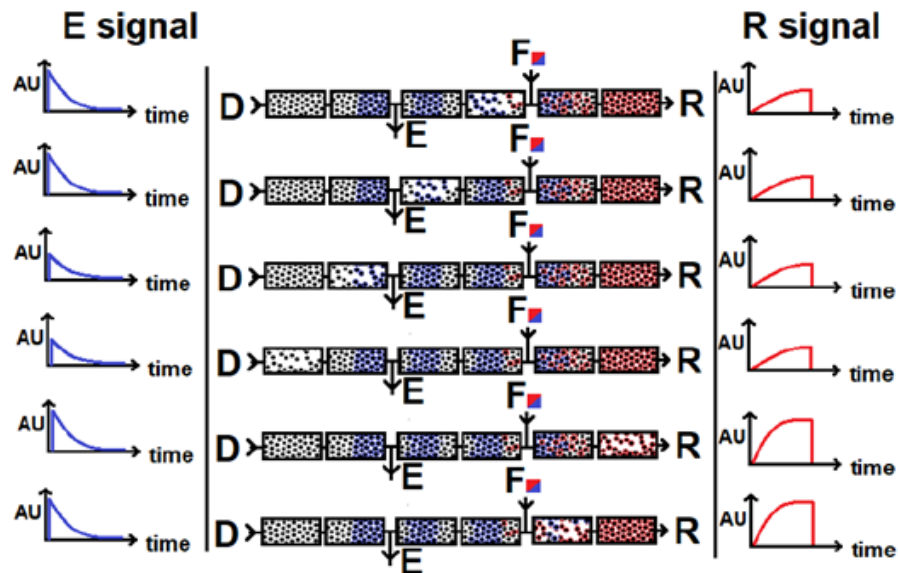


**Figure 5-1 Cyclic signal variation from singular failure-mode**

The single failure mode of ligand loss is hypothesised to modulate the raffinate ('R', RHS) and extract ('E', LHS) outlet-concentration peak shapes as the faulty column (shown with fewer sorbent beads) is shuffled between different SMB zones over the course of port-switches (the individual rows of the figure profile the column movement during the course of six switching periods, which is one cycle time for this system).

In addition to failure mode detection and diagnosis from the monitoring of outlet concentration patterns of feed species through UV spectrometry, raffinate conductivity patterns may also provide useful information when monitoring SE-SMB processes. In the first results chapter, the mechanism by which modulator perturbations in SE-SMB systems are generated was analysed. It was shown that the duration of a MP is a function of the Z2 and Z3 liquid flow rates, and that the modulator concentration of a MP was related to these flow-rates as well as to the desorbent- and feed- modulator concentrations. It is hypothesised that the flow-rate sensitivity of the MP's duration and modulator-concentration may provide a useful means to monitor an SE-SMB. For example, as shown by Figure 5-2, pump flow-rate variations (a class of failure mode) result in different modulator profiles in Z3. Different modulator profiles may be detected by online measurement of the raffinate conductivity, and thus conductivity-monitoring may yield useful information for a fault-detection system.

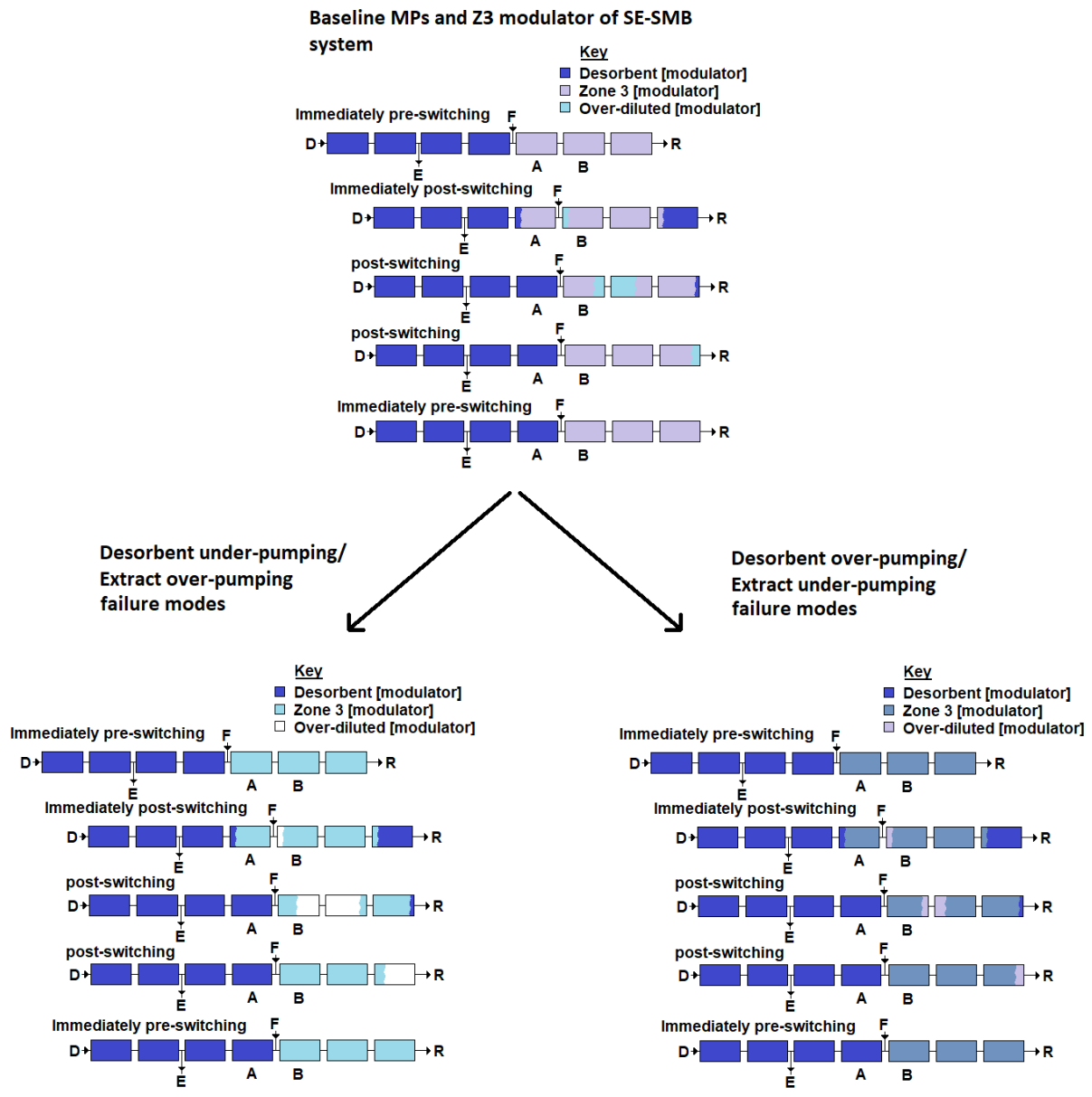


**Figure 5-2 Conductivity measurement of SE-SMBs**  
*The duration of modulator perturbations, as well as the general modulator concentration profile of Z3, is expected to reveal pump flow rate changes as measured by on-line raffinate conductivity.*

Most chromatographic expert systems analyze chromatograms through defined features (i.e. measurable parameters) of a chromatogram, such as peak shape and peak retention-time. Such features may also be used in SMB expert systems, but – unlike in batch chromatography expert system – SMB systems are more complex. In SMB systems, where all columns are connected in series, a disturbance of one column’s concentration profile can affect the concentration profiles of the entire set of SMB columns. It is precisely because of the fact that SMB systems constitute a

series of interlinked columns (and not a set of parallel batch processes), that straightforward re-purposing of batch chromatography expert systems for SMB application is not generally possible. Since fault detection and diagnosis is much more complicated in SMB systems than in batch processes, it is proposed that the task of fault analysis may be simplified by separating it into a two stage process. In this two-step process, the 'local' effects of faults (e.g. pertaining to the component, such as a single column, where the fault is present) may be distinguished from the 'global' effects of faults (e.g. the chromatographic profile changes of the entire multi-column SMB process). Therefore, two levels of analysis may be employed in the construction of SMB expert systems; these are termed 'cycle-signal analysis' and 'column-signal analysis'. Cycle-signal analysis is applied to cycle signals, which are outlet concentration signals generated during one cycle period. By contrast, column-signal analysis applies to the outlet signals generated during each switching period. Figure 5-3 and Figure 5-4 show how cycle-signals and column-signals may be analyzed through feature-extraction from outlet concentration patterns.

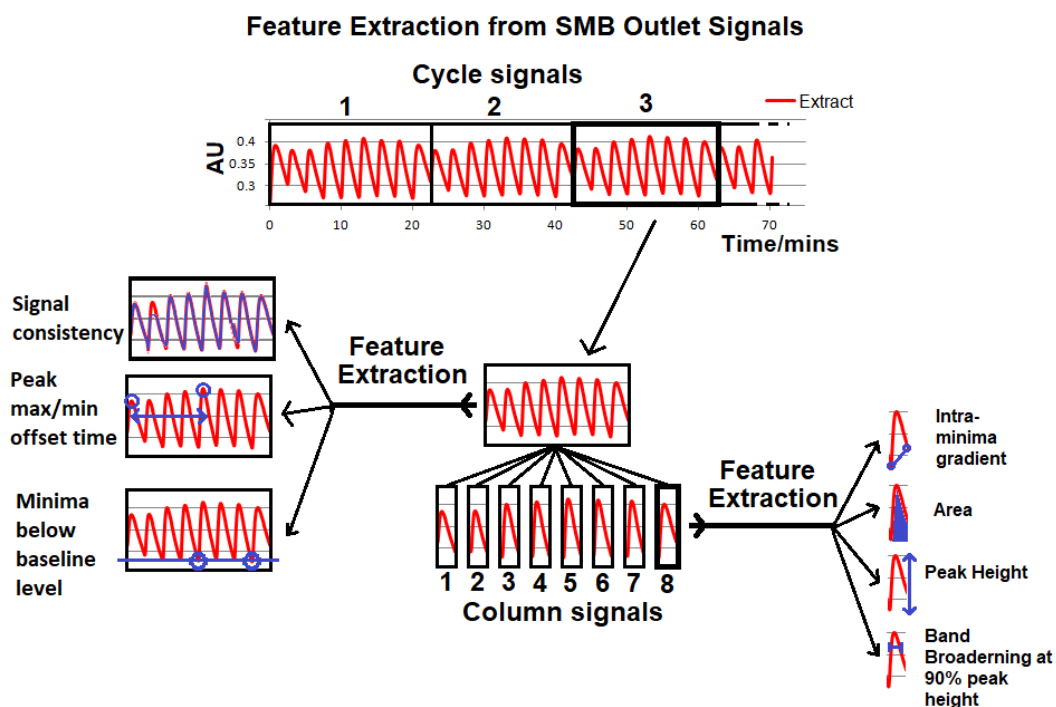


**Figure 5-3 UV signal feature extraction**  
*Two-step feature extraction from SMB outlet concentration patterns: cycle signal analysis and column signal analysis*

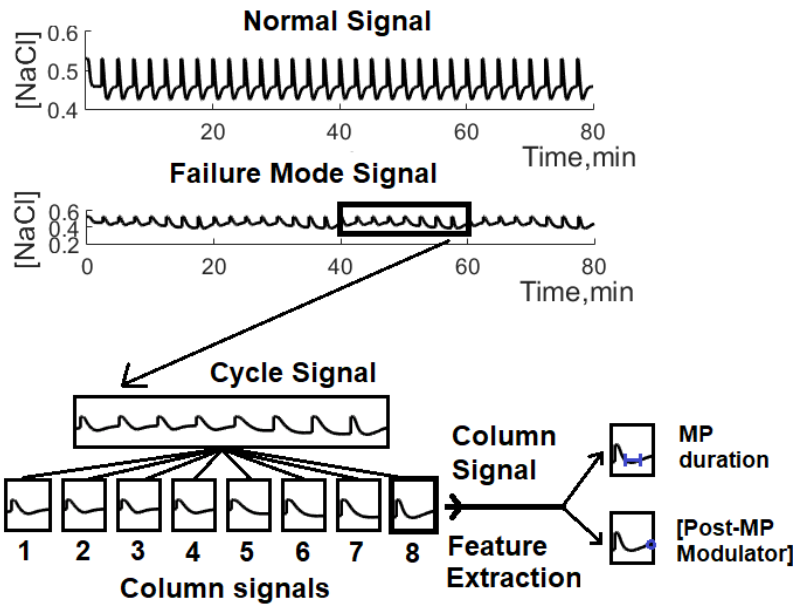


**Figure 5-4 Feature extraction from SMB outlet conductivity patterns**  
 Example of raffinate conductivity failure mode pattern caused by a valve block leak

## 5.3 Results and Discussion

### 5.3.1 The outlet concentration patterns produced by singular column and leak SMB failure modes are cyclical

Experimental extract- and raffinate-outlet UV280 signals were graphed for three SE-SMB runs subject to singular failure modes. Figure 5-5 (Bi,Ci,Di) show the UV signals for the singular failure modes of a fouled column, a degraded column, and a valve-block leak, respectively. The cycle time for these SMB runs was 20 minutes, as eight columns constituted the SMB train, and the switching time was 2.5 minutes.

Simulations of various severities of failure modes were performed in addition to experimental work. Examples of the results from these single failure mode simulations for ligand loss, a valve-block leak, fouling, and column degradation (through channelling) are shown by Figure 5-5 (Dii, Bii, Cii, Diii). A baseline (no faults) signal is shown by Figure 5-5 (A) for comparison with the signals produced by SMB faults. Note that simulation results involving pump flow rate faults are not included in Figure 5-5. The mass-balance of all simulations closed within the range of  $100\% \pm 1\%$ , with the exception of the leak simulations (because the mass balance equations used in the model did not account the loss of material from the leak outlet, and thus the closure of the mass balance was not expected for in these simulations).

The valve-block leak simulation, as detailed in the Materials and Methods section, was constructed with reference to the leak flow rate of the experimental leak failure-mode. During each cycle time roughly 10mL of liquid was eluted through the leak valve. It was found that the leak flow-rate varied based upon its zonal position; of the total of 10mL eluted, most was eluted during switching periods in which the leak was situated in Z1. This observation was used to inform the cyclical modulation of the leak flow-rate in the simulated valve-block failure mode. It should be noted that other SMB laboratory equipment will experience different patterns of leak outflow based upon differing internal pressure drops, valve-block configurations, and back pressures. However, the effect of valve-block leaks on features such as the inlet-outlet mass-balance and an SE-SMB's variable conductivity patterns should be generalizable across different SMB equipment.

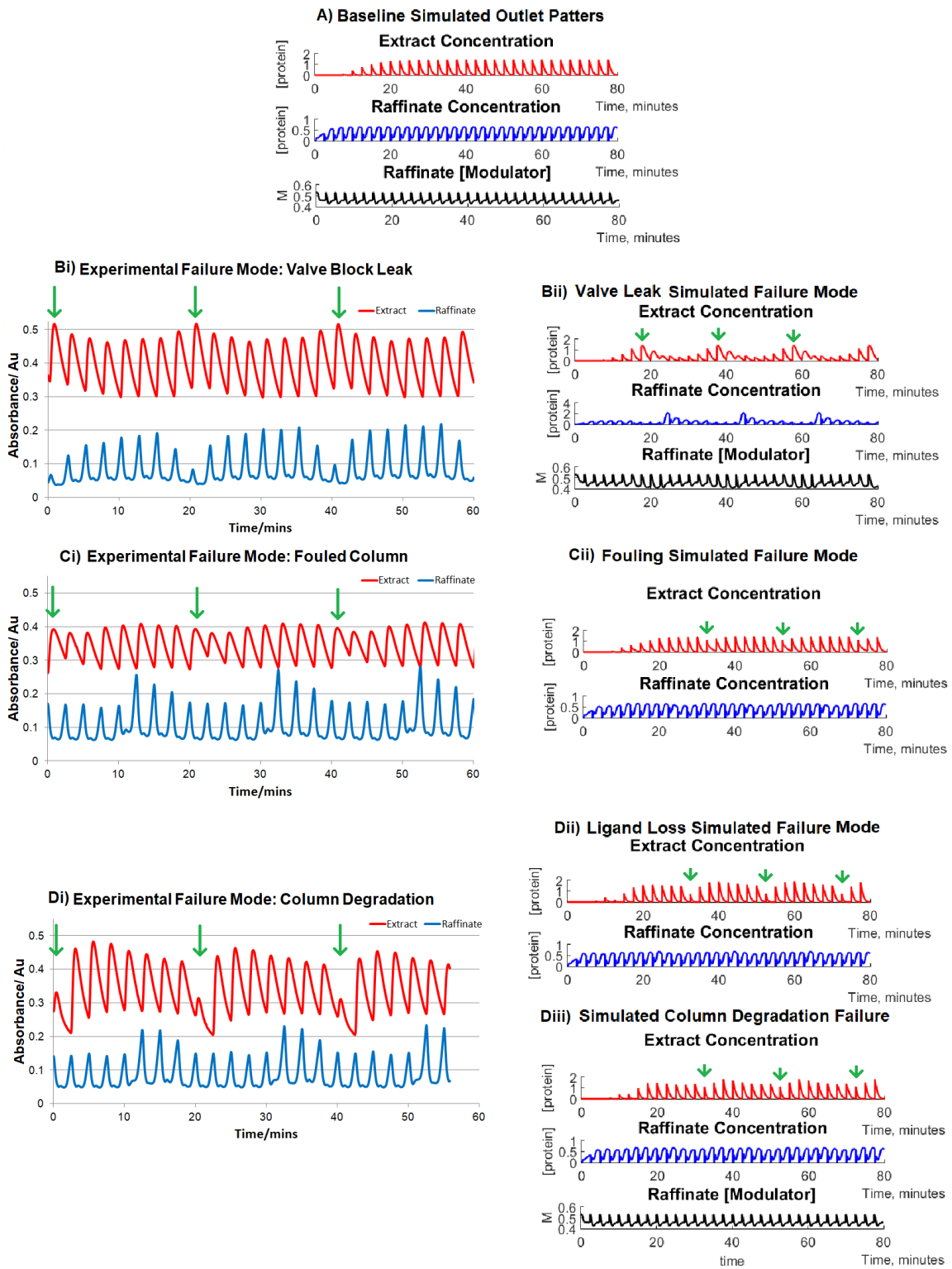


**Figure 5-5 Failure-mode signatures in SE-SMB extract and raffinate outlet concentration patterns**  
 SE-SMB outlet failure-mode signatures generated from experimental models as well as simulated models. Red signals are those outlet concentration/absorbance patterns generated from experimental/simulated extract ports, whilst blue signals are those generated from experimental/simulated raffinate ports. Green arrows indicate certain conserved features of cycle-

signals and/or column-signals which appear in both the simulated and experimental systems. **A)** Baseline (no failure) simulated signal pattern, **Bi)** Experimental outlet UV280nm-absorbance signals from system with valve-block leak, **Bii)** Outlet concentration signals from simulated system with valve-block leak, **Ci)** Experimental outlet UV280nm-absorbance signals from system with a single fouled column in the separation train, **Cii)** Outlet concentration signals from simulated system with a single fouled column in the separation train, **Di)** Experimental outlet UV280nm-absorbance signals from system with a 'degraded' column (here, defined by material loss from a column, **Dii)** Outlet concentration signals from simulated system with a single column subject to 'column degradation' ( here, modelled by loss of ligand from a single column), **Diii)** Outlet concentration signals from simulated system with a single column subject to 'column degradation' ( here, modelled by flow-path channelling within a single column)

It can be seen that experimental failure mode signals are more 'distinct' than their simulated counterparts, because the range of peak amplitudes is larger for the experimental signals than is the case for the simulated signals. It is possible that this difference may be caused by the limitations of the failure-mode simulation models; additional model details, such as three-dimensional modelling of the effect of column fouling on blocking the surface pores of the chromatographic beads, may allow better replication of the distinct failure mode signals obtained experimentally. However, there are two reasons to believe that the current simulation models are sufficiently detailed that they can faithfully capture experimental chromatographic phenomena: 1) The cyclical variation in column-signal peak amplitudes in each cycle-period is replicated by the simulation models, and 2) The pattern of the cycle-signals (e.g. the offset time between the extract column-signal maxima and raffinate column-signal maxima) matches between the experimental and simulation models. Therefore, while experimental signals may be more eminent, simulation models provide a useful investigative basis for failure-mode signal analysis.

Decision trees for the classification of single failure modes in both extract-pump and Z2-pump SMB configurations were constructed (Figure 5-6). It was found that singular failure modes including column fouling, degradation, ligand loss and valve-block leak could be uniquely identified from outlet signal data for both SMB configurations. It was also found that the Z2 pump configuration permitted unique identification of malfunctioning pumps, but – for the extract pump SMB configuration - there was some aliasing between certain desorbent and extract pump failure mode signatures.

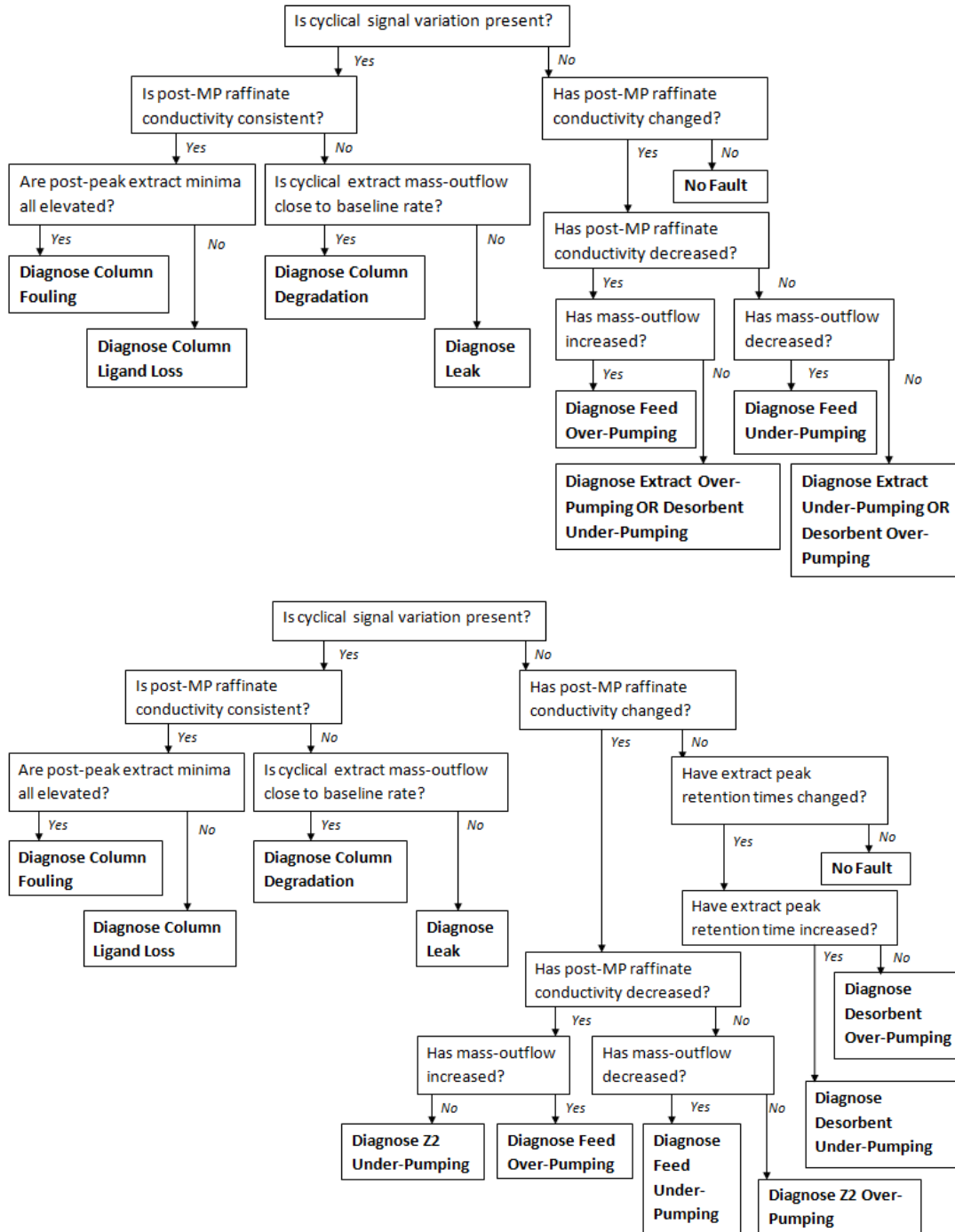


**Figure 5-6 Single failure-modes classification decision trees**

**Top:** Decision tree for Extract-pump SMB configuration, **Bottom:** Decision tree for Z2-pump SMB configuration

A list of the features, and corresponding parameters, used in the Z2-pump SMB failure-mode diagnosis decision tree is given in Table 5-2.

**Table 5-2** Cyclic signal features indicative of failure mode class in step-down SE-SMB system with Z2 pump. Codes for features (of type F#) are detailed in the Materials and Methods Table 2-4.

Cyclic signal feature/ Single failure-mode type	F24	F23	F16	F15	F19	F20	Unique combination of features? (Y/N)
Fouling	T	T	0	0	F	0	Y
Column Degradation	T	F	~	0	T	0	Y
Ligand Loss	T	T	0	0	T	0	Y
Leak	T	F	~	~	T	-	Y
Feed Pump (+)	F	T	-	-	F	+	Y
Feed Pump (-)	F	T	+	+	F	-	Y
Z2 Pump (+)	F	T	+	-	F	0	Y
Desorbent Pump (-)	F	T	0	0	F	0	Y
Z2 Pump (-)	F	T	-	+	F	0	Y
Desorbent Pump (+)	F	T	0	0	F	0	Y
<b>Symbols</b> + indicates increase in feature value - indicates decrease in feature value 0 indicates no change in feature value T indicates logical test is true F indicates logical test is false ~ indicates cyclical variation							

Experimental detection of raffinate conductivity signals was not possible due to equipment limitations. Therefore, it remains to be experimentally demonstrated that online raffinate conductivity measurements are sensitive and accurate enough to permit differentiation between certain failure modes, and other process-monitoring sensors – such as pressure monitors and flow-rate monitors – may be needed to support, or replace, the method of conductivity-measurement for experimental fault detection/diagnosis proposed in this chapter.

### 5.3.2 Identification of general column failure modes

Certain types of column failure modes do not produce cyclical signal patterns when the fault affects all columns in an SMB to a similar degree. This type of failure mode is referred to here as a ‘general failure mode’; two common examples of such a failure mode include general fouling of all columns in an SMB separation train, and general ligand loss from all columns in an SMB separation train.

General failure modes change the retention and band-broadening behaviour of chromatographic peaks within an SMB system, and are therefore uniquely identifiable through analysis of column signal features. Figure 5-7 shows a decision tree which may differentiate general

failure modes from each other and also from singular failure modes (which produce cyclical variation in cycle signals). The decision tree, shown by Figure 5-7 and converted to an algorithm in Matlab, was able to classify the simulated general failure-mode data set with complete accuracy.

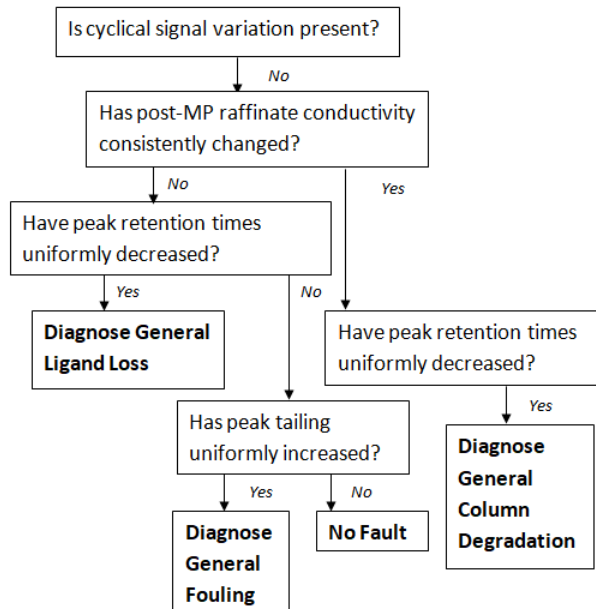


**Figure 5-7 Decision tree for classification of general failure modes**

### 5.3.3 Mechanism of generation of cyclic signal features

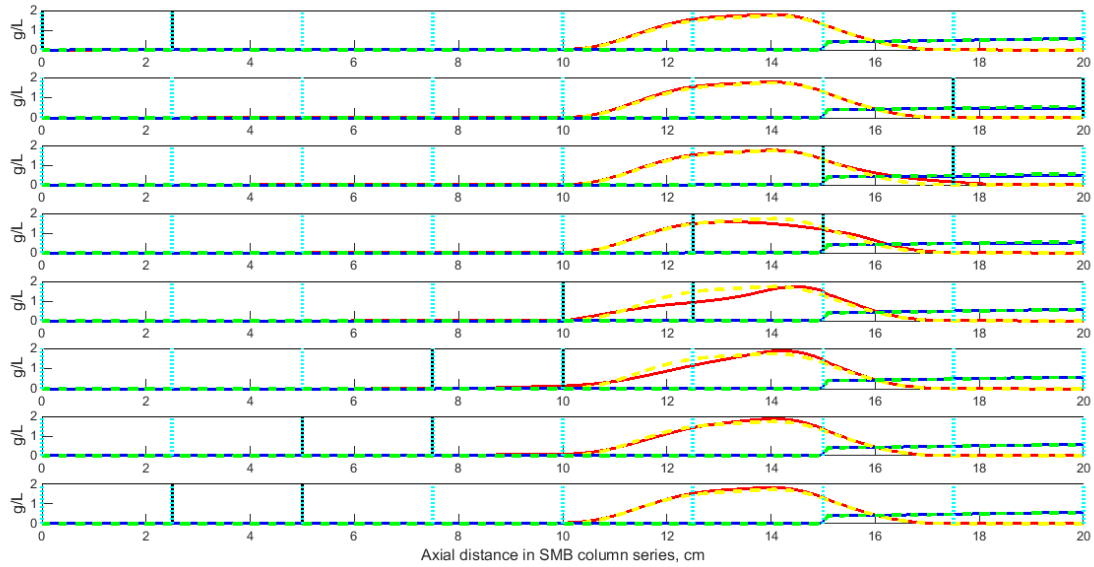
The previous section presented a set of simulated and experimental outlet-signal chromatograms that revealed cyclical patterns of signal variations which were repeated during each cycle signal of a singular failure-mode SMB system. These cyclical signal patterns were sufficiently unique and reproducible to enable automatic fault classification, but the underlying chromatographic phenomena which explain the generation of such signal patterns needs further investigation. This section examines the way in which signals are generated by two singular failure modes (single-column ligand loss and single-column fouling).

The theory section of this chapter hypothesised that cyclical variation in the outlet signals of singular failure modes would occur, because a fault (e.g. a fouled column/leaking valve), during its shuffling between different SMB zones, would distort the SMB feed species concentration profiles of each zone in a sequential and repeating manner. Figure 5-8 shows snapshots of the internal concentration profiles of the MRC and LRC feed species (red and blue curves) over the course of simulated single failure-mode SMB cycles. It can be seen that a faulty column, which is bracketed by

black lines in the figure, is shuffled through every column position in the SMB column series (of total length 20cm) during the course of an SMB cycle. For both of the single column ligand-loss and fouled-column failure modes (Figure 5-8 top and bottom, respectively), the internal concentration profiles experience either minor or major deviations from that of the expected concentration profiles of a non-faulty SMB (shown by yellow and green dashed curves for the MRC and LRC respectively). These deviations may be seen more clearly in Figure 5-9, where the internal concentration profiles of the single failure-mode systems are overlaid.

It can be seen from the Figure 5-8 that significant discrepancies between the normal and faulty internal concentration profiles occur when the faulty column is located in Z3 (spanning 15-20cm on the graph) and also when it is located in Z2 (spanning 10-15cm on the graph). It is these changes to the internal concentration profile, in both Z2 and Z3, which are believed to be responsible for modulation of the outlet signal patterns collected from the extract and raffinate. The raffinate is located downstream of Z3, so it is conceivable the perturbations to the concentration profile in Z3 are directly transmitted to the raffinate concentration profile. Likewise, distortions to the concentration profile of the first column in Z2 will inevitably transmit into perturbations of the extract outlet concentration profile, because port-switching repeatedly shifts the first Z2 column to become the final Z1 column, from where its feed-species contents may be eluted into the extract outlet and into Z2.

### A) Single Fouled Column



### B) Ligand Loss from Single Column

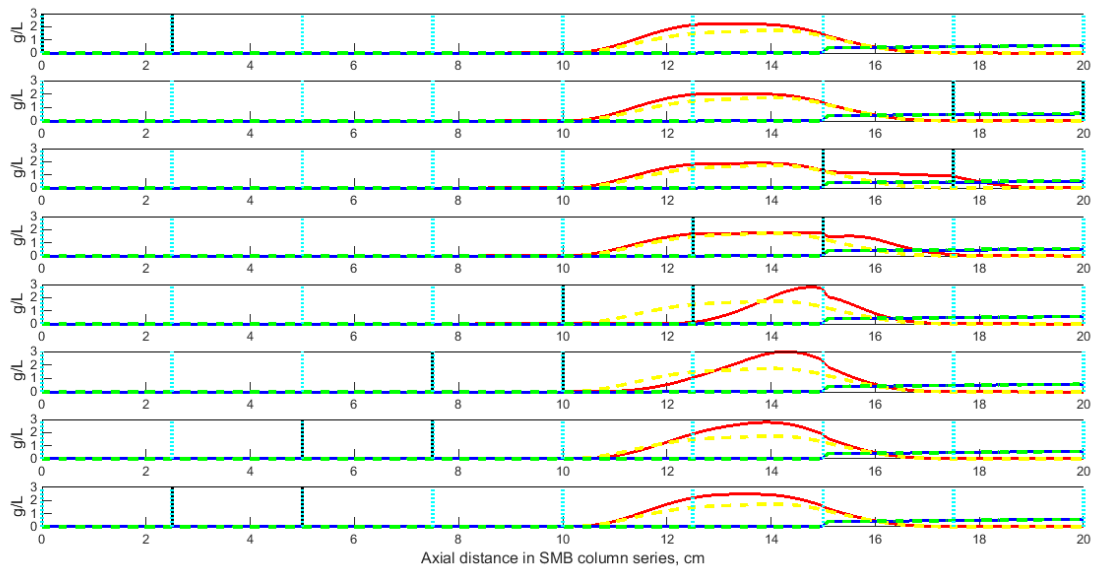
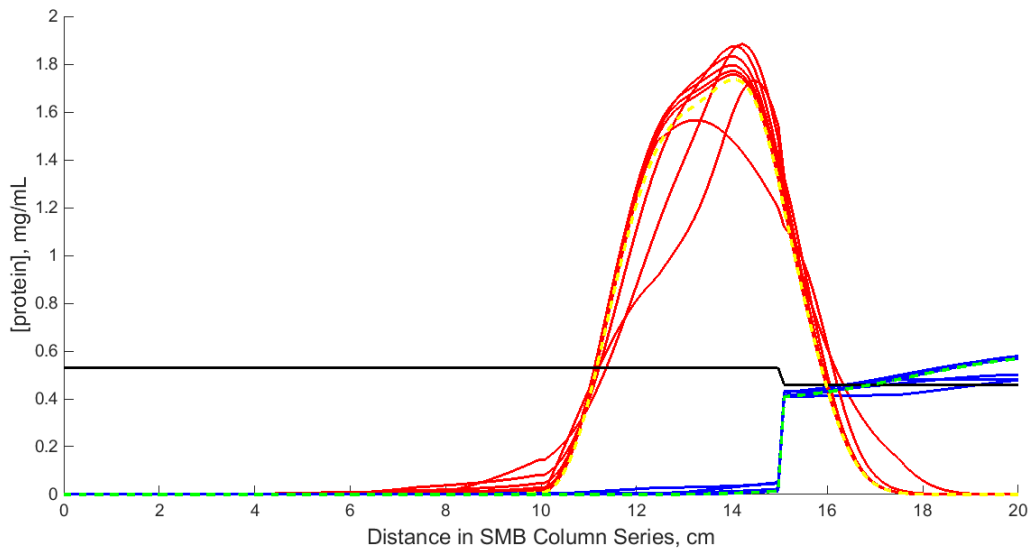


#### Figure 5-8 Mechanisms of failure-mode pattern generation

Internal SMB failure-mode concentration profile ‘snapshots’ taken at the end of each switching time during the course of a cycle period for: **A)** Fouling of a single column, and **B)** Ligand loss from a single column. Each horizontal row of the figures displays the simulated internal concentration profile of columns at the end-time of consecutive ports switching period. The ports are located along the column series as follows: Desorbent at  $z=0\text{cm}$ , Extract at  $z=10\text{cm}$ , Feed at  $z=15\text{cm}$ , Raffinate at  $z=20\text{cm}$ . The column configuration is 4-2-2, and the junctions between simulated columns are delineated by vertical, dashed-cyan lines. The faulty column is bracketed by two vertical dashed black lines. The red and blue curves represent the MRC and LRC concentration profiles respectively, and the dashed yellow and dashed green curves represent the non-faulty SMB’s MRC and LRC internal concentration profiles respectively.

**A) Overlaid concentration profile snapshots (fouling of single-column in an SE-SMB)**



**B) Overlaid concentration profile snapshots (ligand loss from single-column in an SE-SMB)**

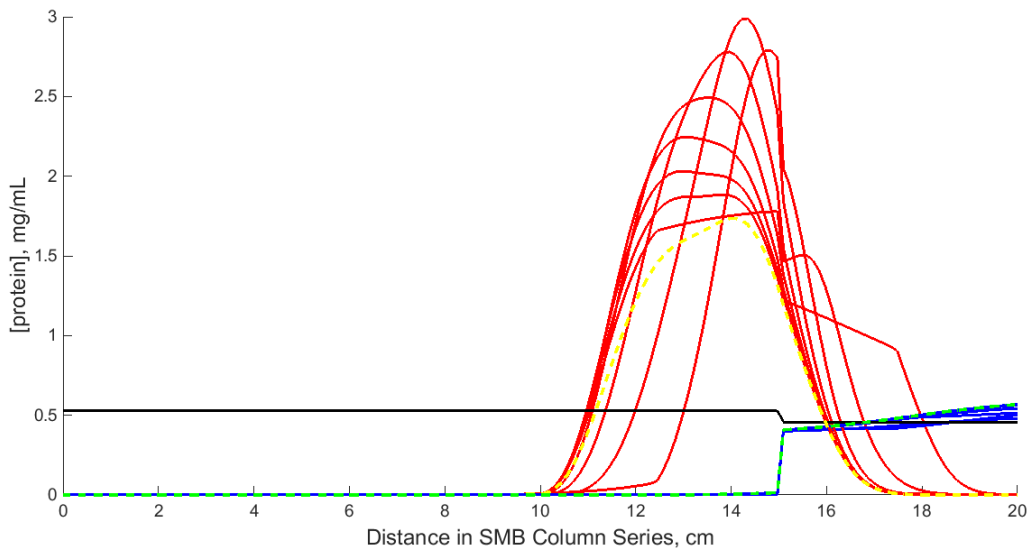


**Figure 5-9 Overlaid internal concentration profile snapshots of single-fault SE-SMBs**

The red and blue curves represent the MRC and LRC concentration profiles respectively, and the dashed yellow and dashed green curves represent the non-faulty SMB's MRC and LRC internal concentration profiles respectively. The black lines are transient modulator concentration profiles. The ports are located as follows: Desorbent at  $z=0\text{cm}$ , Extract at  $z=10\text{cm}$ , Feed at  $z=15\text{cm}$ , Raffinate at  $z=20\text{cm}$ . **A)** A failure mode's (fouling of a single column) overlaid internal concentration profile 'snapshots' from points during the course of a cycle time. **B)** A failure mode's (ligand loss from a single column) overlaid internal concentration profile 'snapshots' from points during the course of a cycle time.

#### 5.3.4 Localization of Faults by column-signal features

In addition to failure mode classification through outlet signal analysis, identification of a faulty component's location in the SMB component series may also be found from analysis of outlet concentration signals.

The previous section examined how internal concentration profiles of a faulty SMB are cyclically perturbed by the movement of a faulty column through the zones. This location-dependent distortion of the SMB concentration profile by a faulty column provides one means to identify the location of the faulty component. When a faulty column transitions between either  $Z2 \rightarrow Z1$  or  $Z1 \rightarrow Z3$ , distinct column signals are produced in comparison to the other column signals in the cycle time. Given prior classification of the failure mode type, it is therefore possible to identify the failure mode location through column signal analysis. Figure 5-10 details decision trees which permit the identification of faulty components after failure mode classification has occurred. It was found that the decision trees in Figure 5-10 were able to discriminate between failure-mode column signals and non-failure-mode column signals present in the same cycle signal, thus subsequent identification of a faults location was possible in both the simulated and experimental data. Note that, for lack of an online conductivity monitor, it was not possible to test the proposed leak-failure-mode decision tree experimentally.

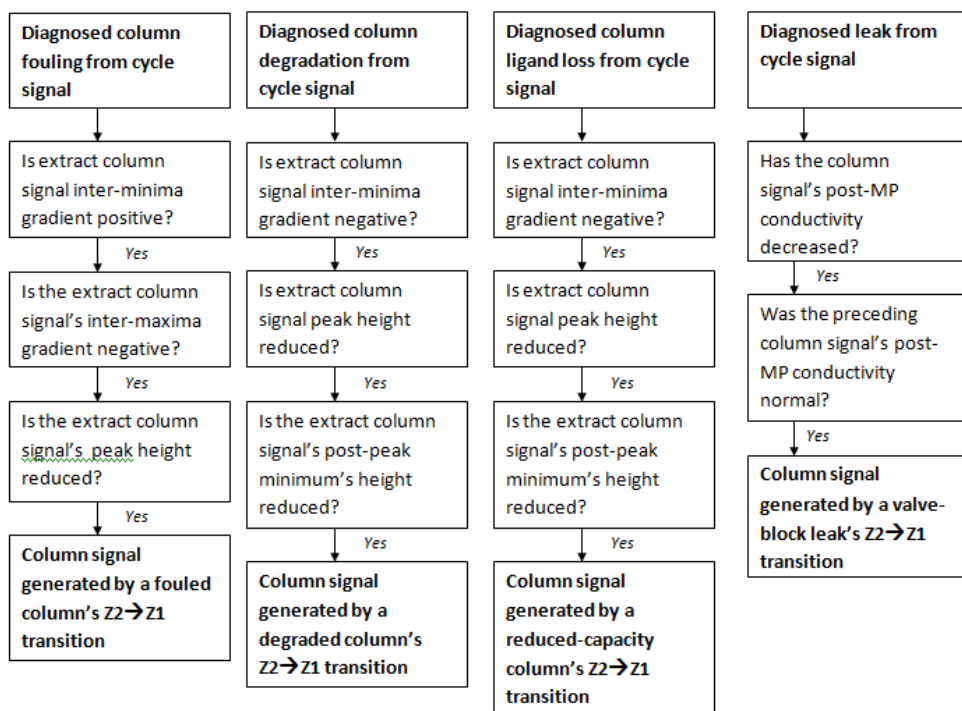


**Figure 5-10 Decision trees for locating malfunctioning component (post-failure-mode classification)**

### 5.3.5 Robustness of fault detection methods to false-positive signals

The robustness of an expert system to false-positive signal features is important for its practical utility. This section presents results which suggest that failure-mode signal patterns may not be easily 'spoofed' by potential process adjustments or one-off anomalies.

Any expert system depending upon rules-based analysis of SMB signal features will be practically useful only if it is robust. In this context, 'robustness' is defined as an expert system's ability to ignore false-positive signals as well as false-negative signals. In the development of other chromatographic expert systems, the issue of robustness to false negative signals has been addressed by means such as: 1) Improved sensitivity and accuracy of detectors, 2) Multiple sensors (e.g. pressure, flow rate and UV absorbance), and 3) The use of Artificial Neural Networks, in conjunction with rules-based algorithms, to increase the robustness of expert systems against noisy data [130]. All of these strategies for improving an expert system's robustness to false negative signals may be employed in the future development of expert SMB systems.

Ignoring false positive signals by batch chromatographic expert systems is achievable by similar means as those used for ignoring false negative signals. However, SMB systems may be more vulnerable to the generation of false-positive signals than batch chromatographic systems, because

any one-off anomalies or perturbations of an SMB system may be perpetuated in cycle signals due to non-batch nature of SMB systems. In turn, this may lead to misclassification of SMB faults or misidentification of faulty components. This section investigates whether generation of false-positive signals is easily achieved in SMB systems.

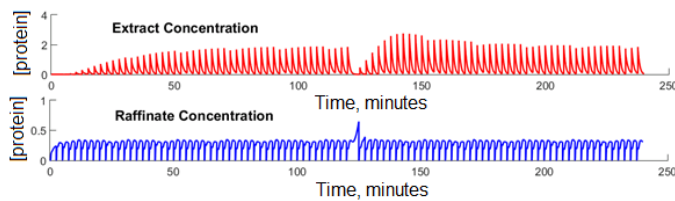
The reproducibility of failure-mode signal patterns between cycle times was observed from the experimental and simulation data presented in a previous section. Figure 5-11E shows an example of this cycle-signal reproducibility more clearly by graphing an overlay of three cycle signals (duration of 20 minutes each) which were collected consecutively from the extract of an experimental SMB system afflicted by a valve-block leak. As can be seen from the figure, the peaks, troughs and band-widths of the three cycle signals closely align, and thus fulfil the definition of a consistent cycle signal.

Four attempts were made to generate false-positive cycle signals. For a linear isotherm process experiencing a failure-mode of a single fouled column (as shown by Figure 5-11A), a port switching event in the middle of the process run (at 120 minutes) was simulated to be deferred by one switching period. It can be seen from Figure 5-11A that this one-off process perturbation did not result in long-lasting changes to the existing cycle signal and column signal features; the signal patterns present before the process interruption are re-asserted by the simulation after approximately one cycle period. A similar result was observed in a different perturbation of another simulated failure-mode SMB system. Figure 5-11B shows the simulation results of a linear-isotherm SMB process which, in addition to being afflicted by ligand loss from a single column, experiences a jump in the input feed concentration - lasting for the duration of a single switching period - midway through the process (at 120mins). This one-off process perturbation also failed to durably alter the signal patterns; after two switching cycles, no differences between the pre-perturbation cycle signals and the re-established cycle signals can be observed.

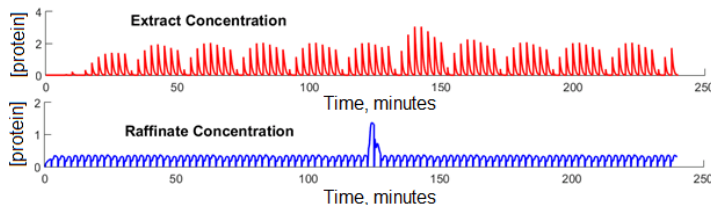
For failure mode detection and diagnosis through outlet-concentration pattern-analysis to attract the interest of industrial SMB practitioners, robustness to cycle-signal spoofing must also be demonstrated for SMB processes operated under overload conditions (i.e. under high feed-concentration, non-linear isotherm conditions). Two attempts were made to generate false-positive cycle signals in otherwise fault-free non-linear SE-SMB processes. The first attempt to spoof a cycle signal delayed a port-switching event for one switching time in the middle of a simulated process (at 75 minutes); shown by Figure 5-11C, this process perturbation did not succeed in producing any

iterative cycle signal in the non-linear isotherm SMB simulation. Similarly, a one-off temporary process perturbation of an increase in feed concentration (occurring at 75 minutes in Figure 5-11D), also failed to produce a lasting modification to the outlet signal patterns from an SMB operated under non-linear isotherm conditions.

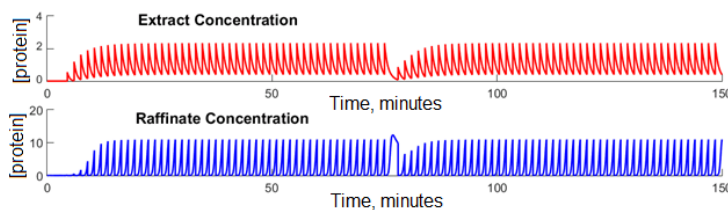
### A) One-off process perturbation (linear isotherm)



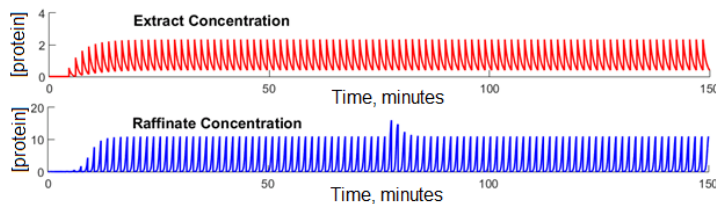
### B) One-off process perturbation of feed (linear isotherm)



### C) One-off process perturbation (nonlinear isotherm)



### D) One-off process perturbation of feed (nonlinear isotherm)



### E) Overlay of experimental cycle signals

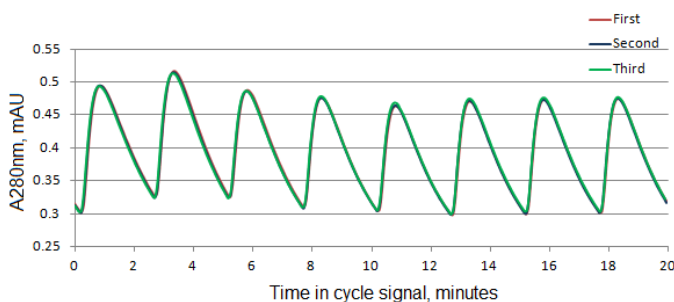


### Figure 5-11 Generating false-positive failure-mode signals

Attempts to 'spoo' decision trees by generating false-positive failure-mode cycle signals. **A)** Extension of one switching period (linear-isotherm process), **B)** Increase in feed concentration during one switching period (linear-isotherm process), **C)** Extension of one switching period (high feed concentration, nonlinear-isotherm process), **D)** Increase in feed concentration during one switching period (high feed concentration, non-linear isotherm process). **E)** Overlay of extract cycle signals from experimental leak failure mode.

### 5.3.6 Failure modes in a directly-coupled SMB ternary cascade

The previous chapter made the case that multi-component (ternary) separations are efficiently achieved through use of raffinate-coupled SMB cascades. The inter-train mixing tank in such raffinate-coupled cascades has the dual advantages of both buffering modulator perturbations generated by the first separation train, but also 're-setting' failure-mode signals from the first separation train (i.e. buffering the concentration variances of outlet feed-species) so that a binary-separation SMB expert system may be applied to multi-component cascades without modification.

This latter benefit of intermediary buffer tanks is useful because failure-mode signals in directly-coupled SMB cascades can be much more complex and subtle. This signal complexity and subtlety may be seen from the example shown by Figure 5-12. The figure shows the outlet concentration patterns of a direct-raffinate-coupled SMB cascade, where – for the purposes of a simple demonstration – the switching times of both cascades are equal, a modulator step is present between the separation trains but not within them (i.e. the binary separation trains are operated isocratically), and both separation trains have the same cycle time of 16 minutes. In this very simple construction of a ternary SMB cascades, it can be seen that a failure mode in the first separation train (ligand loss from a single column) obviously affects the outlet concentration signals from outlet ports in the first separation train. However, the effects of this failure mode – once transmitted through the SMB cascade to the second extract and raffinate ports - is subtle to the extent that it is barely detectable by eye. Furthermore, if an additional fault were to also occur in the second separation train, its detection and diagnosis would require an SMB expert system to apply robust and accurate de-convolution tools to the second train's outlet signals (Extract 2 ('E2') and Raffinate 2 ('R2') in the figure) to parse the identities and origins of both failure modes. It is questionable whether development of these de-convolution strategies for an SMB cascade is warranted, given that buffer-tank mediated cascades can easily avoid the need for such additional complexity in an expert system.

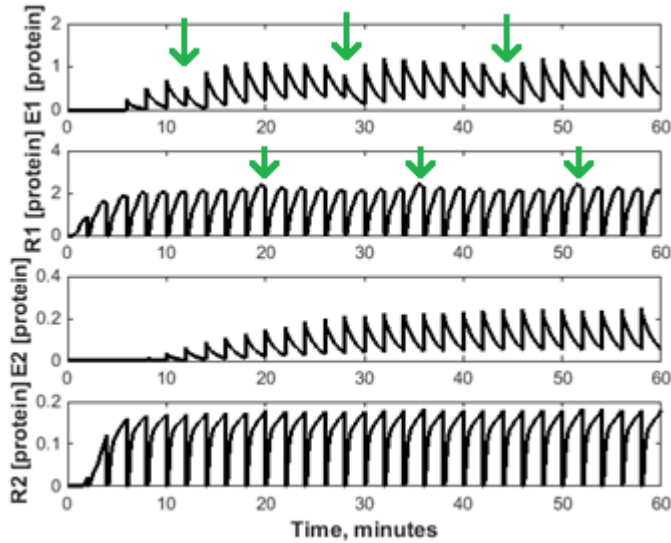


**Figure 5-12 Failure-mode patterns in an SMB cascade**

Failure mode signal patterns, as transmitted from the first separation train (top two rows) to the second separation train (bottom two rows) through a direct raffinate-coupled SMB cascade. Green arrows indicate distinct failure mode signatures in the first separation train, but these signals are indistinct once processed by the second SMB separation train. Outlets of second SMB train are named 'Extract II' (E2) and 'Raffinate II' (R2).

## Conclusion

This chapter has presented an initial set of strategies for the detection and diagnosis of certain failure modes in SE-SMB systems. It was found that common failure modes, including column and pump faults, were amenable to the type of rules-based expert systems that have previously been successfully applied to batch chromatography tasks. It was also found that a simple classification algorithm, when applied to simulated signal patterns, could sensitively detect failure-modes even in non-severe cases of a fault where the purity of the outlet streams was not compromised. However, a considerable amount of investigative and development work remains to be performed before an SMB expert system may find application to industrial or laboratory processes.

Avenues for future development of SMB expert systems include the analysis of 'multiple' and 'complex' failure-modes. 'Multiple failure modes' are failure modes which can co-occur, such as ligand loss and fouling of all columns, or single classes of failure mode that affect multiple components in an SMB system, such as fouling of half of the SMB columns. These failure modes are more complex than singular failure modes, because the large number of possible combinations and

severities of failure modes means that there are very many permutations of outlet concentration signal patterns. It remains to be seen whether the raffinate and extract outlet concentration patterns can provide enough information to diagnose multiple and complex failure modes, so additional means of SMB process monitoring – such as through measurement of internal concentration profiles, online outlet-purity analysis through at-line HPLC sampling, pressure and flow-rate monitoring – may become necessary. An alternative means for process monitoring would be to schedule regular withdraws of columns from an ongoing SMB process, and then subject each column - in isolation - to tests. For example, these tests could include assaying for column degradation (acetone-pulse test) or rapid assessment of ligand density (histidine-pulse test) [133].

In industrial SE-SMB chromatography, it is very likely that additional complexity will arise due to the characteristics of the feed material. This chapter has considered failure-mode occurrence in a linear isotherm, fast mass-transfer system where the feed concentration was fixed, and the modulator concentrations of the input buffers were completely consistent. Such a scenario is unlikely to hold for typical industrial separation challenges; where feed composition may vary during the process, competitive isotherms are expected, buffer conductivity is variable (or only accurate to within  $\pm 5\text{mS/cm}$  of a set-point), and feed species with slow mass-transfer are common. Therefore, the future development of SMB expert systems will require consideration of additional failure-modes; these include (but are not limited to): 1) Changing composition of feed species, 2) Changing concentration of feed species, 3) Small deviances in SMB modulator concentration profile from buffer preparation errors, and 4) Changes to the distribution of residence times for biological macromolecules that are fragile when subject to prolonged periods adsorbed to chromatographic sorbent or immersed in chromatographic buffers.

Another important area for future work on SMB expert systems is the development of ‘fuzzy-logical’ rules-based systems. The decision trees presented in this chapter were capable of classification of faults from simulation data, but signal data produced from simulation is much less noisy than that collected from experimental processes. The noisiness of experimental data will likely require investigators to incorporate fuzzy logical rules into an SMB expert system, as the inaccuracies and uncertainties in the measurement of experimentally-generated features will suit system which can integrate probabilities. Consequently, as has been previously implemented for batch chromatography expert systems, the decision of yes-or-no in future SMB expert systems will require the definition of probabilistic thresholds.

In summary, whilst this chapter has outlined plausible detection and diagnosis mechanisms for certain types of failure modes in SMB systems, many questions remain as to how, and to what degree, SMB processes may be subject to automated and robust process monitoring.

## CHAPTER 6 CONCLUSION

Continuous and intensified chromatographic processes may solve a number of challenges in bioseparation operations. As detailed in the introduction to this thesis, the high manufacturing costs of biopharmaceuticals spur industrial interest in finding bioseparation processes of improved productivity and yield, but which maintain high standards of purity. However, continuous and intensified bioseparation processes hold appeal beyond this straightforward understanding of manufacturing costs. Continuous DSP unit operations bring closer the possibility of fully continuous bioprocesses; such innovations are exciting for their potential to facilitate the manufacture of low-stability biologics from perfusion bioreactors. In addition to being an enabling technology for end-to-end continuous bioprocessing, intensified processes such as SE-SMB chromatography are capable of performing separations to a resolution (at a given productivity) which is impossible to match through use of single-column batch protocols. Furthermore, the separation resolving-power of SMB systems has the potential to improve lot-to-lot product variant and impurity-profile consistency; this could ease the regulatory and validation burden incurred during early bioprocess development work and post regulatory-approval commercial manufacturing.

This thesis documents the author's investigations into SE-SMB systems, which are promising candidates for inclusion into intensified and continuous bioprocesses. In order to make SE-SMB more attractive than the established single-column batch methods for industrial adoption, this body of work focuses on the twin challenges of operational design and process-monitoring of SE-SMB systems. As outlined in the introduction section of this thesis, a number of issues have historically frustrated the appeal of SE-SMB in industrial bioprocessing; these issues – and the outcomes of their investigation by the author – are summarised below:

- 1) The lack of an accurate SE-SMB design space and set of design inequalities, as investigated in the first Results chapter, has resulted in poor-quality separations as reported by some operators of SE-SMB separations. As detailed in this thesis, the definition of an accurate design space permitted the analytical design of a robust and productive SE-SMB separation of a binary protein model mixture for the first time. Furthermore, the scarcity of literature examples of experimental SE-SMB separations of very challenging mixtures was reduced here through the presentation of example purification experiments with ovalbumin variants.

- 2) The absence of a formal understanding of the modulator dynamics of SE-SMB systems, and thus the challenge of stabilizing the modulator step position in the SE-SMB system, may have previously hindered efforts to optimize binary SE-SMB systems for non-linear systems. In such systems, the ability to avoid the delocalization of the modulator step size and position without selection of sub-optimal switching frequencies – by use of the  $\Psi$  number - should be helpful for SE-SMB operators.
- 3) The definition of clear alternatives to the existing intensified chromatographic approaches – which span from various isocratic centre-cut SMB processes to multiple linear-gradient recycle batch-type processes – has been presented in this thesis. Two centre-cut SE-SMB processes were proposed as candidate intensified-chromatographic processes: the established SE-SMB cascade and the new SAW SMB.
- 4) The lack of process optimization-comparison studies which account for the specific interests of the biopharmaceutical industry. Simulations were used to investigate of various intensified processes applied to a separation problem which featured non-isocratic operation, non-linear isotherm conditions, and small separation factors; these features reflect common bio-chromatography challenges. As far as the author is aware, this comparison study is currently one of very few which compare SE-SMB systems with the rival industrial process of single-column recycle-batch chromatography. SE-SMB systems showed significant promise, in the context of these results, as an intensified and continuous process.
- 5) The lack of an SMB fault detection and diagnosis expert system to ‘de-risk’ industrial operation. The work for this thesis did not include the development of an SE-SMB expert system – this is a future task that will require significantly investment of resources and time. However, as a starting point, a number of failure-mode ‘signatures’ have been presented which should immediately enable other investigators to better recognize typical experimental faults. Furthermore, it is hoped that the preliminary work on fault classification decision-trees described in this thesis will be informative for the future development of SMB expert systems.

A number of avenues for future work have been outlined within the previous Results chapters. Most of these proposals follow logically and narrowly from each chapter’s content. However, there are a few research questions which have bearing on all research questions raised in this thesis.

First, the various intensified and continuous chromatographic systems would benefit from comparisons across a broad number of features. While such a comparison would obviously include dimensions such as resolving power and productivity, other qualitative issues such as process controllability, the design space size for robust purifications, and vulnerability to failure modes would also feature in an industrially useful comparison. It is also possible that individual process requirements suit different types of intensified chromatographic processes. For example, a process that requires continuous processing due to low product stability, but doesn't require a superbly high-resolution bio-chromatographic separation, may benefit from a recycle-batch process which has far fewer failure-modes than an MCGSP or SE-SMB process. Conversely, a process which requires a high-resolution and high-productivity chromatographic step, might favour an SE-SMB process despite the additional failure-mode risks that would be involved.

Second, the issue of protein residence time in intensified and continuous separations is of industrial interest. Whilst the residence-time distribution of species in a single-column batch process is easily determined, methods to calculate the residence-time distribution of species in an SMB or generic recycle-chromatographic process are missing from the literature. Since certain biological macromolecules, such as viral vectors, can often be denatured by long exposure to certain chromatographic sorbents, this issue is central to optimal process design.

Finally, an important area of future work may be the definition of constraints to delineate the design space of binary SE-SMB separations run under non-linear isotherm conditions. Even if these constraints were not completely accurate because they were based upon a set of simplifications – such as that of the 'square-wave' modulator perturbation simplification employed by N-theory – the use of these constraints would be much more important than their use for experimental separation problems. An understanding of the phenomena caused by non-linear isotherms in SE-SMB systems would significantly simplify the multi-objective optimization problem of SE-SMB cascades, and would thus provide significant insight into how SE-SMB should be optimally configured. Questions related to: the optimal size of columns for each of the SE-SMB separation trains, the optimal coupling between the trains in the context of flow-rate and ZLB modulator-dilution constraints, and the interaction between the modulator-step sequence (i.e. whether the desorbent modulator level in the first train should be higher than that of the second) and the non-linear isotherm behaviour of feed-species, together constitute fundamental questions in the centre-cut SE-SMB chromatography of protein mixtures.



## CHAPTER 7 BIBLIOGRAPHY

- [1] C.J. Wayne, A. Velayudhan, Modulator Dynamics Shape the Design Space for Stepwise-Elution Simulated Moving Bed Chromatographic Separations, *Biotechnol. J.* (2018) 1700664. doi:10.1002/biot.201700664.
- [2] G. Guiochon, D.G. Shirazi, A. Felinger, A.M. Katti, *Fundamentals of preparative and nonlinear chromatography*, Academic Press, 2006. [https://books.google.co.uk/books?id=1jQCbFCHp\\_8C&printsec=frontcover&dq=guiochon+chromatography&hl=en&sa=X&ved=0ahUKEwi\\_yJSV4ajbAhVIKMAKHVVFAmkQ6AEIMDAB#v=onepage&q&f=false](https://books.google.co.uk/books?id=1jQCbFCHp_8C&printsec=frontcover&dq=guiochon+chromatography&hl=en&sa=X&ved=0ahUKEwi_yJSV4ajbAhVIKMAKHVVFAmkQ6AEIMDAB#v=onepage&q&f=false) (accessed May 28, 2018).
- [3] A.P. Schellinger, P.W. Carr, Isocratic and gradient elution chromatography: A comparison in terms of speed, retention reproducibility and quantitation, *J. Chromatogr. A.* 1109 (2006) 253–266. doi:10.1016/J.CHROMA.2006.01.047.
- [4] E. Tyteca, K. Vanderlinden, M. Favier, D. Clicq, D. Cabooter, G. Desmet, Enhanced selectivity and search speed for method development using one-segment-per-component optimization strategies, *J. Chromatogr. A.* 1358 (2014) 145–154. doi:10.1016/J.CHROMA.2014.06.097.
- [5] E. Tyteca, S.H. Park, R.A. Shellie, P.R. Haddad, G. Desmet, Computer-assisted multi-segment gradient optimization in ion chromatography, *J. Chromatogr. A.* 1381 (2015) 101–109. doi:10.1016/J.CHROMA.2014.12.085.
- [6] M. Herper, Four Reasons Drugs Are Expensive, Of Which Two Are False, *Forbes*. (2015). <https://www.forbes.com/sites/matthewherper/2015/10/13/four-reasons-drugs-are-expensive-of-which-two-are-false/#5bc22e8e4c3b> (accessed September 2, 2018).
- [7] P.M. (GE H.L.S. Galliher, *Strategies and Points to Consider for Continuous Bioprocessing*, in: *Contin. Biomanufacturing Curr. Success Futur. Trends*, Oxford, 2017.
- [8] M.E. Taylor, K. Drickamer, *Introduction to Glycobiology*, 3rd ed., Oxford University Press, 2011. <https://global.oup.com/academic/product/introduction-to-glycobiology-9780199569113?cc=gb&lang=en&> (accessed September 2, 2018).
- [9] A.J. Stankiewicz, J.B. Moulijn, *Process Intensification: Transforming Chemical Engineering*, 2000. [https://www.rvo.nl/sites/default/files/2013/10/Process Intensification Transforming Chemical Engineering.pdf](https://www.rvo.nl/sites/default/files/2013/10/Process%20Intensification%20Transforming%20Chemical%20Engineering.pdf) (accessed September 4, 2018).
- [10] G. Subramanian, *Continuous Biomanufacturing - Innovative Technologies and Methods*, Wiley-VCH Verlag GmbH & Co. KGaA, Weinheim, Germany, 2017. doi:10.1002/9783527699902.
- [11] J.W. Lee, P.C. Wankat, Optimized design of recycle chromatography to isolate intermediate retained solutes in ternary mixtures: Langmuir isotherm systems, *J. Chromatogr. A.* 1216 (2009) 6946–6956. doi:10.1016/j.chroma.2009.08.046.
- [12] A. Tarafder, L. Aumann, M. Morbidelli, Improvement in industrial re-chromatography

- (recycling) procedure in solvent gradient bio-separation processes, *J. Chromatogr. A.* 1195 (2008) 67–77. doi:10.1016/J.CHROMA.2008.04.079.
- [13] F. Charton, M. Bailly, G. Guiochon, Recycling in preparative liquid chromatography, *J. Chromatogr. A.* 687 (1994) 13–31. doi:10.1016/0021-9673(94)00728-4.
- [14] J.R. Crary, K. Cain-Janicki, R. Wijayarathne, External recycle chromatography: A practical method for preparative purifications, *J. Chromatogr. A.* 462 (1989) 85–94. doi:10.1016/S0021-9673(00)91338-4.
- [15] A. Seidel-Morgenstern, G. Guiochon, Theoretical study of recycling in preparative chromatography, *AIChE J.* 39 (1993) 809–819. doi:10.1002/aic.690390509.
- [16] R. Godawat, K. Brower, S. Jain, K. Konstantinov, F. Riske, V. Warikoo, Periodic counter-current chromatography - design and operational considerations for integrated and continuous purification of proteins, *Biotechnol. J.* 7 (2012) 1496–1508. doi:10.1002/biot.201200068.
- [17] F. Steinebach, M. Krättli, G. Storti, M. Morbidelli, Equilibrium Theory Based Design Space for the Multicolumn Countercurrent Solvent Gradient Purification Process, *Ind. Eng. Chem. Res.* 56 (2017) 13482–13489. doi:10.1021/acs.iecr.7b00569.
- [18] J.P.S. Aniceto, C.M. Silva, Simulated moving bed strategies and designs: From established systems to the latest developments, *Sep. Purif. Rev.* 44 (2014) 41–73. doi:10.1080/15422119.2013.851087.
- [19] D.B. Broughton, C.G. Gerhold, Continuous sorption process employing fixed bed of sorbent and moving inlets and outlets, US2985589A, 1961.
- [20] J.W. Lee, P.C. Wankat, Thermal simulated moving bed concentrator, *Chem. Eng. J.* 166 (2011) 511–522. doi:10.1016/J.CEJ.2010.11.009.
- [21] Y.S. Bae, C.H. Lee, Partial-discard strategy for obtaining high purity products using simulated moving bed chromatography, *J. Chromatogr. A.* 1122 (2006) 161–173. doi:10.1016/j.chroma.2006.04.040.
- [22] W. Jin, P.C. Wankat, Thermal Operation of Four-Zone Simulated Moving Beds, *Ind. Eng. Chem. Res.* 46 (2007) 7208–7220. doi:10.1021/IE070047U.
- [23] Y.A. Beste, W. Arlt, Side-stream simulated moving-bed chromatography for multicomponent separation, *Chem. Eng. Technol.* 25 (2002) 956–962. doi:10.1002/1521-4125(20021008)25:10<956::AID-CEAT956>3.0.CO;2-7.
- [24] Z. Zhang, M. Mazzotti, M. Morbidelli, PowerFeed operation of simulated moving bed units: Changing flow-rates during the switching interval, *J. Chromatogr. A.* 1006 (2003) 87–99. doi:10.1016/S0021-9673(03)00781-7.
- [25] O. Ludemann-Hombourger, R.M. Nicoud, M. Bailly, The “VARICOL” process: A new multicolumn continuous chromatographic process, *Sep. Sci. Technol.* 35 (2000) 1829–1862. doi:10.1081/SS-100100622.

- [26] P. Sá Gomes, A.E. Rodrigues, Outlet Streams Swing (OSS) and MultiFeed Operation of Simulated Moving Beds, *Sep. Sci. Technol.* 42 (2007) 223–252. doi:10.1080/01496390601070125.
- [27] S. Li, Y. Kawajiri, J. Raisch, A. Seidel-Morgenstern, Optimization of simulated moving bed chromatography with fractionation and feedback: Part II. Fractionation of both outlets, *J. Chromatogr. A.* 1217 (2010) 5349–5357. doi:10.1016/j.chroma.2010.06.032.
- [28] K.M. Kim, C.H. Lee, Backfill-simulated moving bed operation for improving the separation performance of simulated moving bed chromatography, *J. Chromatogr. A.* 1311 (2013) 79–89. doi:10.1016/j.chroma.2013.08.058.
- [29] Y. Zang, P.C. Wankat, SMB Operation Strategy–Partial Feed, *Ind. Eng. Chem. Res.* 41 (2002) 2504–2511. doi:10.1021/IE010832L.
- [30] T.B. Jensen, T.G.P. Reijns, H.A.H. Billiet, L.A.M. van der Wielen, Novel simulated moving-bed method for reduced solvent consumption, *J. Chromatogr. A.* 873 (2000) 149–162. doi:10.1016/S0021-9673(99)01352-7.
- [31] F. Wei, B. Shen, M. Chen, Y. Zhao, Study on a pseudo-simulated moving bed with solvent gradient for ternary separations, *J. Chromatogr. A.* 1225 (2012) 99–106. doi:10.1016/j.chroma.2011.12.080.
- [32] S. Mun, Optimal design of solvent gradient simulated moving bed chromatography for amino acid separation, *J. Liq. Chromatogr. Relat. Technol.* 34 (2011) 1518–1535. doi:10.1080/10826076.2011.575976.
- [33] H.G. Nam, S.H. Jo, C. Park, S. Mun, Experimental validation of the solvent-gradient simulated moving bed process for optimal separation of phenylalanine and tryptophan, *Process Biochem.* 47 (2012) 401–409. doi:10.1016/j.procbio.2011.11.011.
- [34] J. Houwing, S.H. Van Hateren, H.A.H. Billiet, L.A.M. Van Der Wielen, Effect of salt gradients on the separation of dilute mixtures of proteins by ion-exchange in simulated moving beds, *J. Chromatogr. A.* 952 (2002) 85–98. doi:10.1016/S0021-9673(02)00091-2.
- [35] J. Houwing, H.A.H. Billiet, L.A.M. Van Der Wielen, Optimization of azeotropic protein separations in gradient and isocratic ion-exchange simulated moving bed chromatography, *J. Chromatogr. A.* 944 (2002) 189–201. doi:10.1016/S0021-9673(01)01389-9.
- [36] S. Mun, N.-H.L. Wang, Optimization of productivity in solvent gradient simulated moving bed for paclitaxel purification, *Process Biochem.* 43 (2008) 1407–1418. doi:10.1016/j.procbio.2008.08.011.
- [37] L. Gueorguieva, S. Palani, U. Rinas, G. Jayaraman, A. Seidel-Morgenstern, Recombinant protein purification using gradient assisted simulated moving bed hydrophobic interaction chromatography. Part II: Process design and experimental validation, *J. Chromatogr. A.* 1218 (2011) 6402–6411. doi:10.1016/j.chroma.2011.07.008.

- [38] J.S. Hur, P.C. Wankat, New Design of Simulated Moving Bed (SMB) for Ternary Separations, *Ind. Eng. Chem. Res.* 44 (2005) 1906–1913. doi:10.1021/ie040164e.
- [39] J.S. Hur, P.C. Wankat, J. Il Kim, J.K. Kim, Y.M. Koo, Purification of L-phenylalanine from a ternary amino acid mixture using a two-zone SMB/chromatography hybrid system, *Sep. Sci. Technol.* 42 (2007) 911–930. doi:10.1080/01496390701206264.
- [40] Y. Xie, S. Mun, J. Kim, N.H.L. Wang, Standing wave design and experimental validation of a tandem simulated moving bed process for insulin purification, *Biotechnol. Prog.* 18 (2002) 1332–1344. doi:10.1021/bp025547r.
- [41] S. Mun, Enhanced performance of a tandem simulated moving bed process for separation of paclitaxel, 13-dehydroxybaccatin III, and 10-deacetylpaclitaxel by making a difference between the adsorbent particle sizes of the two subordinate simulated moving bed units, *Process Biochem.* 46 (2011) 1329–1334. doi:10.1016/j.procbio.2011.02.026.
- [42] P.C. Wankat, Simulated Moving Bed Cascades for Ternary Separations, *Ind. Eng. Chem. Res.* 40 (2001) 6185–6193. doi:10.1021/ie010075r.
- [43] X. Yi, C.Y. Chin, D.S.C. Phelps, C.-H. Lee, K.B. Lee, S. Mun, N.-H.L. Wang, A Five-Zone Simulated Moving Bed for the Isolation of Six Sugars from Biomass Hydrolyzate, *Ind. Eng. Chem. Res.* 44 (2005) 9904–9920.
- [44] R. Wooley, Z. Ma, N.H.L. Wang, A nine-zone simulating moving bed for the recovery of glucose and xylose from biomass hydrolyzate, *Ind. Eng. Chem. Res.* 37 (1998) 3699–3709. doi:10.1021/ie9800896.
- [45] J. Nowak, D. Antos, A. Seidel-Morgenstern, Theoretical study of using simulated moving bed chromatography to separate intermediately eluting target compounds, *J. Chromatogr. A.* 1253 (2012) 58–70. doi:10.1016/J.CHROMA.2012.06.096.
- [46] N.-H.L. Wang, C.Y. Chin, Versatile simulated moving bed systems, US7141172B2, 2002. <https://patents.google.com/patent/US7141172B2/en> (accessed May 28, 2018).
- [47] X. Wang, C.B. Ching, Chiral separation of  $\beta$ -blocker drug (nadolol) by five-zone simulated moving bed chromatography, *Chem. Eng. Sci.* 60 (2005) 1337–1347. doi:10.1016/j.ces.2004.10.007.
- [48] H. Khan, M. Younas, Five-zone simulating moving bed for ternary separation, *Iran. J. Chem. Chem. Eng.* 30 (2011) 101–117.
- [49] S. Mun, Improving performance of a five-zone simulated moving bed chromatography for ternary separation by simultaneous use of partial-feeding and partial-closing of the product port in charge of collecting the intermediate-affinity solute molecules, *J. Chromatogr. A.* 1218 (2011) 8060–8074. doi:10.1016/j.chroma.2011.09.015.
- [50] G. Paredes, S. Abel, M. Mazzotti, M. Morbidelli, J. Stadler, Analysis of a Simulated Moving Bed Operation for Three-Fraction Separations (3F-SMB), *Ind. Eng. Chem. Res.* 43 (2004) 6157–6167. doi:10.1021/IE0498293.

- [51] S. Abel, M.U. Bähler, C. Arpagaus, M. Mazzotti, J. Stadler, Two-fraction and three-fraction continuous simulated moving bed separation of nucleosides, *J. Chromatogr. A.* 1043 (2004) 201–210. doi:10.1016/j.chroma.2004.05.094.
- [52] S. Mun, Partial port-closing strategy for obtaining high throughput or high purities in a four-zone simulated moving bed chromatography for binary separation, *J. Chromatogr. A.* 1217 (2010) 6522–6530. doi:10.1016/j.chroma.2010.08.049.
- [53] J.K. Kim, Y. Zang, P.C. Wankat, Single-cascade simulated moving bed systems for the separation of ternary mixtures, *Ind. Eng. Chem. Res.* 42 (2003) 4849–4860. doi:10.1021/ie030373j.
- [54] A.S. Kurup, K. Hidajat, A.K. Ray, Optimal operation of a Pseudo-SMB process for ternary separation under non-ideal conditions, *Sep. Purif. Technol.* 51 (2006) 387–403. doi:10.1016/j.seppur.2006.03.002.
- [55] R.J.S. Silva, R.C.R. Rodrigues, H. Osuna-Sanchez, M. Bailly, E. Valéry, J.P.B. Mota, A new multicolumn, open-loop process for center-cut separation by solvent-gradient chromatography, *J. Chromatogr. A.* 1217 (2010) 8257–8269. doi:10.1016/j.chroma.2010.11.005.
- [56] E.A.B. Da Silva, A.E. Rodrigues, Design methodology and performance analysis of a pseudo-simulated moving bed for ternary separation, *Sep. Sci. Technol.* 43 (2008) 533–566. doi:10.1080/01496390701812491.
- [57] F. Wei, M. Li, F. Huang, M. Chen, H. Jiang, Y. Zhao, A novel pseudo simulated moving bed with solvent gradient for ternary separations, *J. Chromatogr. A.* 1218 (2011) 2906–2911. doi:10.1016/j.chroma.2011.03.001.
- [58] T. Masuda, T. Sonobe, F. Matsuda, M. Horie, Process for fractional separation of multi-component fluid mixture, US5198120A, 1990.
- [59] S. Jermann, S. Katsuo, M. Mazzotti, Intermittent simulated moving bed processes for chromatographic three-fraction separation, *Org. Process Res. Dev.* 16 (2012) 311–322. doi:10.1021/op200239e.
- [60] S. Jermann, M. Meijssen, M. Mazzotti, Three column intermittent simulated moving bed chromatography: 3. Cascade operation for center-cut separations, *J. Chromatogr. A.* 1378 (2015) 37–49. doi:10.1016/j.chroma.2014.12.011.
- [61] S. Katsuo, M. Mazzotti, Intermittent simulated moving bed chromatography: 1. Design criteria and cyclic steady-state, *J. Chromatogr. A.* 1217 (2010) 1354–1361. doi:10.1016/j.chroma.2009.12.065.
- [62] L. Aumann, M. Morbidelli, A continuous multicolumn countercurrent solvent gradient purification (MCSGP) process, *Biotechnol. Bioeng.* 98 (2007) 1043–1055. doi:10.1002/bit.21527.
- [63] C.J. Wayne, A. Velayudhan, Developments in Countercurrent Protein Polishing: Theory and

- Experiment, in: Oxford, 2017.
- [64] M. Krättli, F. Steinebach, M. Morbidelli, Online control of the twin-column countercurrent solvent gradient process for biochromatography, *J. Chromatogr. A.* 1293 (2013) 51–59. doi:10.1016/j.chroma.2013.03.069.
- [65] M.M. Papathanasiou, S. Avraamidou, R. Oberdieck, A. Mantalaris, F. Steinebach, M. Morbidelli, T. Mueller-Spaeth, E.N. Pistikopoulos, Advanced control strategies for the multicolumn countercurrent solvent gradient purification process, *AIChE J.* 62 (2016) 2341–2357. doi:10.1002/aic.15203.
- [66] Van der Wielen, L.A.M., Houwing J, in: *Proceeding First Eur. Symp. Biochem. Eng. Sci.*, 1996.
- [67] L.C. Keßler, L. Gueorguieva, U. Rinas, A. Seidel-Morgenstern, Step gradients in 3-zone simulated moving bed chromatography: Application to the purification of antibodies and bone morphogenetic protein-2, *J. Chromatogr. A.* 1176 (2007) 69–78. doi:10.1016/J.CHROMA.2007.10.087.
- [68] T. Mueller-Spaeth, L. Aumann, L. Melter, G. Stroehlein, M. Morbidelli, Chromatographic separation of three monoclonal antibody variants using multicolumn countercurrent solvent gradient purification (MCSGP), *Biotechnol. Bioeng.* 100 (2008) 1166–1177. doi:10.1002/bit.21843.
- [69] J.W. Lee, P.C. Wankat, Comparison of Recycle Chromatography and Simulated Moving Bed for Pseudobinary Separations, *Ind. Eng. Chem. Res.* 48 (2009) 7724–7732. doi:10.1021/ie900092y.
- [70] S.H. Jo, H.G. Nam, S. Mun, Optimal design and experimental validation of a modified four-zone SMB process for the separation of a ternary amino acid mixture, *Process Biochem.* 45 (2010) 1288–1298. doi:10.1016/j.procbio.2010.04.016.
- [71] S. Wang, Y. Liang, S. Zheng, Separation of epigallocatechin gallate from tea polyphenol by simulated moving bed chromatography, *J. Chromatogr. A.* 1265 (2012) 46–51. doi:10.1016/j.chroma.2012.09.098.
- [72] G. Agrawal, Y. Kawajiri, Comparison of various ternary simulated moving bed separation schemes by multi-objective optimization, *J. Chromatogr. A.* 1238 (2012) 105–113. doi:10.1016/j.chroma.2012.03.064.
- [73] G. Agrawal, Y. Kawajiri, Full Superstructure for Multiobjective Optimization of Multicolumn Chromatography for Ternary Separations, *Chem. Eng. Technol.* 38 (2015) 1677–1682. doi:10.1002/ceat.201500104.
- [74] D.M. Ruthven, C.B. Ching, Review Article Separation, *Chem. Eng. Sci.* 44 (1989) 1011–1038.
- [75] G. Storti, M. Mazzotti, M. Morbidelli, S. Carr, Robust design of binary countercurrent adsorption separation processes, *AIChE J.* 39 (1993) 471–492. doi:10.1002/aic.690390310.
- [76] D.C.S. Azevedo, A.E. Rodrigues, Design of a simulated moving bed in the presence of mass-

- transfer resistances, *AIChE J.* 45 (1999) 956–966. doi:10.1002/aic.690450506.
- [77] M. Mazzotti, G. Storti, M. Morbidelli, Optimal operation of simulated moving bed units for nonlinear chromatographic separations, 769 (1997) 3–24.
- [78] M. Mazzotti, G. Storti, M. Morbidelli, Robust Design of Countercurrent Adsorption Separation Processes : 2 . Multicomponent Systems, *AIChE J.* 40 (2010) 1825–1842.
- [79] S. Abel, M. Mazzotti, M. Morbidelli, Solvent gradient operation of simulated moving beds: 2. Langmuir isotherms, *J. Chromatogr. A.* 1026 (2004) 47–55. doi:10.1016/J.CHROMA.2003.11.054.
- [80] K.U. Klatt, F. Hanisch, G. Duennebier, Model-based control of a simulated moving bed chromatographic process for the separation of fructose and glucose, *J. Process Control.* 12 (2002) 203–209. www.elsevier.com/locate/jprocont.
- [81] G. Duennebier, J. Fricke, K.U. Klatt, Optimal design and operation of simulated moving bed chromatographic reactors, *Ind. Eng. Chem. Res.* 39 (2000) 2290–2304. doi:Doi 10.1021/le990820o.
- [82] C. Wang, K.U. Klatt, G. Duennebier, S. Engell, F. Hanisch, Neural network-based identification of SMB chromatographic processes, *Control Engineering Practice* 11 (2003) 949-959.
- [83] S. Abel, G. Erdem, M. Amanullah, M. Morari, M. Mazzotti, M. Morbidelli, Optimizing control of simulated moving beds-experimental implementation, *J. Chromatogr. A.* 1092 (2005) 2–16. doi:10.1016/j.chroma.2005.04.101.
- [84] M. Rüdts, T. Briskot, J. Hubbuch, Advances in downstream processing of biologics – Spectroscopy: An emerging process analytical technology, *J. Chromatogr. A.* 1490 (2017) 2–9. doi:10.1016/j.chroma.2016.11.010.
- [85] A. Velayudhan, Robustness and Regulatory Considerations in the Development of a Continuous Bioprocess Unit-Operation, in: *Integr. Contin. Biomanufacturing*, Castelldefels, Spain, 2013.
- [86] Y. Kawajiri, L.T. Biegler, Large scale optimization strategies for zone configuration of simulated moving beds, *Comput. Chem. Eng.* 32 (2008) 135–144. doi:10.1016/J.COMPCHEMENG.2007.04.009.
- [87] Z. Ma, N.-H.L. Wang, Standing Wave Analysis of SMB Chromatography: Linear Systems, *AIChE J.* 43 (1997) 2488–2508. doi:DOI 10.1002/aic.690431012.
- [88] H.K. Versteeg, W. Malalasekera, *An introduction to computational fluid dynamics : the finite volume method*, New York, 1995.
- [89] A. Velayudhan, C. Horváth, Adsorption and ion-exchange isotherms in preparative chromatography, *J. Chromatogr. A.* 663 (1994) 1–10. doi:10.1016/0021-9673(94)80490-7.
- [90] S.F. Chung, C.Y. Wen, Longitudinal dispersion of liquid flowing through fixed and fluidized

- beds, *AIChE J.* 14 (1968) 857–866. doi:10.1002/aic.690140608.
- [91] E.J. Wilson, C.J. Geankoplis, Liquid Mass Transfer at Very Low Reynolds Numbers in Packed Beds, *Ind. Eng. Chem. Fundam.* 5 (1966) 9–14. doi:10.1021/i160017a002.
- [92] M.E. Young, P.A. Carroad, R.L. Bell, Estimation of diffusion coefficients of proteins, *Biotechnol. Bioeng.* 22 (1980) 947–955. doi:10.1002/bit.260220504.
- [93] T.E. Bankston, M.C. Stone, G. Carta, Theory and applications of refractive index-based optical microscopy to measure protein mass transfer in spherical adsorbent particles, *J. Chromatogr. A.* 1188 (2008) 242–254. doi:10.1016/j.chroma.2008.02.076.
- [94] G.L. Skidmore, B.J. Hortsman, H.A. Chase, Modelling single-component protein adsorption to the cation exchanger s sepharose® FF, *J. Chromatogr. A.* 498 (1990) 113–128. doi:10.1016/S0021-9673(01)84240-0.
- [95] G. Wang, T. Briskot, T. Hahn, P. Baumann, J. Hubbuch, Root cause investigation of deviations in protein chromatography based on mechanistic models and artificial neural networks, *J. Chromatogr. A.* 1515 (2017) 146–153. doi:10.1016/j.chroma.2017.07.089.
- [96] E.J. Close, Thesis: The derivation of bioprocess understanding from mechanistic models of chromatography, UCL, 2015.
- [97] C.Y. Chin, Y. Xie, J.S. Alford, N.-H.L. Wang, Analysis of zone and pump configurations in simulated moving bed purification of insulin, *AIChE J.* 52 (2006) 2447–2460. doi:10.1002/aic.10852.
- [98] A. Mishra, A. Shukla, Analysis of the Effect of Elite Count on the Behavior of Genetic Algorithms: A Perspective, in: *IEEE 7th Int. Adv. Comput. Conf.*, 2017. doi:10.1109/IACC.2017.163.
- [99] N. Taulier, T. V Chalikian, Characterization of pH-induced transitions of beta-lactoglobulin: ultrasonic, densimetric, and spectroscopic studies., *J. Mol. Biol.* 314 (2001) 873–89. doi:10.1006/jmbi.2001.5188.
- [100] U. Bhaskar, G. Gopaldaswamy, R. Raghu, A simple method for efficient extraction and purification of C-phycoyanin from *Spirulina platensis* Geitler, *Indian J. Exp. Biol.* 43 (2005) 277–279.
- [101] Y. Xie, D. Wu, Z. Ma, N.H.L. Wang, Extended standing wave design method for simulated moving bed chromatography: Linear systems, *Ind. Eng. Chem. Res.* 39 (2000) 1993–2005. doi:10.1021/ie9905052.
- [102] P.C. Wankat, *Rate-controlled separations*, Blackie Academic & Professional, 1994. [https://books.google.co.uk/books/about/Rate\\_Controlled\\_Separations.html?id=PYUiz-kQjkUC&redir\\_esc=y](https://books.google.co.uk/books/about/Rate_Controlled_Separations.html?id=PYUiz-kQjkUC&redir_esc=y)
- [103] M. Mazzotti, S. Abel, L. Aumann, M. Morbidelli, Solvent gradient operation of simulated moving bed processes., *Abstr. Pap. Am. Chem. Soc.* 225 (2003) U241–U241.

- [104] S. Abel, M. Mazzotti, M. Morbidelli, Solvent gradient operation of simulated moving beds - 2. Langmuir isotherms, *J. Chromatogr. A.* 1026 (2004) 47–55. doi:10.1016/j.chroma.2003.11.054.
- [105] P. Li, J. Yu, G. Xiu, A.E. Rodrigues, Separation region and strategies for proteins separation by salt gradient ion-exchange SMB, *Sep. Sci. Technol.* 43 (2008) 11–28. doi:10.1080/01496390701747895.
- [106] S. Mun, N.H.L. Wang, Optimization of productivity in solvent gradient simulated moving bed for paclitaxel purification, *Process Biochem.* 43 (2008) 1407–1418. doi:10.1016/j.procbio.2008.08.011.
- [107] L.C. Keßler, L. Gueorguieva, U. Rinas, A. Seidel-Morgenstern, Step gradients in 3-zone simulated moving bed chromatography. Application to the purification of antibodies and bone morphogenetic protein-2, *J. Chromatogr. A.* 1176 (2007) 69–78. doi:10.1016/j.chroma.2007.10.087.
- [108] P. Jandera, J. Churáček, Gradient elution in liquid chromatography : IX. Selection of optimal conditions in stepwise-elution liquid chromatography, *J. Chromatogr. A.* 170 (1979) 1–10. doi:10.1016/S0021-9673(00)84232-6.
- [109] F. Helfferich, Ion exchange, McGraw-Hill, New York, 1962. [https://trove.nla.gov.au/work/3507138?q&sort=holdings+desc&\\_id=1527590390991&versionid=12340110](https://trove.nla.gov.au/work/3507138?q&sort=holdings+desc&_id=1527590390991&versionid=12340110) (accessed May 29, 2018).
- [110] A. Velayudhan, R.L. Hendrickson, M.R. Ladisch, Simultaneous concentration and purification through gradient deformation chromatography, *AIChE J.* 41 (1995) 1184–1193. doi:10.1002/aic.690410514.
- [111] J.K. Kim, Y. Zang, P.C. Wankat, Single-Cascade Simulated Moving Bed Systems for the Separation of Ternary Mixtures, *Ind. Eng. Chem. Res.* 42 (2003) 4849–4860. doi:10.1021/ie030373j.
- [112] G. Ströhlein, L. Aumann, M. Mazzotti, M. Morbidelli, A continuous, counter-current multi-column chromatographic process incorporating modifier gradients for ternary separations, *J. Chromatogr. A.* 1126 (2006) 338–346. doi:10.1016/j.chroma.2006.05.011.
- [113] S. Mun, Effect of a partial-feeding application on product purities and throughput of a five-zone simulated moving bed process for the separation of a ternary nucleoside mixture, *Process Biochem.* 46 (2011) 977–986. doi:10.1016/j.procbio.2011.01.015.
- [114] V.G. Mata, A.E. Rodrigues, Separation of ternary mixtures by pseudo-simulated moving bed chromatography, *J. Chromatogr. A.* 939 (2001) 23–40. doi:10.1016/S0021-9673(01)01335-8.
- [115] R.J.S. Silva, R.C.R. Rodrigues, H. Osuna-Sanchez, M. Bailly, E. Valéry, J.P.B. Mota, A new multicolumn, open-loop process for center-cut separation by solvent-gradient chromatography, *J. Chromatogr. A.* 1217 (2010) 8257–8269. doi:10.1016/J.CHROMA.2010.11.005.

- [116] S.-H. Jo, J.K. Kim, C.G. Yoo, J.-I. Kim, Y.-M. Koo, S. Mun, Comparative Analysis of Single-Cascade Five-Zone and Two-Zone SMB Systems for the Separation of a Ternary Amino Acid Mixture, *Can. J. Chem. Eng.* 85 (2007) 875–882. <https://onlinelibrary.wiley.com/doi/pdf/10.1002/cjce.5450850608>.
- [117] Y. Zang, P.C. Wankat, Three-Zone Simulated Moving Bed with Partial Feed and Selective Withdrawal, *Ind. Eng. Chem. Res.* 41 (2002) 5283–5289. <http://pubs.acs.org/doi/pdf/10.1021/ie020052s>.
- [118] S. Mun, Enhanced separation performance of a five-zone simulated moving bed process by using partial collection strategy based on alternate opening and closing of a product port, *Ind. Eng. Chem. Res.* 49 (2010) 9258–9270. doi:10.1021/ie100366g.
- [119] J. Nowak, D. Antos, A. Seidel-Morgenstern, Theoretical study of using simulated moving bed chromatography to separate intermediately eluting target compounds, *J. Chromatogr. A.* 1253 (2012) 58–70. doi:10.1016/j.chroma.2012.06.096.
- [120] G. Agrawal, B. Sreedhar, Y. Kawajiri, Systematic optimization and experimental validation of ternary simulated moving bed chromatography systems, *J. Chromatogr. A.* 1356 (2014) 82–95. doi:10.1016/j.chroma.2014.06.028.
- [121] S. Imamoglu, Simulated moving bed chromatography (SMB) for application in bioseparation., *Adv. Biochem. Eng. Biotechnol.* 76 (2002) 211–231. doi:10.1007/3-540-45345-8.
- [122] G. Paredes, S. Abel, M. Mazzotti, M. Morbidelli, J. Stadler, Analysis of a Simulated Moving Bed Operation for Three-Fraction Separations (3F-SMB), *Ind. Eng. Chem. Res.* 43 (2004) 6157–6167. doi:10.1021/ie0498293.
- [123] P. Nikitas, A. Pappa-Louisi, K. Papachristos, Optimisation technique for stepwise gradient elution in reversed-phase liquid chromatography, *J. Chromatogr. A.* 1033 (2004) 283–289. doi:10.1016/J.CHROMA.2004.01.048.
- [124] P. Jandera, J. Churáček, Gradient elution in column liquid chromatography: theory and practice, Elsevier, 1985. [https://books.google.co.uk/books/about/Gradient\\_Elution\\_in\\_Column\\_Liquid\\_Chroma.html?id=9Bp-IAEACAAJ&redir\\_esc=y](https://books.google.co.uk/books/about/Gradient_Elution_in_Column_Liquid_Chroma.html?id=9Bp-IAEACAAJ&redir_esc=y).
- [125] H. Du, M.J. Stillman, Knowledge acquisition for fault diagnosis in gas chromatography, *Anal. Chim. Acta.* 296 (1994) 21–31. doi:10.1016/0003-2670(94)85147-6.
- [126] H. Du, S. Lahiri, G. Huang, M.J. Stillman, Developing an expert system for diagnosis of problem gas chromatographic data, *Anal. Chim. Acta.* 296 (1994) 21–31. doi:10.1016/0003-2670(94)85146-8.
- [127] S. Lahiri, R.S. Roberts, J.W. Elling, Algorithms for the Qualitative Assessment of Gas Chromatograms, *J. Chromatogr. Sci.* 34 (1996) 505–512. doi:10.1093/chromsci/34.11.505.
- [128] C. Kingsford, S.L. Salzberg, What are decision trees?, *Nat. Biotechnol.* 26 (2008) 1011–3. doi:10.1038/nbt0908-1011.

- [129] A.P. Levis, R.G. Timpany, W.E. Austad, J.W. Elling, J.J. Ferguson, D.A. Klotter, S.I. Hruska, Application of knowledge-based network processing to automated gas chromatography data interpretation, in: S.K. Rogers, D.W. Ruck (Eds.), *International Society for Optics and Photonics*, 1995: pp. 294–302. doi:10.1117/12.205137.
- [130] J.W. Elling, S. Lahiri, J.P. Luck, R.S. Roberts, S.I. Hruska, K.L. Adair, A.P. Levis, R.G. Timpany, J.J. Robinson, Peer Reviewed: Hybrid Artificial Intelligence Tools for Assessing GC Data, *Anal. Chem.* 69 (1997) 409A–415A. doi:10.1021/ac971691t.
- [131] P. Sá Gomes, M. Minceva, A.E. Rodrigues, Operation strategies for simulated moving bed in the presence of adsorbent ageing, *Sep. Sci. Technol.* 42 (2007) 3555–3591. doi:10.1080/01496390701710703.
- [132] F.D. Antia, A Simple Approach to Design and Control of Simulated Moving Bed Chromatographs, in: A. Velayudhan, A.S. Rathore (Eds.), *Scale-up Optim. Preparative Chromatogr. Princ. Biopharm. Appl.*, Marcel Dekker, 2003: p. 342.
- [133] T.C. Huuk, T. Briskot, T. Hahn, J. Hubbuch, A versatile noninvasive method for adsorber quantification in batch and column chromatography based on the ionic capacity, *Biotechnol. Prog.* 32 (2016) 666–677. doi:10.1002/btpr.2228.

## CHAPTER 8 APPENDIX

**Table 8-1 MOO final generation's individuals for T1 binary separation**

**Product collected at Raffinate port**

ts, mins	Cd, M	Cf, M	Qd, , mL/min	Qf, mL/min	Productivity g/L/min	Yield, %
0.709	0.278	0.140	6.112	3.607	2.220	100.000
0.685	0.285	0.146	4.694	4.907	2.931	97.087
0.674	0.288	0.165	4.481	5.231	3.109	96.154
0.709	0.278	0.140	6.112	3.607	2.220	100.000
0.709	0.278	0.140	6.112	3.607	2.220	100.000
0.685	0.285	0.146	4.694	4.907	2.931	97.087
0.700	0.281	0.143	5.586	4.089	2.492	99.010
0.688	0.284	0.151	5.145	4.550	2.747	98.039
0.685	0.285	0.146	4.694	4.907	2.931	97.087
0.709	0.278	0.140	6.112	3.607	2.220	100.000

**Table 8-2 MOO final generation's individuals for T1 binary separation**

**Product collected at Extract port**

ts, mins	Cd, M	Cf, M	Qd, , mL/min	Qf, mL/min	Productivity g/L/min	Yield, %
0.709	0.278	0.140	6.753	3.607	1.263	94.340
0.685	0.285	0.146	6.734	4.907	1.338	87.719
0.674	0.288	0.165	6.547	5.231	1.327	88.496
0.709	0.278	0.140	8.164	3.607	1.062	100.000
0.709	0.278	0.140	6.481	3.607	1.374	82.645
0.685	0.285	0.146	6.547	4.907	1.327	88.496
0.700	0.281	0.143	7.278	4.089	1.129	99.010
0.688	0.284	0.151	6.734	4.550	1.338	87.719
0.685	0.285	0.146	8.164	4.907	1.062	100.000
0.709	0.278	0.140	6.753	3.607	1.263	94.340

**Table 8-3 MOO final generation's individuals for Recycle-batch chromatography**

Initial Gradient [NaCl], M	End Gradient [NaCl], M	Gradient length, CVs	Batches per Recycle Run	Column Loading, g/L	Recycle initial Gradient [NaCl], M	Recycle End Gradient [NaCl], M	Recycle batch gradient length, CVs	Productivity g/L/min	Yield, %
0.15	0.20	5.25	3	5.17	0.08	0.15	11.51	0.11	96.57
0.12	0.38	14.31	4	2.42	0.10	0.44	11.94	0.04	98.15
0.13	0.32	8.01	3	3.56	0.10	0.21	12.05	0.06	97.53
0.13	0.22	10.50	2	5.05	0.08	0.34	10.32	0.08	96.94
0.14	0.28	9.46	3	4.31	0.11	0.37	9.90	0.08	97.03
0.11	0.20	3.46	3	8.56	0.11	0.72	5.20	0.21	83.28
0.12	0.37	14.51	3	2.30	0.08	0.45	13.20	0.03	98.19
0.12	0.21	18.60	3	1.98	0.10	0.55	8.20	0.03	98.53
0.10	0.37	18.29	3	2.27	0.08	0.35	11.16	0.03	98.45
0.11	0.27	4.65	2	6.08	0.05	0.61	10.81	0.13	94.75
0.13	0.18	3.43	4	9.19	0.00	0.73	4.48	0.22	78.84
0.12	0.23	4.69	3	5.21	0.07	0.36	10.96	0.11	96.45
0.11	0.29	9.93	6	3.51	0.14	0.51	10.11	0.07	97.42
0.13	0.27	13.38	2	2.69	0.09	0.59	11.89	0.04	98.10
0.10	0.27	12.03	2	1.47	0.09	0.24	12.08	0.02	98.78
0.13	0.36	4.14	3	8.92	0.03	0.65	8.40	0.19	87.74
0.13	0.22	5.02	4	6.10	0.00	0.47	6.80	0.15	94.44
0.14	0.25	6.26	3	2.69	0.10	0.49	16.99	0.05	97.87
0.13	0.27	16.12	3	2.55	0.12	0.57	10.41	0.04	98.18
0.14	0.21	4.81	2	5.43	0.05	0.28	7.91	0.12	96.32
0.13	0.24	12.60	3	3.53	0.10	0.39	8.48	0.06	97.75
0.12	0.33	21.63	4	0.49	0.15	0.58	13.23	0.01	98.95
0.11	0.31	13.90	6	1.93	0.12	0.50	12.71	0.03	98.42
0.13	0.28	15.24	3	0.79	0.10	0.48	16.68	0.01	98.92
0.11	0.32	16.68	3	1.95	0.11	0.56	11.07	0.03	98.47
0.11	0.36	18.98	3	2.19	0.10	0.41	11.16	0.03	98.45
0.15	0.22	13.02	3	2.31	0.10	0.44	15.33	0.03	98.39
0.10	0.21	5.30	3	8.03	0.08	0.53	8.36	0.16	92.07
0.09	0.31	14.75	2	1.16	0.10	0.29	11.93	0.02	98.85
0.14	0.31	7.97	3	4.06	0.09	0.19	12.05	0.07	97.29
0.13	0.34	15.90	3	2.49	0.12	0.45	13.13	0.03	98.23
0.13	0.29	8.51	3	2.37	0.10	0.48	13.28	0.05	98.05
0.12	0.31	10.31	6	3.27	0.13	0.50	11.32	0.06	97.56
0.15	0.21	9.12	3	3.71	0.06	0.59	13.01	0.07	97.47
0.12	0.14	22.22	3	0.21	0.03	0.62	13.19	0.00	99.21

**Table 8-4 MOO final generation's individuals for batch chromatography**

Initial Gradient [NaCl], M	End Gradient [NaCl], M	Gradient length, CVs	Column Loading, g/L	Productivity g/L/min	Yield, %
0.15	0.23	2.53	9.32	0.24	61.22
0.09	0.24	14.56	0.75	0.01	95.97
0.10	0.20	17.31	1.25	0.02	95.69
0.10	0.20	11.06	1.25	0.03	95.37
0.09	0.25	17.56	0.48	0.01	96.37
0.09	0.24	14.65	0.37	0.01	96.39
0.08	0.26	24.57	0.35	0.00	96.64
0.09	0.25	20.21	0.41	0.01	96.51
0.09	0.25	15.64	0.59	0.01	96.25
0.09	0.22	13.58	0.88	0.02	95.90
0.10	0.20	17.31	0.25	0.00	96.67
0.09	0.25	22.40	0.43	0.01	96.53
0.09	0.25	15.09	0.47	0.01	96.33
0.09	0.24	14.43	0.71	0.01	96.02
0.09	0.24	14.65	0.37	0.01	96.39
0.09	0.24	20.90	0.37	0.01	96.54
0.08	0.26	24.57	0.35	0.00	96.64

**Table 8-5 MOO final generation's individuals for SAW SMB**

ts, mins	Qdesorbent	Qextract	Qfeed	Cd, M	Cf, M	Productivity g/L/min	Yield, %
0.51	8.62	1.32	1.03	0.25	0.06	0.354093	70.42254
0.70	9.99	2.59	0.31	0.23	0.00	0.151035	100
0.60	9.30	1.88	0.49	0.24	0.01	0.224585	94.33962
0.56	8.66	1.48	0.76	0.25	0.01	0.296009	80